# SURFACE ENHANCED RAMAN DETERMINATION OF HEADSPACE SAMPLED DIMETHYL TRISULFIDE

---

A Thesis

Presented to

The Faculty of the Department of Chemistry

Sam Houston State University

---

In Partial Fulfillment

of the Requirements for the Degree of

Master of Science

---

by

Md Nure Alam

May, 2017

# SURFACE ENHANCED RAMAN DETERMINATION OF HEADSPACE SAMPLED DIMETHYL TRISULFIDE

by

Md Nure Alam

_____

APPROVED:

David E. Thompson, PhD
Thesis Director

Richard E. Norman, PhD
Committee Member

Darren L. Williams, PhD
Committee Member

John B. Pascarella, PhD
Dean, College of Sciences and Engineering Technology

## ABSTRACT

Alam, Md Nure, *Surface Enhanced Raman Determination of Headspace Sampled Dimethyl Trisulfide*. Master of Science (Chemistry), May, 2017, Sam Houston State University, Huntsville, Texas.

Cyanide is a toxin with many natural and industrial sources. Among several cyanide antidotes dimethyl trisulfide (DMTS) is one of the current promising candidates under investigation. Surface Enhanced Raman Spectroscopy (SERS) is a sensitive, cost effective method that has long term potential for multiplexed, portable sensing. In this research, experiments were carried out to compare three different approaches to sampling DMTS from ethanolic solutions: drop-coating, immersion, and headspace sampling. The SERS experiments in all media show promising sensitivity with detectable signals at 5 micromolar concentrations of DMTS in ethanol. Problems in the reproducibility of signals in the headspace sampling led to the observation that condensation on the sample cell windows and sensor was a problem. A proof of principle experiment using resistive heating to warm the sampling window was successful in removing and preventing condensation. Experiments were also carried out in which DMTS was reduced to produce more volatile products that could be detected more rapidly from the headspace than DMTS. In these experiments, SERS peaks were observed to grow in more rapidly than had been observed from headspace sampling above ethanolic DMTS solutions. Specifically, SERS peaks from reduction products were observed within a minute following the initiation of reaction.



KEY WORDS: Dimethyl trisulfide (DMTS), Surface Enhanced Raman Spectroscopy (SERS)

## ACKNOWLEDGEMENTS

I deeply confer my gratitude to Dr. David Thompson for his thoughtful supervision throughout my master's study at Sam Houston State University. The scientific attributes I acquired from him are precious and I will try my best to carry the legacy throughout my professional career.

I would like to thank Dr. Richard Norman for providing me the actual opportunity and environment to improve my ability as a scientist. I also give a profound thanks to Dr. Ilona Petrikovics to grant me the opportunity of working in her lab to move forward in my research. I am also thankful to Dr. Darren Williams to provide me instruments to advance my research. I am very thankful to Dr. Donovan Haines and Rachell Haines for help with valuable information and updates of appropriate deadlines.

I would like to add my thankfulness to the group members of Dr. Petrikovics' lab and of Dr. Thompson's lab. I am highly indebted to the Chemistry Department at SHSU for supporting me with the platform to grow as a person and as a scholar.

## TABLE OF CONTENTS

**Page**

ABSTRACT ..... iii

ACKNOWLEDGEMENTS ..... iv

TABLE OF CONTENTS ..... v

LIST OF TABLES ..... vii

LIST OF FIGURES ..... viii

CHAPTER

I INTRODUCTION ..... 1

II MATERIALS AND METHODS ..... 15

1. DMTS Raman spectra ..... 16

2. Laser power calibration, warm-up time, and stability ..... 18

3. SERS experiments ..... 19

4. SERS challenges ..... 36

5. Detection of DMTS reduction product ..... 40

III RESULTS AND DISCUSSION ..... 50

1. DMTS Raman spectra ..... 50

2. Laser power calibration, warm-up time, and stability ..... 53

3. SERS experiments ..... 54

4. SERS challenges ..... 74

5. DMTS reduction experiment ..... 81

IV CONCLUSION AND FUTURE DIRECTIONS ..... 96

REFERENCES ..... 99

APPENDIX ..... 102

VITA ..... 103

## LIST OF TABLES

**Table** **Page**

1 Preparation of DMTS standard calibration solutions ..... 17

2 Preparation of DMTS solutions ..... 20

3 Stirring methods ..... 69

4 DMTS peak areas in the absence of grease sealing ..... 79

5 DMTS peak areas in the presence of grease sealing ..... 80

6 $NaBH_4$ reduction ..... 89

## LIST OF FIGURES

**Figure** **Page**


1 Schematic diagram of monolayer of DMTS on gold. ..... 6

2 Pure DMTS and ethanol vapor pressure vs temperature graph. ..... 10

3 Raman probe tip and cuvette for ordinary Raman sampling. ..... 18

4 DMTS dilution scheme. ..... 21

5 Spectrum collection method for drop coating. ..... 22

6 Sensor nanopillar leaning mechanism. ..... 25

7 SERS sensor. ..... 25

8 Immersion Raman spectrum collection technique. ..... 26

9 Glass cap sensor holder preparation. ..... 29

10 Sensor holder. ..... 29

11 Glass cap and steel cap sensor holder operation. ..... 30

12 Headspace SERS sampling apparatus a) empty and b) ethanol headspace. ..... 31

13 Steel cap sensor holder. ..... 33

14 The steel cap sensor holder within temperature controller. ..... 33

15 Sensor cutting. ..... 34

16 Indium tin oxide window is attached with cuvette window by alligator clips. ..... 37

17 Clean and grease smeared vial with DMTS solution inside. ..... 39

18 SPME extraction scheme. ..... 39

19 SERS reduction by DTT experimental setup. ..... 49

20 Gaussview 05 calculated and experimental Raman spectrum comparison. ..... 50

21 Ordinary Raman spectrum comparison. ..... 51

22 DMTS ordinary Raman peaks and Gaussian peak area calculation. ..... 53

23 Laser power test. ..... 54

24 Drop coating SERS experiment. ..... 55

25 Attenuation of the SiH stretch with DMTS exposure. ..... 56

26 Peak ratio of 265 $cm^{-1}$/ 180 $cm^{-1}$ vs volume graph. ..... 58

27 Peak ratio of 265 $cm^{-1}$/ 180 $cm^{-1}$ vs concentration graph. ..... 59

28 50 μM DMTS in-solution sampling. ..... 60

29 Benzenethiol (BT) spectrum. ..... 62

30 Laser power optimization for SERS experiment. ..... 63

31 Bare sensor vs preleaned sensor spectrum comparison. ..... 64

32 Headspace control spectrum. ..... 64

33 Subtracted headspace empty cuvette and ethanol spectrum. ..... 65

34 Room temperature 50 μM DMTS headspace SERS spectrum. ..... 66

35 Room temperature 500 μM DMTS headspace SERS spectrum. ..... 67

36 100 μM DMTS non-stirring vs stirring comparison. ..... 70

37 500 μM DMTS non-stirring vs stirring comparison. ..... 70

38 Temperature controller control experiment. ..... 72

39 Headspace sampling SERS at elevated temperature. ..... 73

40 SERS sensor condensation. ..... 75

41 Condensation on cuvette wall. ..... 76

42 Condensation problem solution. ..... 77

43 DMTS chromatogram extracted by SPME. ..... 78

44 DMTS chromatogram extracted by SPME with grease interference ..... 79

45 DMTS peak area comparison when using grease vs no grease. ..... 81

46 GC headspace analysis of reduction reaction. ..... 82

47 DMTS reduction product test by GC-MS. ..... 83

48 Ordinary Raman analysis of DMTS reduction by $FeCl_2$. ..... 85

49 $FeCl_2$ reduction spectrum fit. ..... 86

50 $FeCl_2$ SERS reduction. ..... 87

51 DMTS reduction by $NaBH_4$. ..... 89

52 DMTS reduction by $NaBH_4$ in presence of HCl. ..... 90

53 Reduction by $NaBH_4$ SERS spectrum. ..... 91

54 DTT reduction analysis by ordinary Raman. ..... 93

55 SERS analysis of DMTS reduction by DTT. ..... 94

56 DTT reduction spectra with longer observation period. ..... 95

# CHAPTER I

# Introduction

## Cyanide and its toxicity

Cyanide is a rapid acting toxin that is released as a chemical protectant when certain plant parts (such as the cassava tuber) are injured.[1] Cyanide is also produced for industrial uses such as electroplating, plastics processing, paint manufacturing, and the mining of gold and silver.[2] Cyanide exposure can occur via a variety of routes, including inhalation, ingestion, and dermal absorption. At high enough doses, cyanide can cause human death via each route of exposure.[3] Because of its toxicity and its widespread industrial use, cyanide is of concern as a terrorist weapon.[4]

## Dimethyl trisulfide (DMTS) as cyanide antidote

Cyanide prevents oxygen from binding to the protein complex in the electron transport chain of cellular respiration, shutting down ATP production, and energy generation. Eventually, individuals poisoned with cyanide die from the inability to generate energy from the oxygen that is abundantly present in the blood.[5] The currently approved therapies for treating cyanide poisoning require intravenous administration, and are suitable for hospital settings; however, they are impractical in mass casualty settings where the number of professional health care workers is likely to be insufficient to setup all of the treatments. One of the most widely used antidotal approaches to CN detoxification is to convert $CN^-$ to thiocyanate ($SCN^-$) via reaction with a sulfur donor such as thiosulfate.

Dimethyl trisulfide (DMTS) has recently been found to be a promising alternative sulfur donor for converting $CN^-$ to $SCN^-$.[6] DMTS is one of a group of novel antidotes that is being formulated for intra muscular administration by an auto injection kit. DMTS is

found naturally in plants such as onion, garlic, Brussels sprouts, broccoli, cabbage, cauliflower and leeks.[7,8] DMTS is also used as a flavor additive in food. When isolated as a pure chemical DMTS is a flammable liquid with a boiling point of 165-170°C.[9]

In antidotal development, and in field studies, it would be valuable to deploy portable instruments capable of rapidly monitoring the blood concentration of DMTS, $CN^-$ and other species related to the biochemistry and pharmacokinetics of DMTS in the context of cyanide poisoning. Because DMTS is an attractant for moths in cabbage pollination, and used as a flavor additive in food, portable methods of detecting its presence would also have potential agricultural, and food applications. DMTS also has the potential to be used as a cathode material for rechargeable lithium batteries.[10] GCMS methods have been reported for detecting DMTS in wine (LOQ = 2.4 μg/L or $1.9 \cdot 10^{-2}$ μM).[11]

The existing methods for DMTS analysis, such as gas chromatography and HPLC, are powerful and sensitive; however, they often require complex sample preparation and serial analysis steps that are time consuming. Conventional GC and HPLC instruments are typically not very portable and are expensive. Lab-on-a-chip technologies are reducing the cost, and improving portability for chromatographic separations. Surface enhanced Raman spectroscopy (SERS) can be implemented as the detection system because it provides a platform with the potential for portable, sensitive and rapid analysis of DMTS.

**Surface enhanced Raman spectroscopy (SERS)**

Raman spectroscopy probes molecular vibrational transitions by illuminating the sample with an intense beam of light, and monitoring the inelastic scattering of that light. C.V. Raman won the Nobel Prize in 1930 for the discovery and explanation of the Raman effect.[12]

Fleischmann and co-authors first observed the surface enhancement of Raman signals while trying to use Raman spectroscopy to monitor the electrochemistry of pyridine at a silver electrode. The Raman signals that they observed were approximately one million times brighter than expected.[13] This enhanced signal was later determined by Van Duyne to have an electromagnetic contribution arising from the strong electric fields generated by the collective movement of electrons in the silver nanoparticles present at the surface of the roughened electrode[14] and by Creighton and Albrecht to have a chemical contribution associated with charge transfer between the analyte molecule and the nanoparticle to which it was adsorbed.[13] Since its discovery, surface enhanced Raman spectroscopy (SERS) has been extensively studied and has found increasing use as a method for detecting trace amounts of analyte.[17] Nanostructured gold, and silver are the most commonly used materials for SERS.[15]

The development of a SERS method for detecting DMTS was begun by our previous lab member Hossain.[16] His work demonstrated the initial promise of using SERS as a method for detecting DMTS from dilute solution. He employed headspace sampling techniques with gold nanoparticles on silicon pillars, and found that the signals increased with sampling time. This thesis builds upon Hossain's prior work.

To detect DMTS with SERS, the DMTS must: (1) be brought to the sensor surface, (2) bind to the gold nanoparticles, and (3) exhibit vibrations that have a nonzero SERS cross-section. The next sections discuss these three conditions. Following this discussion, a mathematical model is used to introduce the factors that are likely to influence rates of analyte detection in headspace sampling.

1. Bringing DMTS to the sensor surface

Three ways for bringing DMTS into contact with the sensor surface are (1) to place a drop of DMTS solution on the SERS sensor and allow it to evaporate, (2) to immerse the sensor in the solution under study, and (3) to sample DMTS from the headspace above the analyte solution.

The simplest of these methods is the drop evaporation method. A key advantage of the drop evaporation approach is that it concentrates analytes at the surface when, as is commonly the case, the analyte is less volatile than the solvent. However, the drop evaporation method is challenging to use for quantitation, because of differences in the spread of replicate drops on the surface, and because of variations in the analyte coverage densities that are associated with variations in drop drying patterns. Drop evaporation is also poorly suited for studying the kinetics of sensor binding because of the spatial and temporal nonuniformities in exposure, and the variability of the evaporation period. Fully immersing the SERS sensor in the analyte solution overcomes many of these quantitation challenges by ensuring uniform spatial and temporal exposure of the sensor to the analyte.

Fully immersed sensing is possible when the sample volume is sufficiently large to enable immersion. An advantage of fully immersed vs. evaporated drop sensing, is that fully immersed sensing is compatible with investigations of the kinetics of binding.

However, in a complex matrix, both drop evaporation and immersed sensing are susceptible to sensor fouling by interferents. For example, in our targeted application of measuring DMTS from blood, cysteine is expected both to be abundantly present, and to bind to SERS sensors. Thus, for complex samples, interference can pose problems for drop evaporated and immersed SERS sensing.

When an analyte is more volatile than the interferents, headspace sampling provides an avenue for partially mitigating the selectivity challenge. SERS has been shown to be effective as a gas phase detection method.[17,18] (Gas phase sensing is also advantageous for sampling in hostile environments such as the diagnosis of combustion, plasma, chemical vapor deposition and gas phase dynamics.)[19] Because DMTS has a higher volatility than many interferents such as cysteine, and proteins, headspace sampling has the potential to reduce interferences when determining DMTS from blood.

Challenges that are associated with headspace sampling include extended sensing times for higher boiling analytes, window fogging, and reliable sealing of the sampling environment.[20]

Even though it is more volatile than many interferents, the volatility of DMTS is impeded by its relatively high boiling point of 165-170˚C.[21] Solution stirring and heating can help to expedite the DMTS transport into the headspace. The electrochemical reduction of DMTS to the volatile products methyl mercaptan and hydrogen sulfide could result in a more dramatic improvement in the rate at which DMTS reductant products are brought to the sensor surface. Many reducing agents might accomplish this task. Here we use the example of iron (II) chloride ($FeCl_2$).

$$4Fe^{2+} + CH_3\text{-}S\text{-}S\text{-}S\text{-}CH_3 + 4H^+ \rightarrow 4Fe^{3+} + 2\ CH_3\text{-}SH + H_2S$$

Because methyl mercaptan and hydrogen sulfide are more volatile than DMTS, these products should partition more favorably out of solution into the headspace, where the sensing surface is located.

2. Binding the DMTS or its reduction products to the gold at the sensor surface

Because sulfur atoms form strong bonds to gold,[22] and methyl groups do not, DMTS is expected to bind to the gold nanoparticles on the SERS sensor via the sulfur atoms. Because thiols react faster with noble metals than polysulfides, the fraction of collisions that result in analyte binding should be higher for the reduction products methyl mercaptan and hydrogen sulfide than for DMTS.[23] Adsorption of organosulfur molecules onto noble metals such as silver and gold has been well studied.[22] For example, Ashish Tripathi *et al*. have shown that the adsorption of benzenethiol to an immersed SERS sensor at pH 8.0 is faster than at pH 4.0.[24]

DMTS may initially physisorb to the gold with the methyls lying down on the surface,[25,26] and this conformation may persist when the number of molecules are lower in number. When the number of molecules on the surface increases, it is anticipated that they will pack more densely, cleave the methyl groups off from the DMTS molecule and self-assemble into a chemisorbed monolayer on the gold.[27] One possible conformation for such a monolayer is shown in Figure 1.

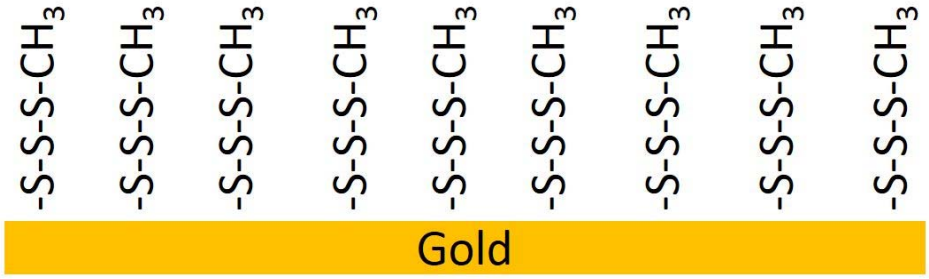


*Figure 1.* Schematic diagram of monolayer of DMTS on gold.

3. The Raman Cross-Section of bound DMTS

Due to their polarizability, the S-S-S and C-S vibrations of DMTS have substantial Raman cross sections.[27] The S-S-S bending and stretching modes are reported in the ranges of 260-270, and 450-490 $cm^{-1}$ respectively.[28,29] The C-S stretch is reported in the 620-730 $cm^{-1}$ range.[30] Solvent molecules are expected to be abundantly present in the gas phase and to collide with the sensor, but are not expected to interfere with the analysis because water and ethanol do not form covalent bonds with gold. Thus, even though it is present at much lower concentration, DMTS will outcompete solvent molecules for binding sites at the SERS sensing surface. Although water and ethanol do not bind to the gold caps, they will be close enough to experience some enhancement due to the evanescent electrical fields of the gold nanocaps. The SERS signal for water and ethanol do not overlap with the sulfur bands that serve as the primary signal for detecting the presence of DMTS.

4. Modeling the rate of DMTS signal growth.

Even if a SERS sensing approach is sensitive, and selective, its utility will be limited by the time required for the analysis. The goal of this section is to present a model for the rate of SERS signal growth in a headspace measurement setting. This model assumes that DMTS is being detected by SERS from the headspace above a volume, V (ranging from 0 – 2000 μL), of an ethanolic DMTS solution whose concentration is C (ranging from 0.01- 1000 μM). This concentration range mimics the expected concentrations of DMTS in blood, or brain over the course of post injection pharmacokinetics studies.[31]

We begin by modeling the solution-headspace partitioning equilibrium. In this equilibrium, n and x represent, respectively, the number of moles of DMTS initially present

in the aliquot being sampled and the number of moles of DMTS that partition into the headspace.

| | *DMTS(EtOH)* ⇋ | *DMTS(g)* |
|---|---|---|
| ***I*** | *n* | *0* |
| ***C*** | *-x* | *+x* |
| | --- | --- |
| ***E*** | *n-x* | *x* |

The equation for the corresponding equilibrium constant is

*Eq. 1*

$$K = \frac{P_{DMTS}}{\chi_{DMTS}}$$

In this equation, P is the equilibrium partial vapor pressure of DMTS in the headspace, and $X$ is the equilibrium mole fraction of DMTS in the liquid solution. Because we are interested in estimating the rate of gas phase collisions with the SERS sensor, it is advantageous to solve for the partial pressure of DMTS in the headspace. Since the DMTS solution is dilute (0.01- 1000 μM) Raoult's law may not predict the behavior of the gas pressure precisely. The equilibrium vapor pressure can be described by Henry's law. [32]

*Eq. 2*

$$P_{DMTS,T} = \chi_{DMTS} \cdot K_h$$

$K_h$ is Henry's law constant.[32] For DMTS the constant has found to be $2.1 \cdot 10^{-5}$ M/pa when using water as solvent.[33] Since the long term goal of this work is to detect DMTS from blood, and since blood contains 650 $g_{water}/kg_{blood}$,[34] the model calculations are based on water as the solvent.

The vapor pressure ($P^o_{298.15}$) and the heat of vaporization ($\Delta H_{vap}$) of pure DMTS have been measured to be 0.143 kPa,[35] and 40.2 ± 3.0 kJ/mol[36] at 298.15K (25 °C).

The Clausius-Clapeyron equation can be used to estimate the vapor pressure of pure DMTS at other temperatures.

*Eq. 3*

$$P^{o}_{DMTS,T} = P^{o}_{298.15} e^{-\left(\frac{\Delta H_{Vap}}{R} * \left(\frac{1}{T} - \frac{1}{298.15}\right)\right)}$$

Figure 2 shows the predicted vapor pressures of pure ethanol, and pure DMTS as a function of temperature.

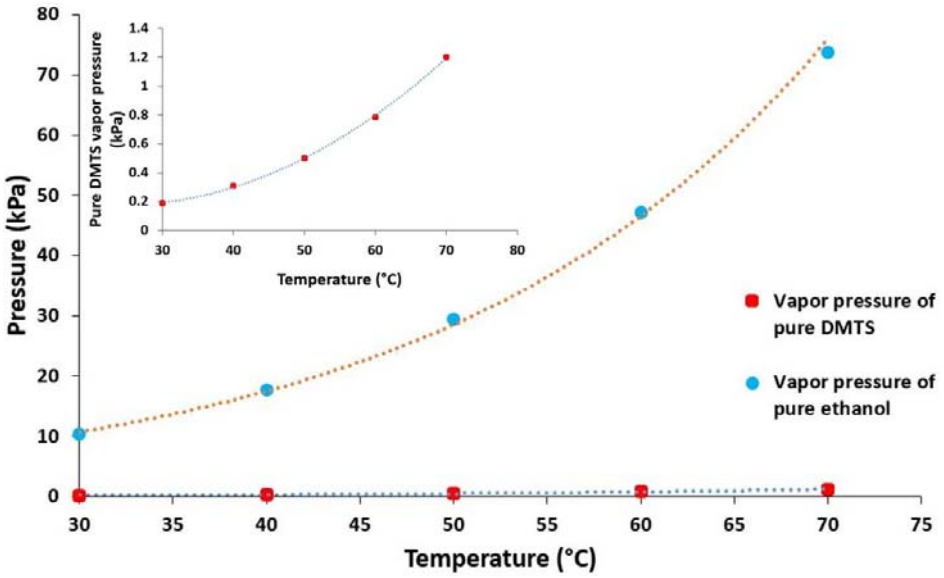


*Figure 2.* Pure DMTS and ethanol vapor pressure vs temperature graph. Inset DMTS vapor pressure vs temperature graph. The vapor pressure is calculated by using the Clausius-Clapeyron equation.

The Clausius-Clapeyron equation provides us with a method for estimating the vapor pressure of pure DMTS, $P^{o}_{DMTS,T}$, at any temperature. The next step is to express the equilibrium mole fraction of DMTS in the sample, in terms of the initial moles of DMTS and solvent (n and $n_{solvent}$), and the extent of evaporation (x and $x_{solvent}$).

*Eq. 4*

$$P_{DMTS,T} = \left(\frac{n - x}{n - x + n_{solvent} - x_{solvent}}\right) \cdot K_h$$

Finally, the equilibrium partial pressure of DMTS in the headspace can be expressed in terms of the ideal gas law.

*Eq. 5*

$$\frac{xRT}{V_{headspace}} = \left(\frac{n-x}{n-x+n_{solvent}-x_{solvent}}\right) \cdot K_h$$

Here, the limitation of the model is that the van der Waals forces are not considered. We now have an equation in which all quantities are known except the extent of reaction x, and the number of moles of evaporated solvent, $x_{solvent}$. The expression is further simplified by assuming that: (1) the number of moles in the headspace ($x+x_{solvent}$) is negligible compared to the number of moles in the solution and (2) that the number of moles of DMTS in solution is much less than the number of moles of solvent. With these two assumptions, the equation simplifies to the following form,

*Eq. 6*

$$\frac{xRT}{V_{headspace}} = \left(\frac{n-x}{n_{solvent}}\right) \cdot \mathrm{K}_h$$

Solving for x,

*Eq. 7*

$$x = \frac{n \cdot K_h \cdot V_{headspace}}{n_{solvent}RT + K_h \cdot V_{headspace}}$$

These simplifications are valid for sample aliquots that are large enough to reach equilibrium with the headspace without substantially decreasing the volume of the original sample, for temperatures below the boiling point, and for initial DMTS concentrations below 100 mM.

Recognizing that the left side of *Eq. 6* is equal to the partial pressure of DMTS in the headspace, *Eq. 6* can be rewritten as,

*Eq. 8*

$$P_{DMTS,T} = \left(\frac{n-x}{n_{solvent}}\right) \cdot \mathrm{K}_h$$

Substituting x from *Eq. 7* into *Eq. 8* gives,

*Eq. 9*

$$P_{DMTS,T} = \frac{n}{n_{solvent}} \cdot \left(1 - \frac{K_h V_{headspace}}{n_{solvent} RT + K_h V_{headspace}}\right) \cdot K_h$$

The definitions of solute molarity, and solvent density can be used to express the mole ratio $n/n_{solvent}$ in terms of experimentally known quantities,

*Eq. 10*

$$P_{DMTS,T} = \frac{C \cdot MW_{solvent}}{\rho_{solvent}} \cdot \left(1 - \frac{K_h}{\frac{\rho_{solvent} RT}{MW_{solvent}} \cdot \frac{V}{V_{headspace}} + K_h}\right) \cdot K_h$$

$$\frac{MW_{solvent}}{\rho_{solvent}} = \frac{18.015 \frac{g}{mol}}{\frac{1000 g}{L}} = 0.018015 \frac{L}{mol}$$

$$\frac{\rho_{solvent} R}{MW_{solvent}} = \frac{\frac{10^6 g_{water}}{m^3}\left(8.314 \frac{kg\ m^2}{s^2\ mol\ K}\right)}{\frac{18.015 g_{water}}{mol}} = 46150\ \frac{Pa}{K}$$

$$P_{DMTS,T} = C \cdot 0.018015 \cdot \left(1 - \frac{K_h}{461504\ T \cdot \frac{V}{V_{headspace}} + K_h}\right) \cdot K_h$$

Accounting transportation of DMTS in the gas phase with a certain rate at which molecules strike the surface area of the SERS sensor, collision flux. Z, can be used to calculate the number of collisions within the area in a given time interval.[32]

The equilibrium collisional flux, $Z_t$, at the SERS sensor is predicted to be:

*Eq. 11*

$$Z_t = \frac{P_{DMTS,T,t} \cdot N_A}{\sqrt{2\pi MW_{DMTS} RT}} = \frac{P_{DMTS,T,t} \cdot \frac{6.022 \cdot 10^{23} collisions}{mol}}{\sqrt{2\pi \frac{0.12626 kg}{mol} \frac{8.314 kg\, m^2}{s^2\, mol\, K} T}} = \frac{2.3448 \cdot 10^{23}}{\sqrt{|T|}} \frac{collisions}{m^2 \cdot s \cdot Pa} \cdot P_{DMTS,T,t}$$

Substituting in the expression *Eq. 11* for the equilibrium headspace pressure of DMTS, an expanded version of the equilibrium collisional flux equation is obtained:

*Eq. 12*

$$Z = \frac{2.3448 \cdot 10^{23}}{\sqrt{T}} \cdot \left[ C \cdot 0.018015 \cdot \left( 1 - \frac{K_h}{461504\, T \cdot \frac{V}{V_{headspace}} + K_h} \right) \cdot K_h \right]$$

To begin using this equation predictively, we assume that Z is in units of collisions $m^{-2}s^{-1}$; that all pressures are in units of Pascals (1Pa = 1 $N/m^2$ = 1 kg/(m $s^2$); that C is the initial concentration of DMTS in units of molarity; and that T is Kelvin.

*Eq. 13*

$$Z = \frac{4.224 \cdot 10^{21} \cdot C}{\sqrt{T}} \cdot \left( 1 - \frac{K_h}{461.5\, T \cdot \frac{V}{V_{headspace}} + K_h} \right) \cdot K_h$$

Where $K_h$ is the Henry's law constant.

**Estimation of the number of binding sites in the laser probe spot:**

Because the goal of this work is to detect DMTS as fast as possible, the rate of collision and binding DMTS to the sensor is important. To estimate the maximal surface area covered by a DMTS molecule, DMTS was modeled as a rectangle with a length of 0.743 nm, a width of 0.180 nm (estimated with Gaussview 05), and an estimated area of 0.134 $nm^2$. For minimal surface area DMTS was modeled as a cylinder with a length of 0.743 nm, a diameter of 0.180 nm, and an estimated area of 0.0254 $nm^2$.

*Eq. 14*

$$|Z|\frac{collisions}{m^2 s}\cdot 0.0254\cdot 10^{-18}\frac{m^2}{binding\ site} < Rate_{\substack{binding\\site}} < |Z|\frac{collisions}{m^2 s}\cdot 0.134\cdot 10^{-18}\frac{m^2}{binding\ site}$$

The sensor is not homogeneously dispersed with gold atoms. The construction of the nanopillars are made of silicon and gold is coated on top of the pillars. The nanopillars are 50-80 nm wide and each $\mu m^2$ covered 18 nanopillars.[37]

An estimate of the number of molecules that can fit in the spot illuminated by laser can also be calculated. If the diameter of the laser spot on the sensor is 100 μm, then the area of the probed spot on the sensor is

*Eq. 15*

$$A_{laser\ spot} = \pi r^2 = \pi\cdot\left(50\cdot 10^{-6} m\right)^2 = 7.85\cdot 10^{-9} m^2$$

Dividing the laser spot area by the minimal and maximal DMTS coverage areas, the number of molecules probed by the laser on a fully coated sensor is estimated to range from 4.40 x $10^8$ to 7.05 x $10^{13}$ molecules (0.73 fmol to 117.12 pmol). That promises improved detection compared to the recent SERS method.[38]

# CHAPTER II

## Materials and Methods

Dimethyl trisulfide (purity ≥98%) was purchased from Sigma Aldrich; ethanol (190 proof) was purchased from VWR. The Raman spectrometer that was used in these experiments was assembled from: a Thorlabs 785nm laser diode in temperature controlled housing, a Thorlabs diode current controller, a Bayspec fiber optic Raman probe, a Bayspec 2020 spectrometer, Bayspec software, and a Northwest qpod 2e cuvette temperature controller. The SERS sensors were purchased from the Silmeco Company in Denmark. An Ohaus Explorer Pro analytical balance was used for weighing samples. An Ophir VEGA power meter was used to measure the laser power. An AutoCAD designed sensor holder was used for positioning the sensor inside the temperature controller. A Nikon D700 DSLR camera was used for taking the pictures of the sensor. A 7890A gas chromatography instrument purchased from Agilent with a 5975C quadrupole mass spectrometer in Dr. Petrikovics lab was used for grease interference experiments. A DB-5MS, 30 m x 0.25 m, 0.1 μm column was used as the stationary phase, carrier gas was helium. A solid phase micro extraction (SPME) fiber coated with CAR/PDMS 85 μm bought from Sigma-Aldrich, and a Hamilton sample lock gas syringe was used for GC experiments. A FLIR ONE thermal imaging camera for iPhone 5/5s from Dr. Williams lab was used for taking InSnO (ITO) window pictures.

## 1. DMTS Raman spectra

### 1.1. Calculated DMTS Raman spectrum

In order to determine the vibrational origin of peaks, Raman spectra of DMTS and methyl mercaptan (MeSH) were calculated using the Hartree-Fock method in Gaussian 09w (Job type: # opt freq=raman hf/6-31g(d) geom=connectivity). GaussView 5.0 software were used to build the molecule and to analyze the results and the frequency is scaled by factor 0.8929.[39] A Raman spectrum of pure DMTS was collected for comparison. We were interested in the methyl mercaptan spectrum because it can be generated by reducing DMTS, and because it has the potential to be detected more rapidly than DMTS.

### 1.2. Determining the limit of detection for DMTS with Raman spectroscopy

To set a baseline for this work, experiments were carried out to determine the limit of detection and quantitation for unenhanced Raman spectroscopy. Prior to starting the measurements, the lens at the tip of the Raman probe was cleaned by Sticklers fiber optic splice & connector cleaner. A 1-cm pathlength glass cuvette was cleaned and rinsed with ethanol, and then placed into the CHV100 cuvette holder mounted in front of the Raman probe. The experiment was carried out inside the fume hood to minimize odors.

A 1.0 M ethanolic stock solution prepared by diluting 2625 μL of DMTS (FM 126.265 g/mol, density 1.202 g/mL at 25 °C) to the mark in a 25.0-mL volumetric flask. From this stock solution, ethanolic DMTS calibration standards ranging from 0.010 to 1.0 M were prepared as shown in Table 1. After dilution, each solution was vortexed for one minute and then inverted 20 times to ensure good mixing. VWR disposable sterile pipette tips were used to transfer pure DMTS from the shipped bottle. Hamilton syringe and VWR micropipettes were used to transfer solutions for dilution procedures.

Table 1

*Preparation of DMTS standard calibration solutions*

| Stock solution concentration (M) | Volume of stock solution (mL) | Volume of diluted solution (mL) | Final DMTS concentration $C_{final}$ (M) |
|---|---|---|---|
| 1.0 | 7.5 | 10.0 | 0.75 |
| 1.0 | 5.0 | 10.0 | 0.50 |
| 1.0 | 2.5 | 10.0 | 0.25 |
| 1.0 | 2.5 | 25.0 | 0.10 |
| 0.10 | 7.5 | 10.0 | 0.075 |
| 0.10 | 5.0 | 10.0 | 0.050 |
| 0.10 | 2.5 | 10.0 | 0.025 |
| 0.10 | 1.0 | 10.0 | 0.010 |

The collection of Raman spectra began immediately after completing the preparation of the calibration solutions. Three mL of each standard solution was transferred into the 4-mL glass cuvette. Raman spectra were collected in 180$^{o}$ geometry using the home assembled Raman system with the Bayspec probe (Figure 3).

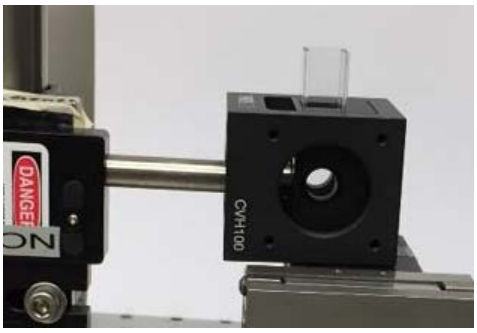


*Figure 3.* Raman probe tip and cuvette for ordinary Raman sampling. Experiments with high concentrations of DMTS were carried out in the hood.

Linear least squares regression was used to fit a line to the data in Microsoft Excel. The limit of detection and the lower limit of quantitation were calculated, respectively, by the formulas 3s/m and 10s/m. The variables s and m represent the standard deviation of the signals from the calibration line, and the slope of the calibration line, respectively. The slope is found by plotting the concentration of DMTS on the X-axis and corresponding peak areas on the Y-axis. Using the slope (m), peak areas are predicted and the standard deviation is calculated by the following equation.

*Eq. 16*

$$s = \sqrt{\sum_{i=0}^{n} \frac{(y_{peak\ area\ predicted\ from\ line} - y_{peak\ area})^2}{n-2}}$$

**2. Laser power calibration, warm-up time, and stability**

Prior to beginning SERS experiments, the home assembled Thorlabs diode laser was run through a simple series of experiments to associate specific diode currents with specific output powers, to determine the laser warm-up time, and to obtain a measure of the laser stability.

Laser diode power calibration experiment: To correlate diode current with optical power, an Ophir VEGA power meter was used to record the optical power at the sample position over the working range of diode currents (0-340 mA). Because the power meter can be damaged if placed at the focus, care was taken to ensure that the detector was placed sufficiently far from the focal spot (at least 8 mm) that the beam had started to expand and formed a spot of ~ 5 mm diameter on the sensor face, but not so far that it overfilled the detector. The laser power at each diode current was recorded using Ophir StarCom32 software.

Laser diode warm up, and stability experiment: To assess the warm-up period for the laser and optical probe, and the power stability of the 785 nm Thorlabs laser, the laser diode current was fixed at 180 mA. The laser power at the sample position was recorded from this cold start by the Ophir VEGA power meter over a period of 80 minutes. The experiment was repeated using a slightly longer 120-minute duration (data is shown only for 80 min Figure 23 b).

## 3. SERS experiments

A series of experiments were carried out to map out the SERS response to DMTS under different exposure conditions. Distinct sets of SERS sensors were exposed to DMTS via drop coating, immersion in DMTS solution, and sampling in the headspace above a DMTS solution. Then SERS spectra were collected. The methods used in these DMTS SERS experiments are described in this section.

### 3.1. Drop coated SERS

The recommended method for applying analyte to the Silmeco SERStrate sensor is to allow a drop of analyte containing solution to evaporate from the sensor surface. In this

experiment, SERStrate sensors were drop-coated with DMTS standard solutions, prior to SERS measurements.

Table 2

*Preparation of DMTS solutions*

| Stock solution concentration (M) | Volume of stock solution (mL) | Volume of diluted solution (mL) | Final DMTS concentration $C_{final}$ (M) |
|---|---|---|---|
| 0.50 | 1.0 | 10.0 | 0.050 |
| 0.050 | 1.0 | 10.0 | 0.0050 (5000 μM) |
| 0.0050 | 1.0 | 10.0 | 0.00050 (500 μM) |
| 0.00050 | 2.0 | 10.0 | 0.00010 (100 μM) |
| 0.00050 | 1.0 | 10.0 | 0.000050 (50 μM) |
| 0.000050 | 1.0 | 10.0 | 0.0000050 (5 μM) |
| 0.0000050 | 1.0 | 10.0 | 0.00000050 (0.5 μM) |

*Note.100 μM DMTS solution preparation is shown in this table, but is not used for this experiment. 100 μM solutions were used for stirring and room temperature unstirred experiment.*

A 0.5 M ethanolic DMTS stock solution was prepared by diluting 520 μL of DMTS (FM 126.265 g/mol, density 1.202 g/mL at 25 °C) to the mark in a 10.0-mL volumetric flask. From this stock solution, a series of ethanolic DMTS calibration standards ranging from 0.50 μM to 0.050 M to were prepared as shown in Table 2 and Figure 5. After dilution,

each solution was vortexed for one minute and then inverted 20 times to ensure good mixing.

Only five concentrations of ethanolic DMTS solutions were used for this experiment (0.5, 5, 50, 500, 5000 μM).

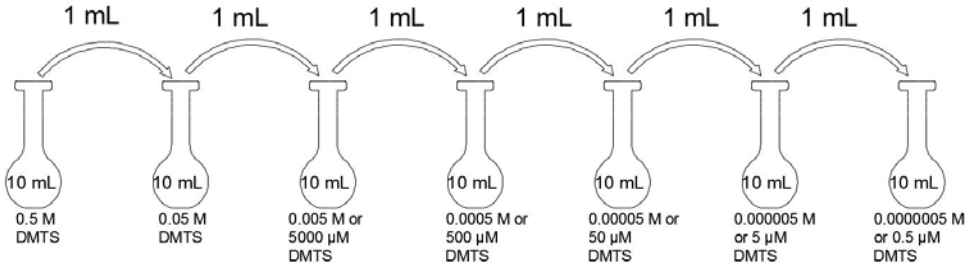


*Figure 4.* DMTS dilution scheme.

Silmeco SERStrate sensors were used as SERS substrates. One SERS sensor was designated as an alignment reference, and the second SERS sensor served as the sensor for DMTS detection.

Using an abundance of caution, the alignment reference sensor was exposed to benzenethiol vapor. Benzene thiol (BT) is a strong Raman and SERS scatterer. It is also toxic. To ensure safety, exposures were carried out in the fume hood, with the exhaust set on the emergency higher flow rate setting. A 25.0-mL bottle of BT was placed in an empty desiccator next to an empty bottle that prevented the BT bottle from tipping over. The BT bottle was opened. The sensor(s) to be exposed were placed above the open BT bottle. Each new 4 mm x 4 mm SERS sensor to be exposed was held in an Eppendorf tube whose bottom tip had been cut off to allow vapor exposure. The Eppendorf tubes were held in a plastic tray designed for holding Eppendorf tubes. The holder was lowered into the desiccator immediately after the BT bottle was opened. The greased desiccator lid was then

applied to seal in the BT vapor. After a 15 minute exposure period, the BT lid was removed. The plastic tray holding the BT coated sensors was removed, the BT bottle was capped and placed within another larger dedicated storage bottle at the back of the hood. All gloves were left in the hood. Everything was allowed to degas for approximately an hour, until the sensors could be removed and no odor of BT sensed. The hood was then returned to normal flow rate. These BT coated sensors served as alignment references in all subsequent experiments.

One new 4 mm x 4 mm SERS sensor was unpacked from the Eppendorf tube in which it had been packaged by the manufacturer, and mounted to a glass sensor holder by a small amount of Dow Corning vacuum grease. A BT alignment reference sensor was attached above the new sensor. The sensor holder consisted of two pieces of glass glued together to form and inverted "T". During the attachment process sensors were held and manipulated with a PELCO 7X.SA tweezer. The mounted sensors were then attached to a Newport xyz translation stage, and placed in front of the Raman probe (Figure 5).

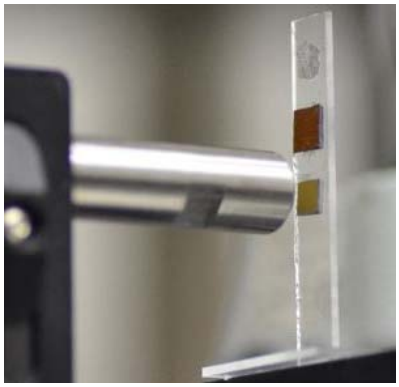

*Figure 5.* Spectrum collection method for drop coating. The steel cylinder represents the Raman laser probe directed toward two square SERS sensors. The top sensor was a benzenethiol sensor (dark brown) used to optimize the distance between the laser probe and sensor. The bottom sensor (light yellow) was the experimental sensor.

The laser power was set to 4 mW. The laser beam was centered on the BT alignment reference sensor. The CCD on the Bayspec spectrometer was turned on and set to collect 2 spectra each second. These spectra were not stored but updated the display in the computer monitor as they were collected. The sensor holder was translated to find the distance at which the BT thiol SERS spectrum was most intense.

Following this rough alignment procedure, the sensor was systematically translated along the optical axis through the optimal focal region by using micrometer z-axis 100 micrometers at a time. Between each 100-micrometer translation, a high quality spectrum was collected and saved. The peak height at 1560 $cm^{-1}$ was then extracted from each saved spectrum and plotted versus micrometer position to find the position where the BT SERS signal was most intense. Once the optimum distance was obtained the experimental sensor (ethanol evaporated sensor in this case) was raised into the laser beam, without changing the distance between probe tip and sensor. Spectra of the unexposed SERS sensor were collected, using a laser illumination powers of 4 and 10 mW. Each raw spectrum was based on 5 second CCD illumination period. Ten raw spectra were averaged to obtain one saved spectrum.

After collecting a spectrum of the unexposed SERS sensor 2-μL drops of ethanol were applied respectively to five new SERS sensors. After the ethanol had evaporated, each sensor was mounted, and aligned. In this manner, a SERS spectrum was collected from each ethanol treated sensor.

The five SERS sensors were then each dedicated to one (0.5, 5, 50, 500, and 5000 μM) of the five standard ethanolic DMTS solutions. A 2-μL drop of the appropriate solution was applied to the dried area of the prior drop, allowed to evaporate, and then

another series of SERS spectra were collected. This cycle was repeated three more times, so that when the final round of SERS spectra was collected, each sensor had been exposed to 2 μL of ethanol, and 8 μL of one DMTS solution. After each exposure, spectra at 4 and 10 mW laser power were collected from each sensor. In total, 50 spectra (5 sensors x 5 additive drop coating DMTS exposures x 2 spectra per DMTS exposure) were collected. Due to time limitations, only the 4mW data were analyzed. Analysis was carried out using Microsoft Excel 2016.

### 3.2. Immersed SERS

The drop-coating experiment was followed by an immersion experiment, in which a single SERS sensor was dipped into a 50 μM DMTS solution. Raman spectra were collected as a function of time to obtain data on the rate of DMTS binding.

The gold-coated silicon nanopillars on the new sensor were preleaned prior to the experiment. The new sensor was transferred into a VWR polystyrene petri dish. A 10 μL drop of Type-I deionized water (3$^{rd}$ floor CFS building) was gently applied to the sensor surface and allowed to evaporate at room temperature for approximately one and half hours. As the evaporation proceeds, the nanopillars are pulled in toward each other, (via intermolecular forces between the water and the silica on the surface of the nanopillars), until the gold caps touch.

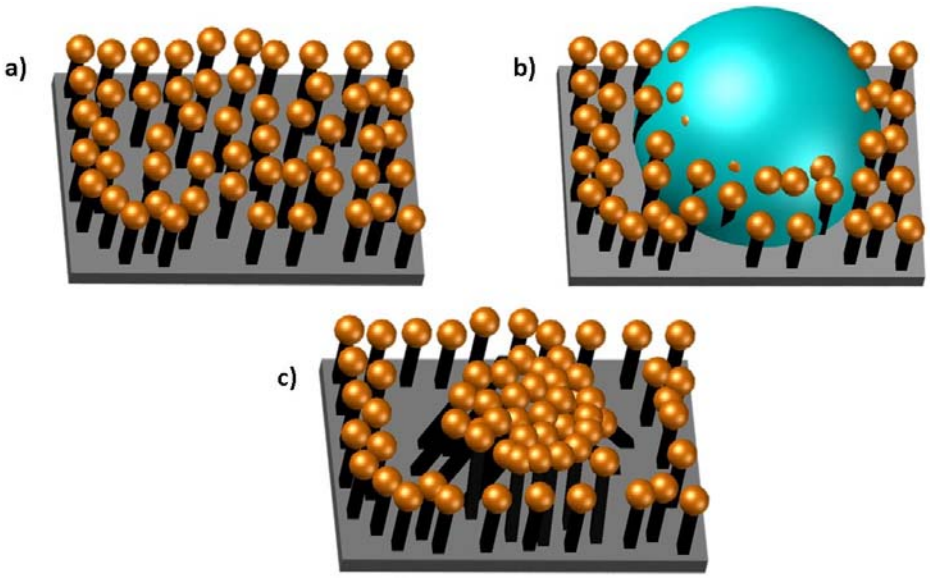


*Figure 6.* Sensor nanopillar leaning mechanism. a) Silicon nanopillar with gold coated top. b) Water droplet (blue region) on the nanopillars, c) Nanopillars leaned upon water evaporation.

An analyte molecule bound near the junction of two adjacent gold nanocaps will experience multiplicative enhancement. The junctions formed by pre-leaning the nanopillars are called hotspots because of their stronger SERS signals. As the nanocaps aggregate upon leaning, their localized surface plasmon resonances shift. As shown in Figure 7 this causes the color of the sensor surface to darken where it has been preleaned.

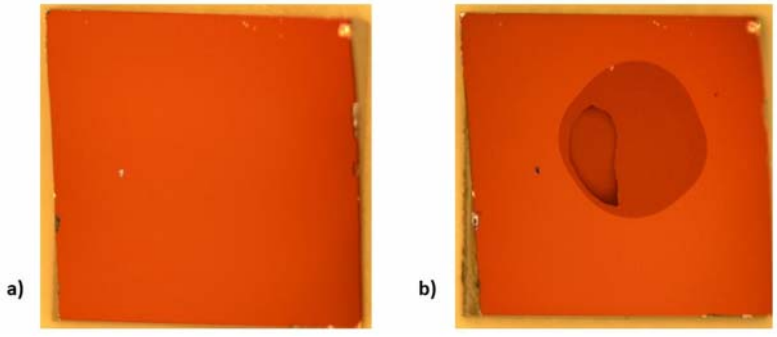


*Figure 7.* SERS sensor. a) New b) Nanopillar leaning upon 10 µL Type-I DI water evaporation.

The preleaned sensor was attached to a “T” shaped sensor holder with vacuum grease. Then 1.2 mL of 50 µM ethanolic DMTS solution was transferred by micropipette into the 4.0-mL quartz cuvette. The “T” shaped sensor holder was inverted and inserted into the cuvette (Figure 8), so that the experimental sensor was fully immersed in the 50 µM ethanolic DMTS solution. Dow Corning grease was used to seal the base of the sensor holder to the top of the cuvette.

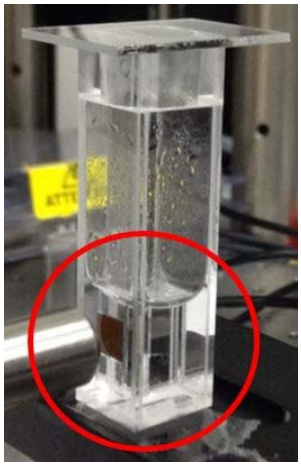

*Figure 8.* Immersion Raman spectrum collection technique. The red circle is showing a square dark brown sensor in a 50 µM DMTS solution inside the quartz cuvette. The cylindrical steel object is the Raman laser probe.

As discussed in the drop coating section, the distance from the sensor to the laser probe is critical. The focal point of the Raman probe shifts from 4.2 mm in air to 4.6 mm in ethanolic solution. In this immersion experiment, the sensor was not aligned using a BT reference, but rather was aligned to approximately 4.66 mm from the probe tip by visual adjustment with the aid of a caliper. Once alignment was completed, spectra were collected under the following conditions: 20 mW laser power, 5 second integration time and 10 spectra were averaged to store as one spectrum. The interval from scan to scan was 5 minutes. In total, 35 scans were stored and analyzed using Microsoft Excel 2016.

### 3.3. Headspace Sampling SERS

When a slightly volatile analyte, such as DMTS, is present in a complex matrix like blood, headspace sampling has the potential to reduce sensor fouling, and to improve method selectivity. The experiments described in this section explored the possibility of using headspace sampling for DMTS. Although the long-term goal is to use headspace sampling with complex matrices such as blood, the solutions used in these experiments were simple ethanolic DMTS solutions.

#### *3.3.1. Control*

Several control experiments were carried out in preparation for the headspace sampling experiments.

##### *3.3.1.1. SERS laser power optimization*

Prior to probing DMTS, a SERS experiment was carried out to characterize signal-to-noise ratios as a function of illuminating laser power. A BT coated alignment reference sensor was attached to a "T" shaped glass sensor holder, and the holder was mounted on the Newport xyz translation stage. Precise alignment of the sensor was carried out as described earlier in the drop coating section. SERS spectra of the BT were collected at eight different laser diode current settings: 110, 120, 130, 140, 150, 160, 170, and 180 mA. The integration time was 5 seconds and 10 spectra was averaged to store as one spectrum. This experiment was repeated two additional times.

The peak area at 1560 $cm^{-1}$ from each benzenethiol spectrum was calculated using Gaussian peak fitting in Microsoft Excel 2016. At each diode current setting, the average peak area, and the standard deviation of the replicate measurements were calculated as shown respectively, in Eq. 17 and Eq. 18.

*Eq. 17*

$$\bar{A} = \frac{Aa+Ab+Ac}{3}$$

*Eq. 18*

$$S_{\bar{A}} = \sqrt{\frac{(Aa-\bar{A})^2 + (Ab-\bar{A})^2 + (Ac-\bar{A})^2}{3-1}}$$

The signal to noise ratio at each diode current setting was then calculated as the coefficient of variation (Eq. 19).

*Eq. 19*

$$\frac{Signal}{noise} = \frac{\bar{A}}{S\bar{A}}$$

Finally, the signal to noise ratio versus laser power was plotted and discussed in the Results and Discussion section.

*3.3.1.2. Sensor preparation*

The nanopillars on the SERS sensors were preleaned by evaporating a water drop from the sensor surface (Figure 6, Figure 7). The preleaned region of the sensor (e.g. circular dark spot in Figure 7 b) was probed by the Raman laser in the headspace sampling experiments.

*3.3.1.3. Control of headspace sampling*

In these experiments, two types of sensor holder were used to suspend the sensor in the headspace: a glass capped glass sensor holder, and a steel capped glass sensor holder Figure 10.

During the preparation of the sensor holders, two major factors were taken into account. First, the holder needed to be long enough to hold the sensor near the solution, but not so long that the sensor would touch the solution. Secondly, the width of the holder

needed to be smaller than the inner width of the cuvette (10 mm) to enable the sensor to be translated within the cuvette for alignment purposes.

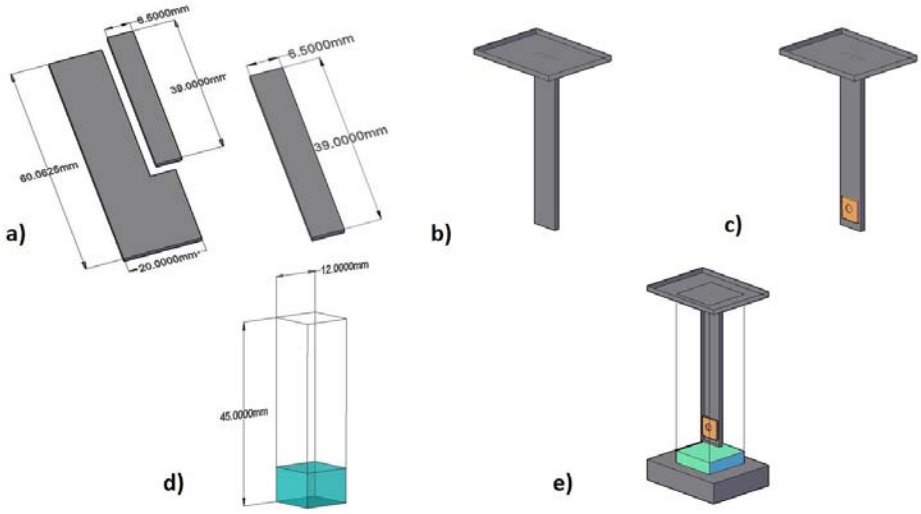


*Figure 9.* Glass cap sensor holder preparation. a) Microscopic glass slide cutting with 39 x 6.5 mm dimension, b) Glass slide attached to another glass slide (glass cap) using UV curing glue, c) SERS sensor (yellowish brown square object) attached with the holder, d) Cuvette with solution inside with dimension f) Sensor holder insert inside glass cuvette with solution.

A 60 by 20 mm (3" x 1") Corning glass microscope slide was cut, using a Wheeler Rex Pipe tool, into 39 mm length and ~6.5 mm width. This was placed in a right-angle jig, and glued to either a steel or a glass cap using UV-curing adhesive. The sensor (dimension 5mm by 5mm) was attached to the holder using Dow Corning high vacuum grease.

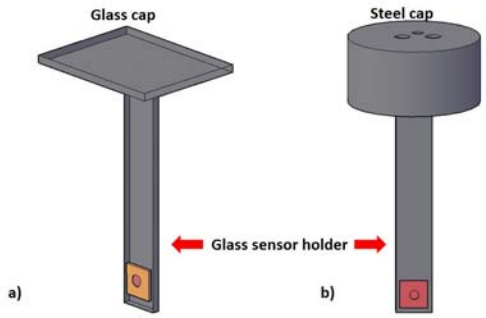


*Figure 10.* Sensor holder. a) Glass cap sensor holder. b) Steel cap sensor holder.

For headspace sampling the sensor was suspended above the solution (Figure 11 a) and for immersion sampling the sensor was immersed in the solution (Figure 11 b). The steel capped sensor holder (Figure 11 c) was used for experiments inside the Quantum Northwest Qpod temperature controller.

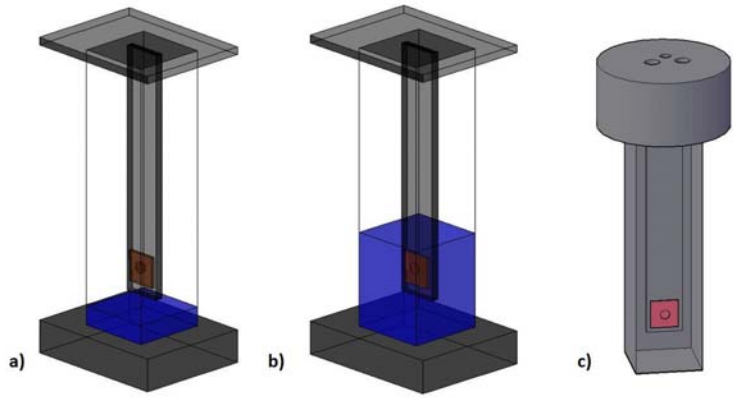


*Figure 11.* Glass cap and steel cap sensor holder operation. a) Headspace and b) in-solution sampling by glass cap sensor holder. c) Steel cap sensor holder with cuvette for special use inside temperature controller.

Fifty and 500 μM DMTS solutions were prepared using a dilution procedure similar to that shown in Table 2. A glass cuvette was cleaned by piranha solution (3 parts of concentrated sulfuric acid mixed with 1 part of 30% hydrogen peroxide)[40], rinsed with ethanol and dried in the fume hood. A preleaned SERS sensor was attached with the sensor holder by using Dow Corning vacuum grease, suspended in an empty cuvette, and mounted on a translation stage in front of the Raman probe. The distance from the SERS sensor to the laser probe was adjusted to be ~4.2 mm with the aid of calipers. (Manpinder Kaur has shown that in air the working distance of this particular Raman probe is 4.2 mm.)[41] The laser was turned on and set to a power of 10 mW. A SER spectrum was collected from the headspace of the empty cuvette (Figure 32). Then, 200 μL of ethanol was transferred into the cuvette. After the insertion, parafilm was used to seal the cuvette. The sensor was

realigned using the General Ultratech calipers. A SER spectrum was collected from the headspace above the ethanol.

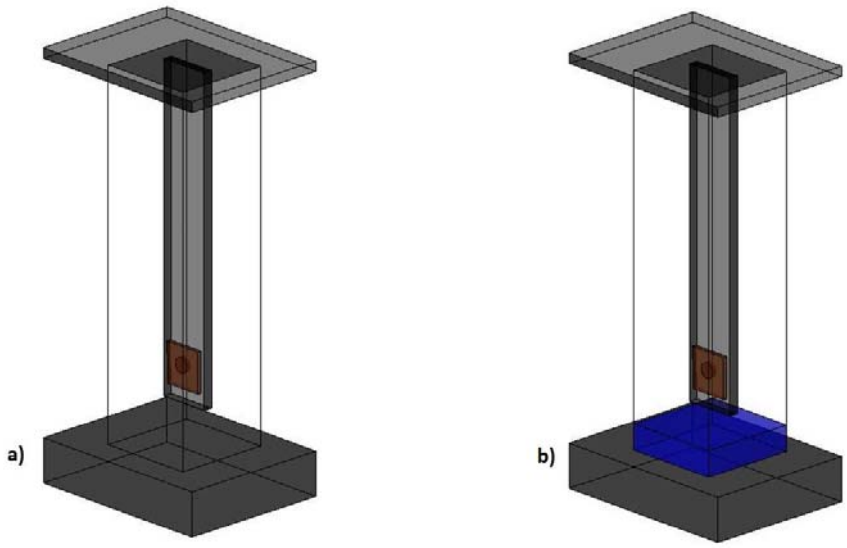


*Figure 12.* Headspace SERS sampling apparatus a) empty and b) ethanol headspace.

### *3.3.2. DMTS SERS Unstirred unheated*

The ethanol was replaced with 50 μM ethanolic DMTS solution. The cuvette was resealed with parafilm, and realigned with the calipers. Twenty minutes elapsed between the insertion of the sensor above the 50 μM ethanolic DMTS solution, and the collection of the first SERS spectrum. The time was due to the care required to do a careful alignment with the calipers. Using the same settings as had been used for the empty cuvette, and pure ethanol experiments, SERS spectra collected with the Bayspec 2020 spectrometer were saved every 5 minutes, over a period of 3 hours and 15 minutes. The 59 spectra were exported to Microsoft Excel 2016 for analysis.

Four changes were made prior to collecting SERS spectra from the headspace above the 500 μM ethanolic DMTS solution. To speed up the time between the first exposure of the sensor to the sample, and collection of the first spectrum, a steel capped

sensor holder that allowed alignment prior to sample introduction was used instead of glass capped sensor holder (described in section 3.3.4 and Figure 13, Figure 14). Grease was used in place of parafilm for sealing the cuvette. A benzenethiol (BT) coated sensor was used to align the sensor with the laser beam (described previously in the drop coated method) in place of the calipers. The laser power was lowered to 4 mW. By using the steel capped sensor holder, the interval between sampling time and first spectrum collection was shortened to 2 minutes. Using the same parameters (other than laser power), SERS spectra were collected every five minutes over a period of 17 hours 10 minutes, from the sensor placed in the headspace of the 500 μM ethanolic DMTS solution.

### *3.3.3. SERS DMTS stirred*

Ashish Tripathi and coworkers have shown that stirring hastens analyte transport to an immersed sensing surface.[24] To see if the same effect would be observed in our experiment, SERS spectra were collected from the headspace above 100 and 500 μM DMTS solutions (prepared as described in Table 2) while they were stirred.

A Quantum Northwest temperature controller was purchased to give us the ability to precisely control both stir rate and the temperature of a sample solution in a standard 1-cm pathlength cuvette. When the cuvette is placed inside this temperature controller, the cuvette position is fixed relative to the Raman probe. Since we had previously moved the entire cuvette to achieve alignment, a novel method was required to align the sensor surface to the focal spot of the Raman probe.

In order to be able to precisely manipulate the position of the sensor holder, the glass base of the T-shaped sensor holder was replaced with a steel cap that had holes for

receiving alignment pins. The detailed design of the steel-capped holder and its mechanism is shown in Figure 13 and Figure 14.

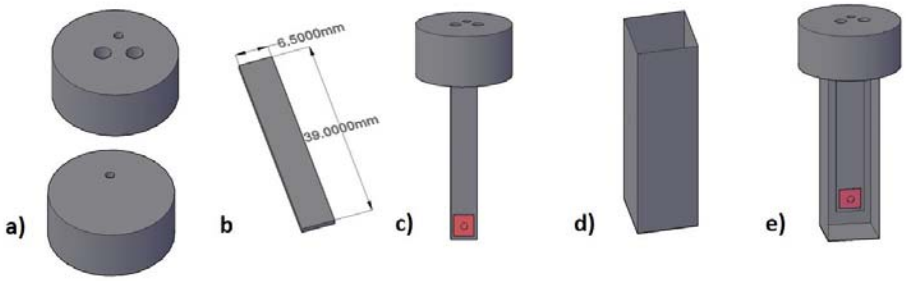


*Figure 13.* Steel cap sensor holder. a) Steel cap top and bottom view b) Previously cut glass slide as sensor holder c) Steel cap attached with the sensor holder and the sensor d) Empty cuvette e) Steel cap sensor holder inserted inside cuvette.

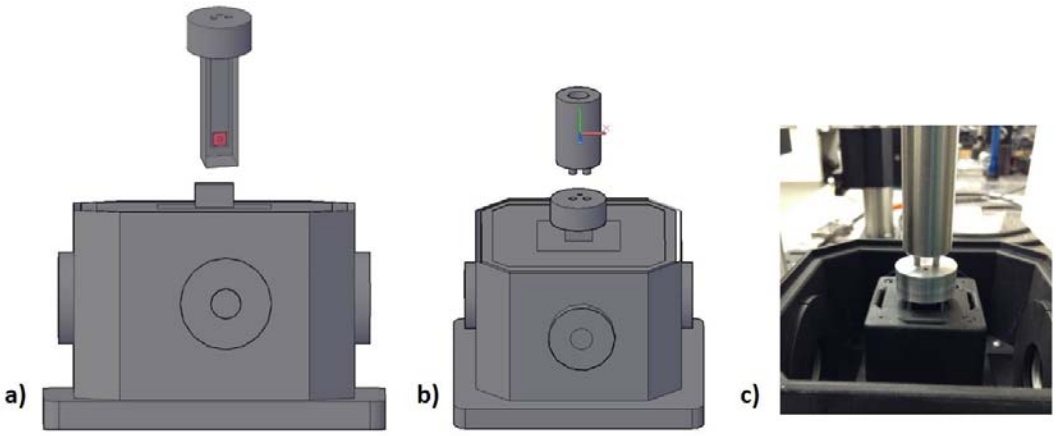


*Figure 14.* The steel cap sensor holder within temperature controller. a) Cuvette with steel cap sensor holder is inserted in the temperature controller b) steel cap manipulator was introduced; manipulator was attached to Newport 3D micrometer c) real picture of steel cap sensor holder setup.

In addition to the two alignment holes (which did not open into the cuvette), an additional sample loading hole was incorporated into the steel cap that enabled sample to be introduced into the cuvette after the alignment had been completed. Since the steel cap was designed to be translated left right and forwards and backwards to align the sensor

within the cuvette, a vapor sealing mechanism was required that had the potential to maintain a good seal as the cap was translated with respect to the top of the cuvette. For this purpose, the parafilm seals used previously were replaced with vacuum grease seals.

The seals cannot be maintained if the steel cap is lifted off of the cuvette. In order to enable the reference and analytical sensors to be translated in and out of the fixed laser beam without breaking the seal, the BT reference sensor needed to be moved from its earlier position above the analytical sensor to a side by side arrangement. The sensors are wide enough that putting two full sensors side by side in the cuvette would severely limit the amount of translation. Thus for this experiment, both a BT alignment sensor and freshly preleaned sensor were cut in two pieces that were approximately 2 mm wide. These were small enough that they could be positioned side by side, and each could be translated in and out of the probe beam as shown in Figure 15.

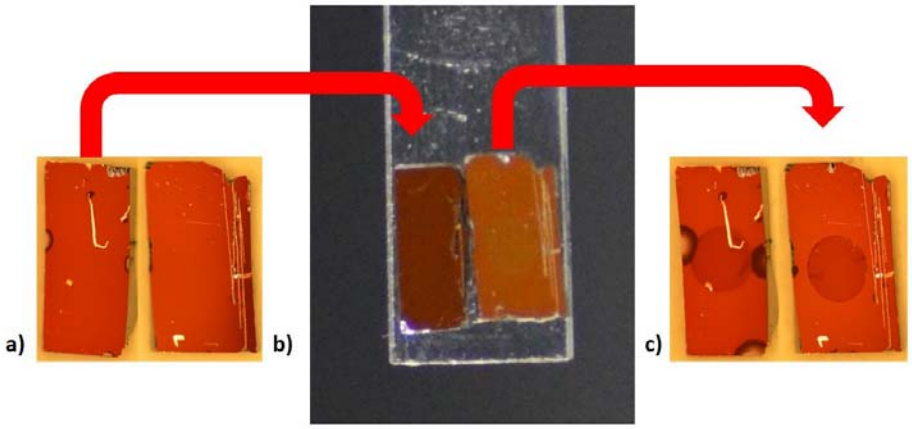


*Figure 15.* Sensor cutting. a) A Benzenethiol sensor is cut in two pieces a) One part of benzenethiol sensor was attached with the sensor holder showing by a red arrow (For experiment a different sensor was used) b) Two sensors were attached side by side, left sensor was reference benzenethiol sensor and the right one was experimental sensor c) Experimental sensor cut in two piece and used one piece for the experiment a red arrow was shown.

The sensor holder was then inserted into the temperature controller. The cap was coupled to the Newport xyz stage, and translated to place the BT sensor in the beam path. The sensor was translated along the optical axis to maximize the BT signal as previously described, and then translated orthogonally to the optical axis to bring the sensor into the focus of the Raman probe. Soon after this we realized that SERS spectra contained an Si-H stretching mode[42] at 2120 $cm^{-1}$ that was always present in the spectra from preleaned sensors, and that this peak could be used as an internal reference for aligning the sensor. This enabled the experiment to be carried out with a single preleaned, uncut sensor.

After aligning the sensor, 200 μL of 100 μM DMTS was introduced into the cuvette using the through hole. The solution was magnetically stirred at 1400 rpm. It took 2 minute to collect the first spectrum after introducing the solution into the cuvette. SERS spectra were collected at one minute intervals over a three-hour period. The laser power was set to 10 mW. The integration time of the detector was set to 5 seconds. Ten raw spectra were averaged into each saved spectrum.

The experiment was repeated with the 500 μM ethanolic DMTS solution. This experiment was moved out of the temperature controller because its opaque sides precluded visual alignment of the sensor, and because this experiment didn't require temperature control. The steel cap holder was again used to hold the sensor. The solution was stirred at 600 rpm by using a VWR magnetic stirrer. A BT reference sensor was used for alignment. Four hundred twenty-three SERS spectra were saved at intervals of ~50 seconds. The laser power in this experiment was reduced to 4 mW. The CCD integration period was 5 seconds per raw spectrum. Ten raw spectra were averaged into each saved spectrum. Data were analyzed by Microsoft Excel 2016 and discussed in the results and discussion section.

### *3.3.4. SERS DMTS heated*

Ashish Tripathi and coworker showed that elevated temperature accelerated the adsorption of benzenethiol on gold.[17] The goal of this experiment was to explore the effect of elevated temperatures on DMTS sensing. Half of a preleaned sensor and half of a BT thiol reference sensor were mounted side-by-side on the glass portion of a steel capped holder. This was placed inside a cuvette, and the cuvette was lowered into the Quantum Northwest temperature controller. The laser was turned on and set to a power of 10 mW. The BT SERS signal was used to align the sensor surface into the focal plane of the Raman probe. The holder was then translated orthogonally to the optical axis to bring the preleaned experimental sensor into the focal plane of the Raman probe. Then a Hamilton syringe was used to transfer 200 μL of 100 μM DMTS solution into the cuvette. Collection of SERS spectra was initiated, simultaneously with a temperature program that raised the temperature of the solution from 20 to 80 °C at a rate of 2 °C/min. The delay between introduction of the sample and the collection of the first SERS spectrum was 2 minutes. The CCD integration time for each raw spectrum was 5 seconds. Ten raw spectra were averaged into each saved spectrum. Spectra were saved every 60 seconds.

## 4. SERS challenges

In the 500 μM DMTS headspace SERS experiment condensation was observed on the cuvette walls. Because such condensation interferes with Raman excitation and signal collection, further experiments were carried out to test methods of mitigating the problem. Additionally, because we were concerned that DMTS might be partitioning into the vacuum grease (used for mounting sensors and sealing), a series of GCMS experiments were run to determine whether or not this was a problem.

### 4.1. Condensation

Condensation on the cuvette walls was first noted in the 500 μM DMTS headspace sampling experiment with stirring. This experiment was external to the temperature controller. When cuvettes were placed inside the temperature controller at room temperature much less condensation was observed. A set of experiments were carried out in which ethanol was incubated in a sealed cuvette surrounded by different amounts of heat conducting material: free of any holder, partially wrapped with black aluminum foil, in a Thorlabs cuvette holder with three thick blackened aluminum sides, and a fourth thinner blackened aluminum side, and with the cuvette fully surrounded on all sides by the thicker aluminum walls of the Quantum Northwest Qpod temperature controller. In each set of conditions photographs were taken after incubation to assess how much condensation formed.

Experiments were also carried out in collaboration with SHSU undergraduate researcher Reece Thompson to explore the possibility of heating a cuvette window to keep it condensation free. A glass microscope slide coated with indium tin oxide (ITO) on one side, and having an electrical resistance of 15-25 $\Omega/cm^2$ was attached to the optical window of a glass cuvette using double sided tape with the ITO side facing the cuvette (Figure 16).

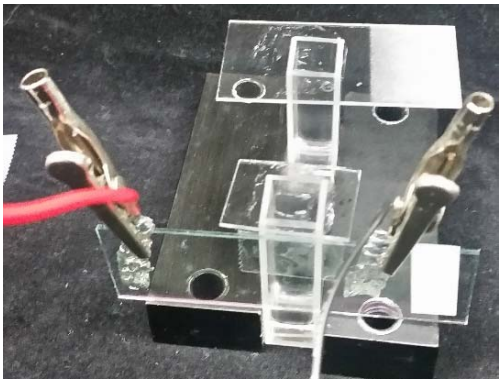

*Figure 16.* Indium tin oxide window is attached with cuvette window by alligator clips.

After adding 500 μL of ethanol to the cuvette, the top was sealed using grease and a piece of glass. A second sealed cuvette containing 500 μL of ethanol served as a control. After 2 hours, an abundant amount of condensation was present on the walls of both cuvettes. Two AA batteries were wired in series across the ITO coated slide using alligator clips over aluminum foil (added to improve uniformity of contact) to deliver 51.3 mA of warming current. IR camera images were taken to see if the ITO was heating evenly. Photographs were taken of the cuvette wall before and after heating. After 30 minutes, the temperature of the solution in each cuvette was taken by placing a thermometer inside the solution in each cuvette, and allowing the temperature to stabilize for 5 minutes. In both cuvettes, the temperature of the solution was found to be 22°C. Thermal mass of the thermometer was likely greater than the measured value. A small thermocouple may provide more accurate reading.

### 4.2.Grease challenge

We were concerned that the grease used to attach sensors and to seal the cuvettes might provide a sink into which DMTS could partition. A GC-MS experiment was carried out to see if DMTS was being lost to the grease.

Ten 2.0-ml crimp top vials were chosen for this experiment. Five vials were used for a control experiment on the first day that employed no grease. On the second day the experiment was repeated with vacuum grease. Photographs of representative vials from the control and experimental groups are shown in Figure 17.

A 0.50 mL aliquot of 500 μM DMTS solution was added to each vial. The vials were crimp sealed, with caps having PTFE (polytetraflouroethylene) septa on the sample

side. Immediately, a solid phase microextraction (SPME) fiber was inserted into the first glass vial (0-minute incubation).

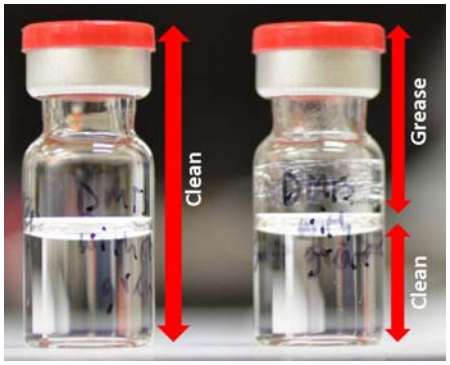


*Figure 17.* Clean and grease smeared vial with DMTS solution inside. There was no contact between the grease and solution.

After 5 minutes of sampling the SPME fiber was retracted, inserted in GC-MS injection port and a total ion chromatogram was collected. The injection temperature was maintained at 300 °C. The initial oven temperature was held at 35 °C for 3 minute, ramped at 10 °C/min to 220 °C, and held at 220 °C for 5 minute.

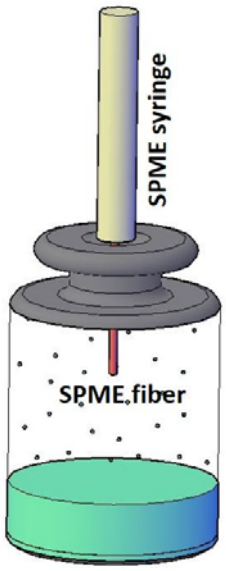


*Figure 18.* SPME extraction scheme.

Vials 2, 3, 4, and 5 were sampled by SPME, respectively 46, 80, 140, 185-min after the initial addition of solution. GC-MS analysis of each sample was carried out using parameters that were identical to those used for the 0-minute chromatogram. An empty vial that had been smeared with grease, and crimp sealed served as the first control sample. A second control contained only ethanol. Both control samples were SPME sampled, and analyzed by GC-MS in an identical manner to the 500 μM DMTS samples. Data are shown in Figure 43.

On the second day, the experiment, was repeated with one important change: grease sealing was used. Dow Corning vacuum grease was smeared inside and on top of the sealing edge of the 5 new vials. The mass of grease added to each vial was determined by subtracting the vial mass before, from the vial mass after application of grease. Weighings were carried out on an Ohaus Explorer Pro analytical balance. In the experiment with grease the sampling times were slightly shift to 0, 50, 95, 145, and 180-minutes after the addition of 500 μM ethanolic DMTS solution. Data are shown in Figure 44. All chromatograms were analyzed in Microsoft Excel 2016.

**5. Detection of DMTS reduction product**

One way of potentially accelerating headspace detection of DMTS, is to chemically reduce DMTS to yield more volatile products like methyl mercaptan and hydrogen sulfide. Because both methyl mercaptan and hydrogen sulfide are gases at room temperature, they are expected to partition into the headspace more rapidly and to have much higher equilibrium partial pressures than DMTS. Since thiols have been shown to adsorb more rapidly to noble metals than sulfanes,[23] the fraction of collisions with the SERS sensor that result in binding should also be higher for the reduction products. Because both methyl

mercaptan and hydrogen sulfide are toxic to humans, care was taken to use sample amounts that were low enough to be safe. As an additional safety precaution all of the sample preparation, and ordinary Raman and SERS experiments described in this section were carried out inside a fume hood. Three reducing agents were tested: iron (II) chloride ($FeCl_2$), sodium borohydride ($NaBH_4$) and dithiothreitol ($C_4H_{10}O_2S_2$) or (DTT).

### 5.1. Iron(II) chloride ($FeCl_2$)

Three experiments were carried out to explore the potential of using $FeCl_2$ as a reducing agent for DMTS. $FeCl_2$ was chosen because it was readily available, and because other experiments carried out by Xinmei Dong in our lab were lending support to the hypothesis that DMTS in blood is reduced by the heme iron of hemoglobin. A possible chemical reaction for reducing DMTS with Fe(II) to produce methyl mercaptan and hydrogen sulfide is shown below:

$$CH_3\text{-}S\text{-}S\text{-}S\text{-}CH_3 + 4\ Fe^{2+} + 4\ H^+ \rightarrow 2CH_3\text{-}SH + H_2S + 4\ Fe^{3+}$$

Gas chromatography, ordinary Raman and SERS were employed to study reaction mixtures of $FeCl_2$ and DMTS.

#### *5.1.1. GC analysis*

GC-MS method was initially utilized to test the reduction of DMTS by $FeCl_2$. The mole ratio of DMTS: $FeCl_2$: HCl needs to be 1.0: 2.0: 2.0 if each DMTS is to be reductively cleaved once, and 1:4:4 if each DMTS is to be reductively cleaved twice as shown in the hypothetical reaction above. Two reduction experiments were run in which DMTS, $FeCl_2$, and HCl were mixed in a 1.0: 10.0: 10.0 mole ratio that ensured that DMTS was the limiting reagent.

A 5000 and a 10000 μM $FeCl_2$ stock solution were prepared by diluting, respectively 6.5 and 13 mg of solid $FeCl_2$ (1 mol $FeCl_2$/126.751 g $FeCl_2$) to 10.0 mL. A 5000 and a 10000 μM HCl stock solution were prepared by diluting, respectively, 520 and 1040 μL of 0.096 M (stock) HCl solution to 10.0 mL. A 500 and a 1000 μM DMTS solution were prepared as described previously in Table 2. All dilutions were carried out with ethanol using class A volumetric flasks. After dilution all flasks were vortexed one minute and inverted twenty times to ensure good mixing. The solution turned to pale yellow color.

Sixty microliters each of the 5000 μM $FeCl_2$ and 5000 μM HCl solutions were added to a 2.0 mL headspace sampling vial. The vial was crimp sealed with a PTFE (polytetraflouroethylene) septa held between the cap and the vial. Then 60 μL of 500 μM DMTS solution was injected through the crimped septa into the vial using a 100 μL Hamilton syringe. After 40 minutes of incubation, a 400 μL sample of the headspace gas in the vial was collected by a 500 μL Hamilton sample lock gas syringe. This 400 μL sample was compressed to 250 μL and then injected into the Agilent GC-MS. A split less injection was used with an inlet temperature of 110 °C. The oven temperature was held at 35 °C for 3 minutes, ramped at 10 °C/min to 150 °C, held at 150 °C for 5 minute, ramped at 20 °C/min to 220 °C, and held at 220 °C for 3 minutes. Before the reaction headspace run, 400 μL air of the lab was collected and run as control. This experiment was repeated a second time as described above with one important change: the concentrations of $FeCl_2$, HCl and DMTS were doubled, respectively, to 10000, 10000, and 1000 μM. The chromatograms of the headspace gas from the original $FeCl_2$ reduction vial, and from the doubled concentration vial are shown in Figure 47.

Control samples were gathered from vials containing, respectively: 60 μL of 10000 μM DMTS; 60 μL of 500 μM DMTS; 60 μL of 500 μM DMTS mixed with 60 μL of 5000 μM $FeCl_2$; 60 μL of 500 μM DMTS mixed with 60 μL of 5000 μM HCl (data not shown); and 60 μL of 5000 μM $FeCl_2$ mixed with 60 μL 5000 μM HCl. The headspace gas samples were gathered from each control vial 40 minutes after crimping, and were analyzed by GC-MS using the same program as was used to analyze the gas samples from the $FeCl_2$/DMTS reduction experiments. The data from the control experiments is shown in Figure 46.

### *5.1.2. Ordinary Raman*

After the GC-MS experiment, an unenhanced Raman experiment was used to study the reduction of DMTS by $FeCl_2$. Because of the lower sensitivity of unenhanced Raman, a higher DMTS concentration of 0.50 M was used in these experiments. Both methyl mercaptan and hydrogen sulfide are gases, having boiling points respectively of -60.55 and 6.11 °C.[43,44] Because both are toxins, the maximum amounts of each that could be produced under the proposed conditions of this experiment were calculated assuming a case in which 1 mol of DMTS would produce 3 moles of either methyl mercaptan or hydrogen sulfide. The calculations are shown in the appendix. The total production in the experiments as designed falls below the lower limit of permissible exposure.[44,43] Nonetheless, to add an extra measure of safety, all sample handling and Raman experiments were carried out inside the fume hood.

A 0.50 M DMTS stock solution was prepared as described in Table 2. A 1.0 M $FeCl_2$ stock solution was prepared by dissolving 1.3 g $FeCl_2$ (1 mol $FeCl_2$/126.751 g $FeCl_2$) to 10.0-mL. A 1.0 M HCl stock solution was prepared by diluting 828 μL of 37% (w/w) aq HCl (density of 37% HCl is 1.2 g/mL) to 10.0-mL. All dilutions were carried out with

ethanol using class A volumetric flasks. After dilution all flasks were vortexed one minute and inverted twenty times to ensure good mixing. No extra caution was taken to minimize oxygen exposure.

A 200 μL aliquot of each stock solution was added to a glass cuvette inside the fume hood. This ~600 μL mixture was illuminated with the 785 nm laser using 10 mW of power. Raman spectra were gathered as a function of time. The CCD integration time was 5 seconds for each raw spectrum. Ten raw spectra were averaged into each saved spectrum. Immediately following this experiment, Raman spectra were collected from a control mixture containing 200 μL of 0.50 M DMTS and 383 μL of ethanol.

### *5.1.3. SERS*

Following the GC-MS, and unenhanced Raman experiments, the final experiment used to study the reduction of DMTS by $FeCl_2$ was a headspace sampled SERS experiment. In this experiment, 100 μM ethanolic DMTS solution was mixed with 1000 μM aq $FeCl_2$ and 1000 μM aq HCl.

A 100 μM ethanolic DMTS solution was prepared as described in Table 2. A 1000 μM $FeCl_2$ solution was prepared in by dissolving 6.5 mg $FeCl_2$ to 50.0 mL with DI water. A 1000 μM HCl solution was prepared by diluting 525 μL of 0.096 M HCl to 50.0 mL with water.

A preleaned SERS sensor was mounted on a steel capped sensor holder and suspended in a cuvette. The cuvette was placed in the Qpod 2e temperature controller. Previously a benzenethiol sensor was used for the sensor alignment with the Raman laser beam. In this experiment a Newell Sharpie permanent marker was used to deposit ink on the side of the experimental sensor. At 203 $cm^{-1}$ the Sharpie ink gives a sharp peak (data

not shown). Using this peak the sensor was positioned into the focal plane of the Raman probe. The sample holder was then translated orthogonally to place an unexposed sensing region into the focus of the Raman excitation laser.

Following this alignment, 60 μL of $FeCl_2$, HCl and DMTS were introduced sequentially into the cuvette. The solution was stirred at a rate of 1400 rpm using a magnetic stirrer. SERS Spectra were collected as a function of time using 3 mW laser power. The CCD integration time was set at 5 seconds per raw spectrum. Five raw spectra were averaged into each saved spectrum.

## 5.2. Sodium borohydride ($NaBH_4$)

We originally thought that reduction by $FeCl_2$ was slow. So, a stronger reducing agent was needed. Hence, sodium borohydride was chosen for this experiment. Both ordinary and SERS experiments were carried out to study the reduction of DMTS by $NaBH_4$.

### *5.2.1. Ordinary Raman*

Reduction experiment by $NaBH_4$ is similar with $FeCl_2$ reduction. Only $NaBH_4$ was used instead of $FeCl_2$. A 1.0 M $NaBH_4$ solution was prepared by diluting 0.4 g $NaBH_4$ (1 mol $NaBH_4$/37.83 g $NaBH_4$) with ethanol to 10.0-mL in a volumetric flask. Two Raman experiments were carried out. In the first experiment, 200 μL of 1.0 M $NaBH_4$ was added to 200 μL of 0.50 M DMTS in a cuvette in the hood. Spectra were collected for 22 minute using a 10 mW laser power. The CCD integration time was set at 5 seconds per raw spectrum. Ten raw spectra were averaged into each saved spectrum. The spectra gathered in this experiment are shown in Figure 51. In the second experiment the reduction reaction was carried out under acidic conditions. Raman spectra were gathered from a mixture of

200 μL of 0.50 M DMTS, 200 μL of 1.0 M $NaBH_4$ with 200 μL of 1.0 M HCl. Spectra were  were collected for 10 hours, using the same instrumental settings as were used for the nonacidified reaction.  A subset of this data is shown in Figure 52.

#### *5.2.2. SERS*

During the ordinary Raman experiment a strong smell was sensed, which is different from DMTS itself. That is a substantial proof of either producing methyl mercaptan ($CH_3$-SH), hydrogen sulfide ($H_2S$) or disulfide compound. In this experiment reduction by sodium borohydride ($NaBH_4$) was analyzed by headspace SERS sampling. For this experiment no acid was used.

A 500 μM DMTS solution was prepared as described in Table 2. A 1000 μM $NaBH_4$ solution was prepared by diluting 4.3 mg $NaBH_4$ (1 mol $NaBH_4$/37.83 g $NaBH_4$) to 10.0 mL. Previously sensor nanopillar leaning was carried out by evaporation of 5.0 μL type-1 DI water from a sensor. This evaporation differed from all others in this thesis because it was carried out in an oven for 30 minute at 110 °C, rather than under ambient conditions in the lab. The preleaned sensor was mounted on the steel capped sensor holder, suspended in a cuvette, and aligned into the focal plane of the Raman probe. Then 60 μL of 1.0 M $NaBH_4$ and 60 μL of 0.50 M DMTS were introduced into the cuvette through the hole of the steel cap. Raw spectra were collected as a function of time at 4 mW laser power and 5 second integration time. Ten raw spectra were averaged into each saved spectrum.

### 5.3. Dithiothreitol (DTT)

$FeCl_2$ is a relatively weak, and $NaBH_4$ is a very strong reducing agent. In this experiment, dithiothreitol (DTT) was tested as a reagent with the potential to provide rapid reduction without generating elemental sulfur. It has been found, that disulfide reduction

by dithiothreitol happens in a minute at pH of 8.[45] Both ordinary Raman and SERS experiments were used to study the reduction of DMTS by DTT.

### *5.3.1. Ordinary Raman*

In the analysis of the reduction by DTT, 0.15 M DMTS was reacted with 0.20 M DTT and NaOH. 0.15 M DMTS is prepared by taking 3 ml of 0.50 M DMTS and diluted with ethanol up to 10 mL in a volumetric flask. 0.50 M DMTS was prepared by the previously described method. The flask is vortexed for one minute and inverted 20 times. To prepare 0.20 M DTT, 0.3089 g DTT was (1 mol DTT/ 154.25 g DTT) added to ethanol in a 10.0-mL volumetric flask and diluted with ethanol up to 10 mL mark and vortexed for 1 minute and inverted 20 times. To prepare 0.20 M NaOH, 0.0834 g NaOH (1 mol NaOH/39.9971 g NaOH) was added to 10.0 mL volumetric flask and diluted with ethanol up to 10.0 mL mark and vortexed for 1 minute and inverted 20 times. After three solutions were prepared 200 µL of each solution were mixed in a cuvette. Then Raman spectra were collected immediately after mixing the solution. By using a benchtop Agility Raman spectrometer, the laser was controlled at 480 mW with 1.5 second integration time 10 spectra were averaged to store as one spectrum. And the pH was measured to be 8.5 using McolorpHast pH-indicator strips. After the experiment the solution is stored in a waste container. Then the cuvette was rinsed with ethanol. Subsequently, control experiments were carried out by mixing DMTS, DTT, NaOH and ethanol (EtOH) at different combinations. At first 200 µL of DMTS is added with 200 µL DTT and NaOH then spectrum was collected from that solution mixture. Similarly, solutions are mixed with the order it shows: DMTS + NaOH + EtOH 200 µL of each; DTT + NaOH + EtOH 200 µL each; DMTS + EtOH + EtOH 200 µL each.

All Raman spectra were collected with the Bayspec 2020, rather than the Agility spectrometer because of its superior resolution. Data are shown in Figure 54.

### *5.3.2. SERS*

The unenhanced Raman study was followed by a headspace SERS experiment. To maintain a similar concentration ratio with the ordinary Raman analysis 1500 μM DMTS solution was reacted with 2000 μM DTT and NaOH solution.

A 1500 μM DMTS solution was prepared by diluting 3.0 mL of 0.0050 M DMTS (Table 2) to 10 mL with ethanol. A 0.020 M DTT solution was prepared by diluting 30.80 mg DTT (1 mol DTT/ 154.25 g DTT) to 10.0 mL with ethanol. Then 1.0 mL of 0.020 M DTT solution was diluted to a 10.0 mL with ethanol to prepare the 2000 μM DTT solution. Similarly, a 0.020 M NaOH solution was prepared by dissolving 8.1 mg NaOH to 10.0 mL with ethanol. Then 1.0 mL of the 0.020 M NaOH solution was diluted to 10.0 mL with ethanol to prepare the 2000 μM NaOH solution.

A preleaned sensor mounted to a steel capped holder was suspended inside a cuvette. A BT reference alignment sensor mounted above the preleaned sensor was used to align the sensors into the focal plane of the Raman probe. An indium tin oxide (ITO) glass slide was mounted to the cuvette as shown in Figure 19.

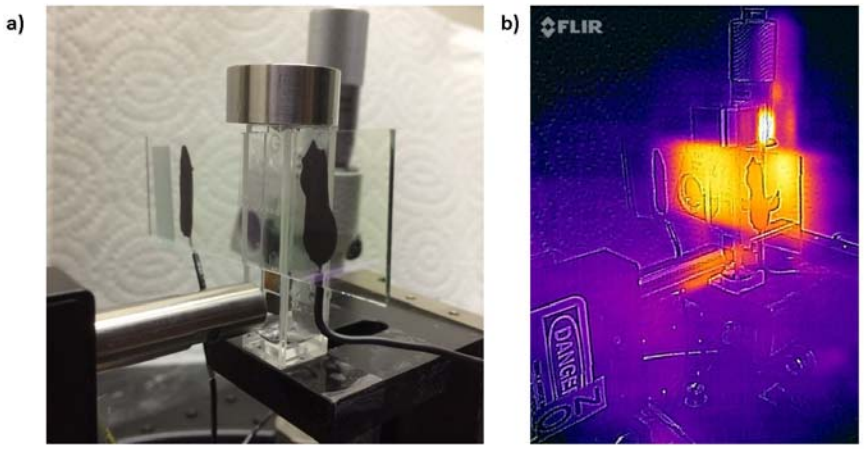


*Figure 19.* SERS reduction by DTT experimental setup. a) The setup for collecting SERS signal at 10 mWs 5 second integration time and 10 spectral average. b) IR picture of the ITO window to maintain the cuvette window condensation free.

Two AA batteries wired in series provided a 51.3 mA current across the ITO slide. The purpose of this current was to prevent condensation on the cuvette wall by gently warming it. SERS spectra were collected through the warmed cuvette wall using an excitation laser power of 10 mW. Raw spectra were collected using a 5 second CCD integration time. Ten spectra were averaged into each saved spectrum. After the collection of spectra had been initiated, a 100 µL Hamilton syringe was used to introduce 66.67 µL of 2000 µM DTT through the access port of the steel cap into the cuvette. This was followed immediately with 66.67 µL of 2000 µM NaOH and 66.67 µL of 1500 µM DMTS. The access port was then sealed with Dow corning vacuum grease and covered with a microscope cover glass slide. SERS spectra were collected continuously before, during, and after the sample introduction. A total of 103 SERS scans were saved for analysis.

# CHAPTER III

## Results and discussion

### 1. DMTS Raman spectra

#### 1.1. Calculated DMTS Raman spectrum.

Raman spectra of DMTS and methyl mercaptan (MeSH) were calculated using the Hartree-Fock method in GaussView 5.0 software. A Raman spectrum of pure DMTS was collected for comparison. These calculated and experimental spectra are shown in Figure 20. The methyl mercaptan spectrum was modeled as a potential product of DMTS reduction reactions that is expected to partition more rapidly than DMTS into the headspace.

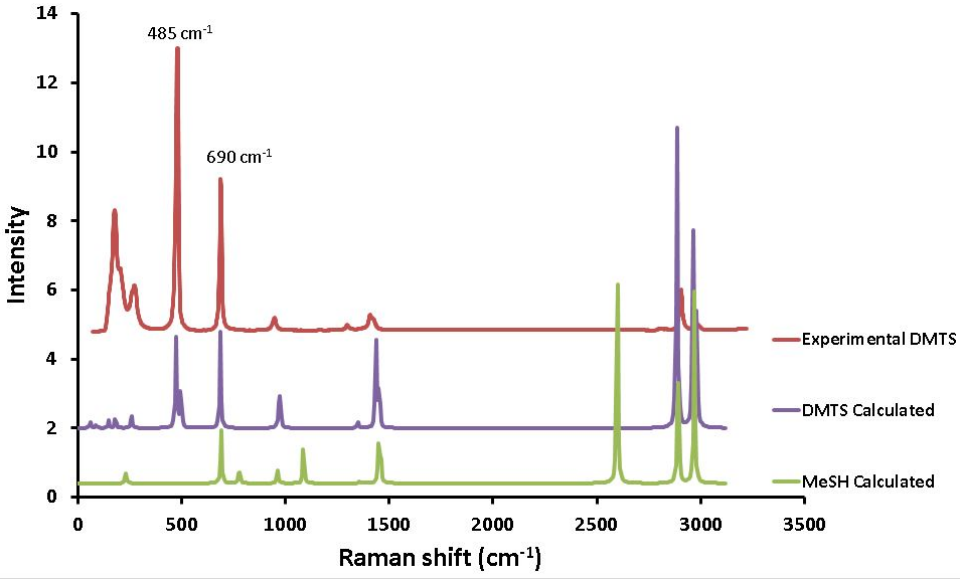


*Figure 20.* Gaussview 05 calculated and experimental Raman spectrum comparison. DMTS and MeSH Raman spectra were calculated by the Hartree-Fock method by using GaussView 5.0 software. Ordinary Raman spectrum of pure DMTS was collected at 20 mW laser power with 5 second integration time and 10 spectral average (scaled to fit with calculated spectrum).

The trisulfide (SSS), and carbon sulfur (CS) stretches were the vibrations of greatest initial interest for this work. The SSS symmetric and asymmetric stretches generally fall near 460

and 490 $cm^{-1}$,[46,29] and symmetric stretch is seen here in both the calculated and measured DMTS spectra. As expected these SSS stretches are absent from the calculated MeSH spectrum. CS stretches are generally observed between 620 and 730 $cm^{-1}$ in primary aliphatic disulfides,[30] and are observed in all three of these spectra near 690 $cm^{-1}$. The peaks at the lower energy of the spectrum arise from less characteristic vibrations.

**1.2. Determining the limit of detection for DMTS with Raman spectroscopy.**

A key goal of this study is to develop a sensitive and selective method for detecting DMTS at low concentrations from aqueous biological solutions such as blood, and saliva. However, the relatively low solubility of DMTS in water (0.15 ± 0.01 mg/ml at 25° C),[47] limits the concentration range for unenhanced Raman experiments. The experiments in this thesis employed ethanolic solutions because the higher solubility of DMTS in ethanol enables experiments to be carried out over a wide range of concentrations.

The first experiment was to determine the limits of detection and quantitation for DMTS on our equipment using unenhanced Raman spectroscopy.

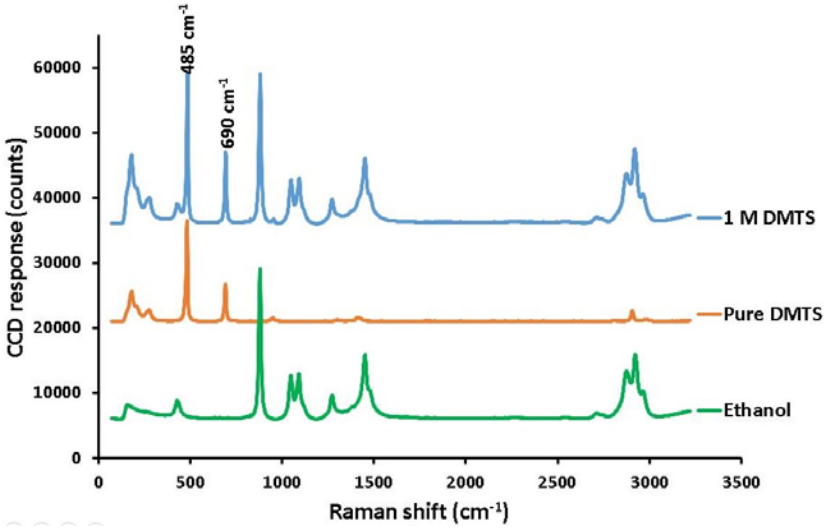


*Figure 21.* Ordinary Raman spectrum comparison. 1 M DTMS and ethanol spectrum was taken at 31.6 mW laser power and pure DMTS spectrum was taken at 3 mW.

The control spectra collected for ethanol, DMTS, and an ethanolic solution of DMTS are shown in Figure 21. Ethanol has a broad peak centered at 430 $cm^{-1}$ whose shoulder overlaps the peak arising from the SSS stretch in DMTS at 485 $cm^{-1}$. The DMTS peak arising from the CS stretch at 690 $cm^{-1}$ has no interferences from the ethanol spectrum. At the lower energy region of the spectrum, the signature feature of DMTS also shows up and can be clearly differentiated from ethanol. Due to the fact that there is less intensity compared to features at 485 and 690 $cm^{-1}$, these peaks were not initially targeted for analyses, although we later found interesting responses suggesting that these peaks should be further studied.

The Raman spectra of ethanolic DMTS calibration standards ranging from 0.010 to 1.0 M were collected (Figure 22a). A sum of Gaussian functions was fit to each spectrum in Microsoft Excel (Eq. 20). A representative fit is shown in Figure 22b.

*Eq. 20*

$$y = h_{P1}e^{-\frac{1}{2}\left\langle\frac{x-x_{P1}}{s_{P1}}\right\rangle^2} + h_{P2}e^{-\frac{1}{2}\left\langle\frac{x-x_{P2}}{s_{P2}}\right\rangle^2} + h_{P3}e^{-\frac{1}{2}\left\langle\frac{x-x_{P3}}{s_{P3}}\right\rangle^2} + Ax^2 + Bx + C$$

The areas under the SSS and CS peaks at 485 and 690 $cm^{-1}$ were calculated by integrating the corresponding Gaussian fitting functions as shown in Eq. 21, and plotted vs. DMTS concentration.

*Eq. 21* $$Peak\ area = h_{max}s\sqrt{2\pi}$$

As seen in Figure 22c, the Raman signal increases linearly with DMTS concentration.

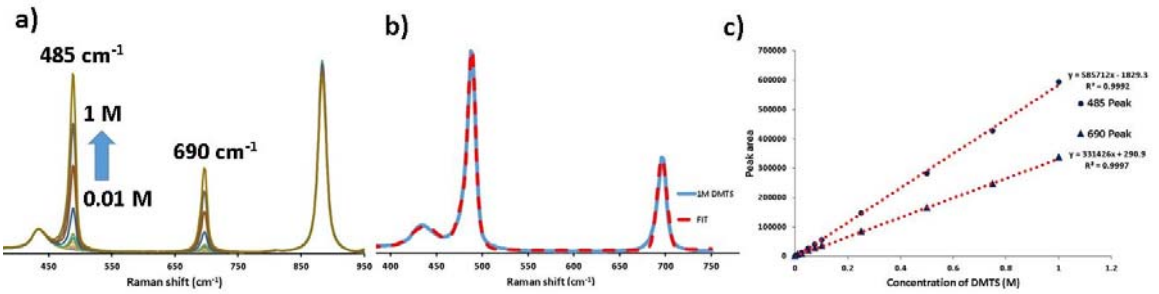


*Figure 22.* DMTS ordinary Raman peaks and Gaussian peak area calculation. a) Different concentrated DMTS peaks. b) Gaussian fit of 1 M DMTS blue represent the original spectrum and red represent Gaussian fit. c) Peak area vs concentration graph. Laser power: 480 mW, integration time: 1.5 s, raw spectra averaged per saved spectrum: 10.

The limits of detection and quantitation were found to be 0.040 and 0.10 M for the 485 $cm^{-1}$ data. Even though the absolute peak areas were smaller, improved limits of detection and quantitation of 0.020 and 0.060 M were found for the 690 $cm^{-1}$ data. These improvements are most likely due to the cleaner background subtraction associated with the absence of interfering ethanol peaks near 690 $cm^{-1}$.

**2. Laser power calibration, warm-up time, and stability**

During drop coating and headspace sampling experiments, the laser was used for extended periods while a sequence of spectra are collected. An example would be a SERS experiment to follow the kinetics associated with the binding of DMTS to gold nanoparticles. For such experiments, it is important to tune the laser power accurately. Figure 23 a shows the output power at the sample position as a function of the Thorlabs laser diode current. This data provides us with a means of initially setting the laser power in each experiment by careful adjustments of the diode current. To test for warm up drift, the laser power was followed out from a cold start at 10mW power over a period of 80 minutes as shown in Figure 23 b.

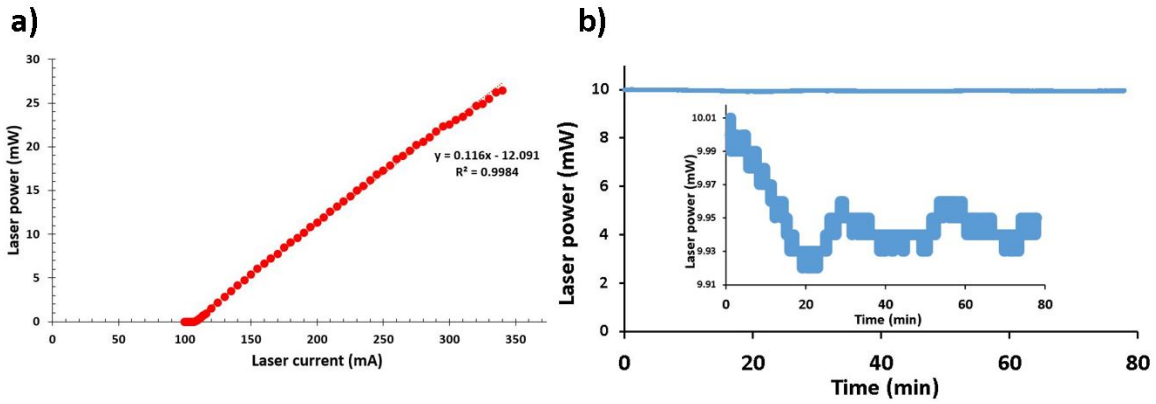


*Figure 23.* Laser power test. a) Laser power vs laser current graph. b) Laser power vs time graphs to test stability at 10 mW laser power. Inset expansion.

Based on this data, the warm up period from a cold start is about 20 minutes, and after this the coefficient of laser power variation was found to be 0.2%. The coefficient of variation was subsequently replicated in other experiments whose data is not shown here.

## 3. SERS experiments

In order to map out the SERS response to DMTS, and to compare with prior data obtained by Hossain, distinct sets of SERS sensors were exposed to DMTS via drop coating, immersion in DMTS solution, and sampling in the headspace above a DMTS solution. The SERS data obtained following exposure by these methods is presented in this section.

### 3.1. Drop coated SERS

In the drop coating experiment a 2 μL drop of ethanolic DMTS solution was deposited on a SERS sensor, allowed to evaporate, and then a SERS spectrum was collected. Another 2 μL drop was applied to the dried area of the prior drop, allowed to evaporate, and then another SERS spectrum was collected. This cycle was repeated two more times, so that the final SERS spectrum was of a sensor that had been exposed to 8 μL

of DMTS solution. The same experiment was carried out for a series of solutions, all of which had DMTS concentrations below the 20 mM detection limit that we obtained for ordinary Raman detection of DMTS. The last SERS spectra collected for each DMTS standard are plotted in Figure 24.

A notable feature of this drop-coated SERS data is that the peak at 475 $cm^{-1}$ arising from the SSS stretch is absent (or very weak) in all but the 5000 µM SERS spectrum. The delayed appearance of the SSS stretch is likely due to an initial binding geometry in which the DMTS molecules lie down. In this geometry, interactions between multiple sulfurs in a single molecule with gold are likely to inhibit stretching.

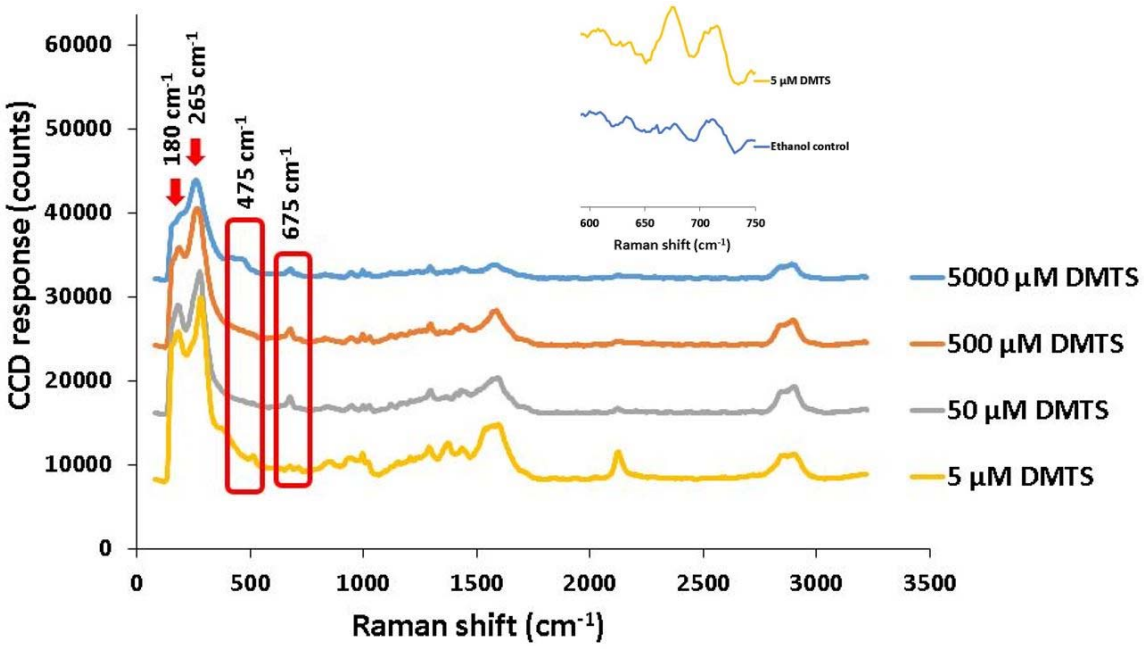


*Figure 24.* Drop coating SERS experiment. Inset 5 µM DMTS 675 $cm^{-1}$ is shown by zooming in on the data with an ethanol control. Laser power: 4 mW, integration time: 5 s, raw spectra averaged per saved spectrum: 10.

At higher concentrations, self-assembled monolayers form, lifting one end of the DMTS molecules off of the surface into a configuration that no longer inhibits the SSS stretch.[25] This delayed growth of the SSS peak observed in the drop-coated SERS

experiments stands in contrast to the unenhanced Raman spectra of DMTS in solution, where the SSS stretches are unconstrained and prominent in all spectra.

The 2120 $cm^{-1}$ peak is associated with a Si-H stretching mode.[42] The attenuation of the 2120 $cm^{-1}$ peak with increasing concentration (Figure 24), and with increasing number of drops deposited (Figure 25) is striking. This peak appears upon preleaning. The origin of the peak may be due to the increased exposure of silicon stems of the nanopillars to the laser. Another potential explanation would be that some small silanes on the sensor surface are solubilized, and transported to the SERS hotspots in the preleaning process. If the first hypothesis is correct, then the attenuation of this stretch with increasing exposure may indicate that DMTS deposits on the pillars and masks the Si-H stretch, or that its binding leads to some deleaning of pillars, or both. If the second hypothesis is correct, then the attenuation is likely due to DMTS molecules displacing silanes from hotspots in the gold. Both hypotheses suggest that the interactions causing the drop in Si-H signal are likely to be non-specific, and reproducible with analytes other than DMTS.

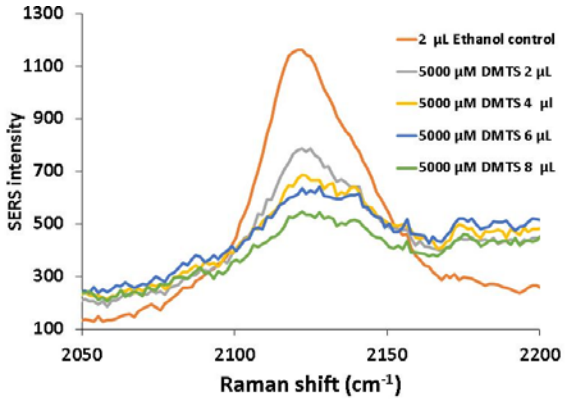


*Figure 25.* Attenuation of the SiH stretch with DMTS exposure. The peak at 2120 $cm^{-1}$ is observed to be systematically attenuated as repeated 2 mL aliquots of DMTS are applied to, and evaporated from, the same region on a specific sensor.

The CS stretch at 675 $cm^{-1}$ shows up clearly at all four concentrations (5 to 5000 µM). The presence of the CS stretch in all of these spectra suggests that drop-coated SERS

improves the DMTS limit of detection approximately a thousand-fold (from ~20 mM to ~5 μM) over unenhanced Raman.

Although these drop-coated SERS experiments clearly outperform unenhanced Raman experiments in terms of sensitivity, the reverse appears to be true with quantitation based on the CS stretch. The unenhanced Raman signals from the CS stretch are linearly correlated with concentration (Figure 22c). The same cannot be said of the CS peak areas in these preliminary drop-coated SERS spectra. If the response were linear, then the area of the CS peak in the SERS spectra would increase 10-fold with each new sample. Systematic growth in the peak area is observed between the 5 and 50 μM samples as expected. However, CS peak area increases less than 10-fold between 50 and 500 μM spectra, and decreases between 500 and 5000 μM spectra.

Why do the CS peak areas exhibit a nonlinear response over the concentration range of the standards? At 50 μM it is likely that the sensor is saturated with DMTS, and saturation explains why the 500 μM spectrum shows little increase in the area of the CS peak. The evaporation of the 8.0 μL of 5000 μM DMTS deposits far more DMTS that can be bound to the gold for surface enhancement. The excess DMTS is likely deposited as a film over the gold bound DMTS, which masks both the laser illumination of, and the SERS signal from, the underlying gold-bound DMTS. This provides a potential explanation for the drop in the area of the CS peak in the 5000 relative to the 500 μM solution. An alternate explanation is that this sensor was not properly positioned at the focal spot of the laser probe beam. This alternate explanation is possible, but unlikely, because the sensor was positioned in each experiment following a careful protocol that found the focal spot of the laser using a benzene thiol coated reference sensor.

Although the response of the CS peak appears to have been strongly affected by saturation effects in these experiments, spectral changes at lower frequencies in Figure 24 show monotonic correlations with concentration: peak intensities at 180 and 265 $cm^{-1}$ showed, respectively, systematic decreases and systematic increases with DMTS concentration. Prior reports suggest that the 180 $cm^{-1}$ peak may arise from the bending mode of Au-S-C, and that the 265 $cm^{-1}$ peak is likely due to the radial Au-S stretching modes which generally appear in the 220-280 $cm^{-1}$ range.[48] The ordinary Raman signal from DMTS also provides signals in the 220-280 $cm^{-1}$ range that are not analyzed extensively.

In their quantitative determination of hydrogen peroxide by SERS in a living cell, Xin Gu et al. reported that the ratio of an increasing to a decreasing peak correlated linearly with the logarithm of the concentration.[49] Following this example, the ratio of areas of the 265 and 180 wavenumber peaks were plotted versus the number of drops applied. The resulting plot is shown in Figure 26. Saturation effects are apparent in the 5000 μM plot, however the 500 μM data shows good linearity through 6.0 μL, and the slight onset of saturation only after evaporation of the fourth 2.0 μL aliquot.

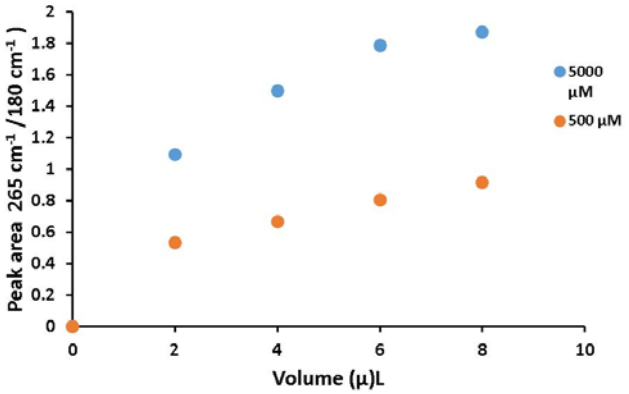


*Figure 26.* Peak ratio of 265 $cm^{-1}$/ 180 $cm^{-1}$ vs volume graph. The data is shown for 500 and 5000 μM DMTS.

A second plot, Figure 27, was prepared in which the ratio of the 265 and 180 wavenumber peak areas were plotted versus $\log_{10}$[DMTS]. The linearity of the 2.0-µL line is striking, while the curves associated with higher doses at each concentration (see the 6-µL line in Figure 27b) show an upward curvature that is likely the consequence of saturation effects. Development of a model that explains this logarithmic relationship in terms of transport and kinetic principles is ongoing.

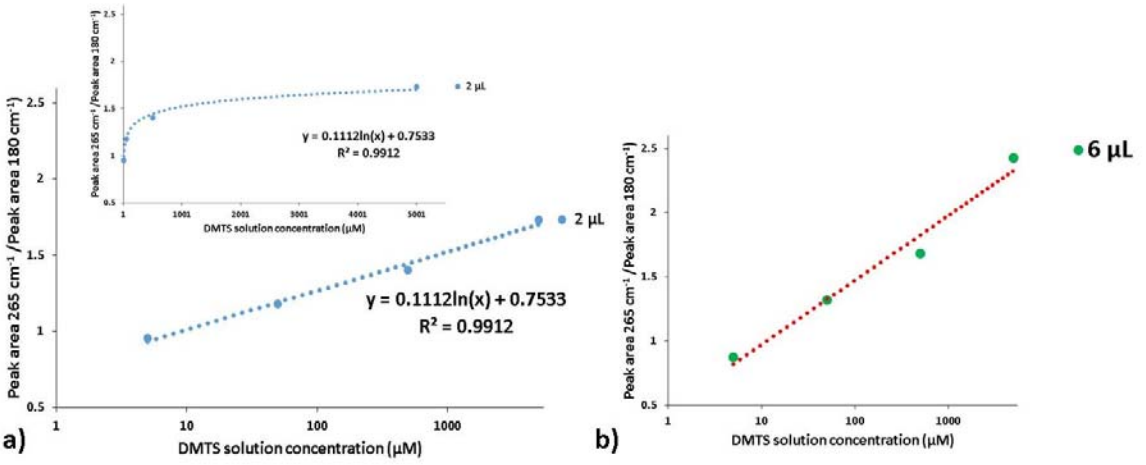


*Figure 27.* Peak ratio of 265 $cm^{-1}$/ 180 $cm^{-1}$ vs concentration graph. a) Peak ratio of 265 $cm^{-1}$/ 180 $cm^{-1}$ vs $\log_{10}$[concentration] graph of 2 µL. Inset with linear axis. b) Peak ratio of 265 $cm^{-1}$/ 180 $cm^{-1}$ vs $\log_{10}$[concentration] graph of 6 µL.

### 3.2. Immersed SERS

The drop-coated SERS experiments were followed by immersed SERS experiments. A drop of water was evaporated from each sensor prior to immersing it, with the goal of preleaning the nanopillars to generate hotspots that strengthen SERS signals.

The region from which the drop is evaporated in the preleaning process is generally left darkened relative to the unwetted portion of the sensor. Upon immersion, the strong visual contrast between the darker pre-leaned circle, and the lighter outer regions of the

sensor, disappeared. If the darkening associated with preleaning is due to residual solvent left on the sample, then the loss of contrast upon immersion may be due to uniform wetting and darkening of the entire sensor. Alternately, if the darker color in the preleaned regions arises from plasmonic interactions between the leaned gold caps on the nanopillars, then the loss of contrast upon immersion may be due to deleaning of the previously leaned nanopillars. Further experiments are needed to test these hypotheses, and to determine what leads to the loss of color contrast between preleaned and nonpreleaned portions of the sensor upon immersion.

SERS spectra gathered as a function of time from a single SERS sensor immersed in a 50 µM ethanolic DMTS solution are shown in Figure 28.

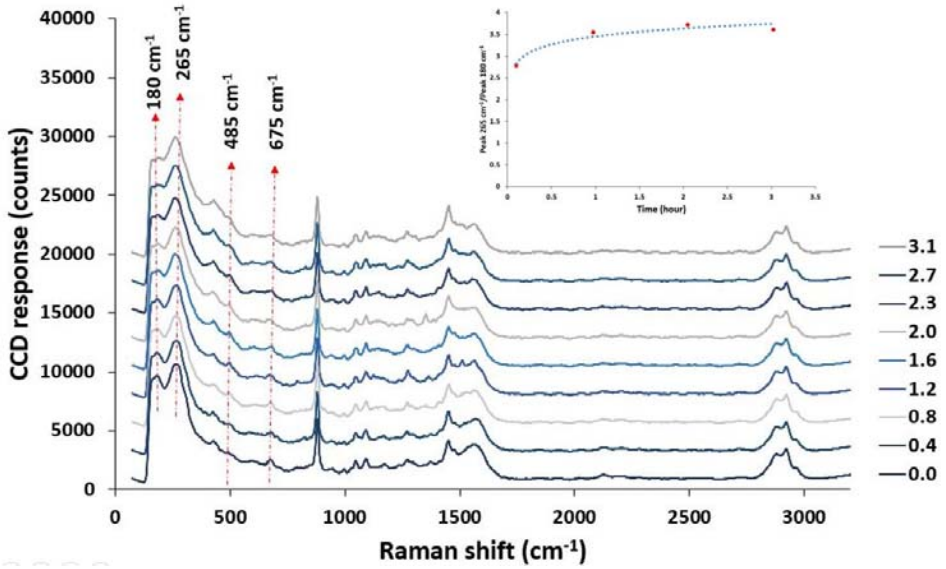


*Figure 28.* 50 µM DMTS in-solution sampling. Laser power: 20 mW, integration time: 5 s, raw spectra averaged per saved spectrum: 10. The numbers on the right side of each spectrum represent time in hours. Inset peak ratio (265 $cm^{-1}$/180 $cm^{-1}$) vs time graph.

Because the laser passes through the dilute ethanolic solution to reach the sensor, the immersed SERS spectra shown in Figure 28 contain the ordinary Raman spectrum of

ethanol (Figure 21) overlayed upon the SERS spectrum of DMTS. As observed with the drop coating exposures, the CS stretch appears almost immediately upon immersion, while the SSS stretches grow into the spectrum over a period of hours. Although the CS peak is present almost immediately, it is attenuated relative to that observed in the drop-coated experiments. This attenuation of SERS signal upon immersion is consistent with other experiments in our lab showing that SERS signals from gold capped nanopillar sensors are attenuated when the sensors are immersed in ethanol or water. The plot of the ratio of the areas of the 265 and 180 $cm^{-1}$ peaks versus time is shown in the inset to Figure 28, and shows monotonic increases through the first two hours of exposure similar to those observed when this ratio was plotted versus the DMTS concentration in the Figure 27a inset. In conclusion, the signals from the immersed sensor are lower, but replicate the same patterns observed in the drop coated experiments. Additionally, the immersed experiments open a door for future detailed study of the binding kinetics.

### 3.3. Headspace sampled SERS

#### *3.3.1. Controls*

##### *3.3.1.1. SERS laser power optimization*

Following the drop-coated, and immersion experiments, attention was directed toward headspace sampled SERS experiments. Prior to probing DMTS, a control experiment was carried out to characterize SERS signal to noise ratios.

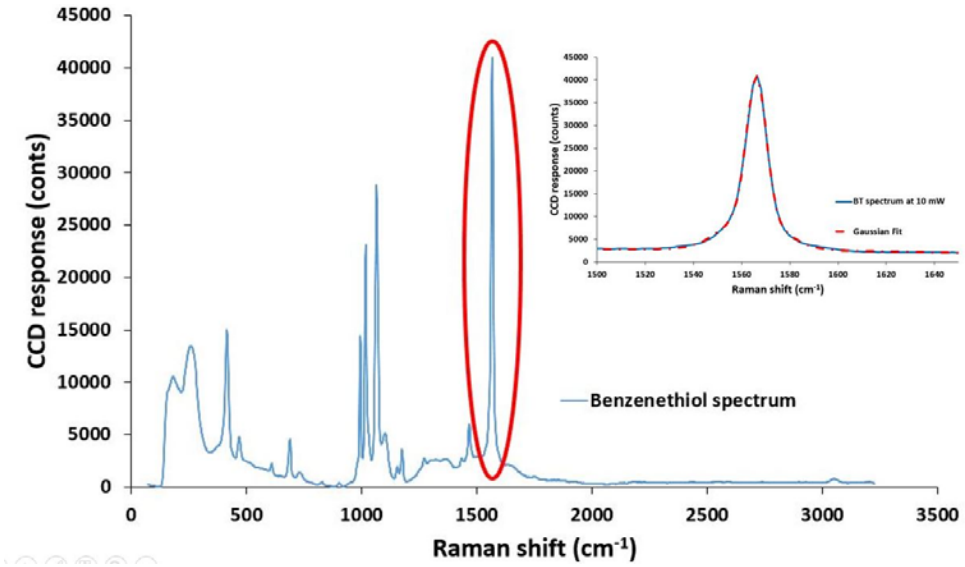


*Figure 29.* Benzenethiol (BT) spectrum. Laser power: 4 mW, integration time: 5 s, raw spectra averaged per saved spectrum: 10. Inset Gaussian peak fitting of the 1560 $cm^{-1}$ peak. (Circled in red)

Because benzenethiol has a strong Raman scattering cross section, and because it binds tightly to gold, the control experiment was carried out with a benzenethiol coated SERS sensor. Multiple SERS spectra were collected from the benzene thiol coated sensor at a specific laser power. The experiment was repeated at laser excitation powers (at the sample position) ranging from 0.1 to 9.0 mW. Figure 29 shows a representative SERS spectrum of benzenethiol.

In each spectrum, a Gaussian equation was fitted to the 1560 $cm^{-1}$ peak, and then the fitted function was integrated to estimate the peak area. The inset in Figure 29 shows the quality of the Gaussian fit to the 1560 $cm^{-1}$ peak. The benzenethiol SERS signal increased linearly with the power of the illuminating laser power as shown in Figure 30 a. The coefficient of variation of peak areas at a single laser illumination power was used as an estimate of the signal to noise ratio. The signal to noise ratios calculated in this way are

plotted versus laser power in Figure 30 b. Illumination powers at the upper end of the range (8 and 9 mW) showed the best signal to noise ratios.

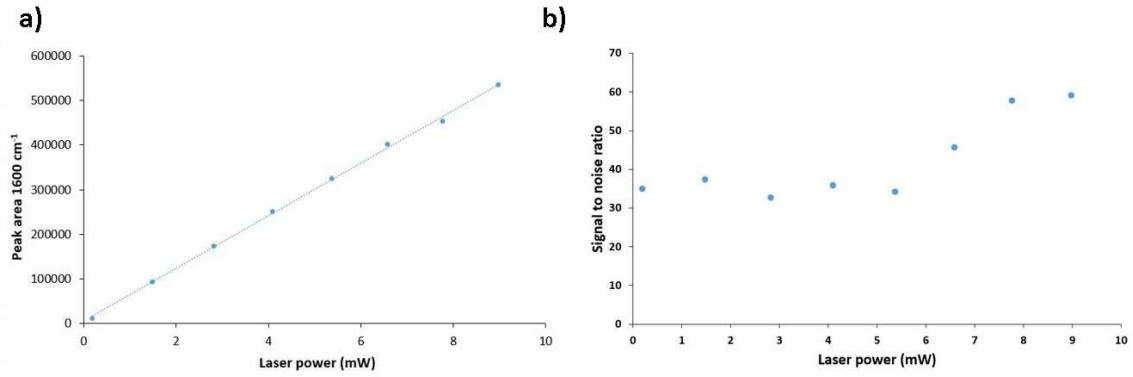


*Figure 30.* Laser power optimization for SERS experiment. a) Peak area at 1600 $cm^{-1}$ (1560 $cm^{-1}$) from benzenethiol vs laser power and b) Signal to noise ratio vs laser power graph.

*3.3.1.2. Sensor preparation*

Figure 31 shows the difference in the SERS background spectra obtained from the preleaned and unpreleaned regions of a sensor. Although the changes in the structure of the background spectrum complicate the overall spectrum, the increases in SERS intensity obtained from the preleaned regions (dark spot on the sensor) outweigh the challenges of working with a more complex background. An alternative to preleaning is the post leaning technique in which the sensor is exposed to gas phase analyte first, followed by evaporation of a drop of solvent to lean the nanopillars.[37] Because preleaning gives slightly higher enhancement than post leaning, preleaning techniques were used in the headspace sampled SERS experiments reported here.

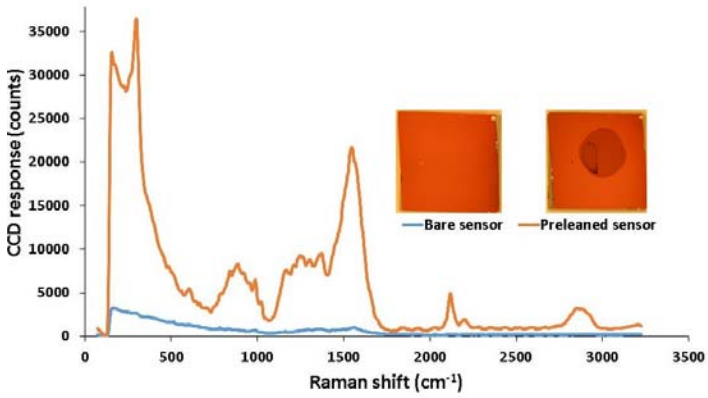


*Figure 31.* Bare sensor vs preleaned sensor spectrum comparison. Both spectra were taken at Laser power: 10 mW, integration time: 5 s, raw spectra averaged per saved spectrum: 10. Leaning of the nanopillar was carried out by evaporating 10 µL Type-I DI water.

*3.3.1.3. Control of headspace sampling*

A control experiment was carried out to observe the changes in the SERS background with time for a preleaned sensor hung in dry cuvette (Figure 32a), and for a preleaned sensor hung in the headspace above ethanol (Figure 32b).

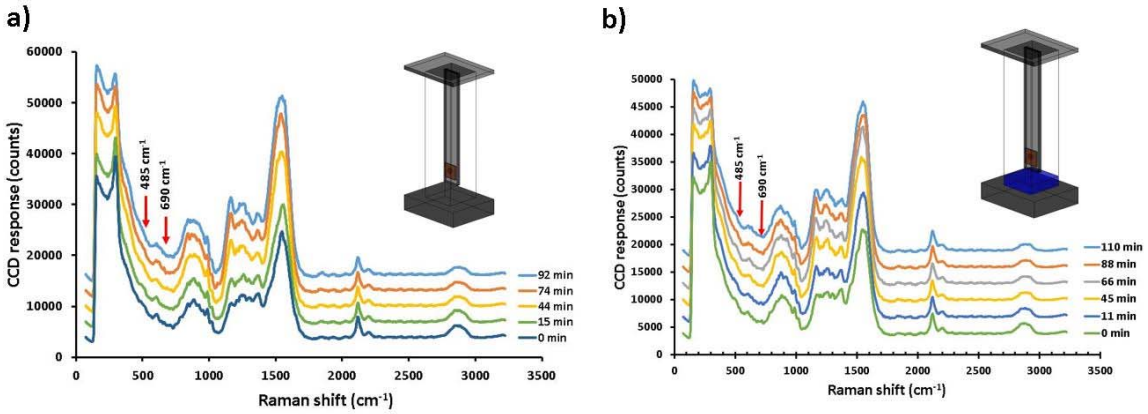


*Figure 32.* Headspace control spectrum. a) Headspace spectrum of preleaned sensor inside empty cuvette at different times (Inset empty cuvette headspace scheme). b) Headspace preleaned sensor with ethanol inside cuvette (Inset ethanol inside cuvette headspace scheme). Laser power: 10 mW, integration time: 5 s, raw spectra averaged per saved spectrum: 10. Red arrows are showing the region of the DMTS signature peak.

While the background pattern remains remarkably similar from spectrum to spectrum, the background intensity changes with time. To highlight such changes, Figure 33 subtracts the initial spectrum from all spectra.

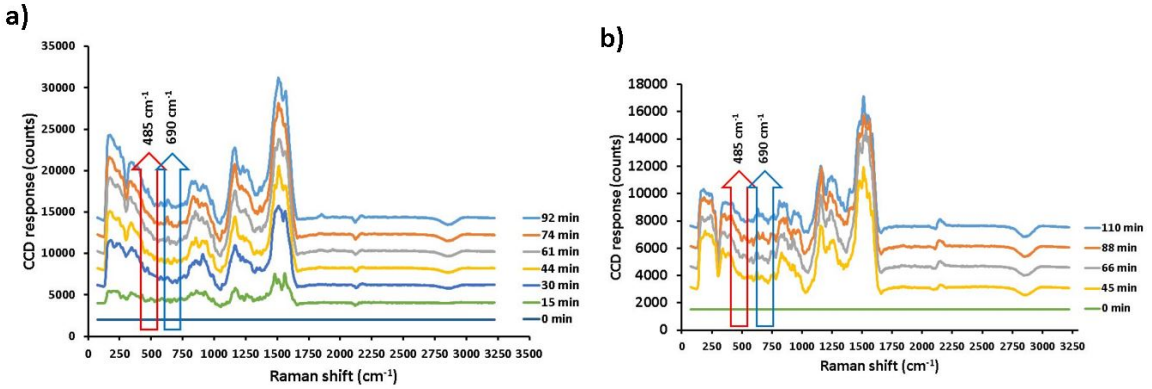


*Figure 33.* Subtracted headspace empty cuvette and ethanol spectrum. a) Headspace empty cuvette spectrum with 0 minute subtracted. b) Headspace ethanol inside cuvette spectrum with 0 minute subtracted.

The growth in the background peaks is especially pronounced for the sensor in the dry cuvette. This is likely due to evaporation of residual solvent from the preleaned region that is facilitated by the warming effect of the laser upon the surface. Joie Games has shown that dry and wet sensors provide varying signals. If this hypothesis is correct, then the effect should be much less pronounced in an ethanol saturated headspace. Figure 33b shows that the intensities reach equilibrium significantly faster in the saturated than in the dry headspace. The rapid equilibration of the background, and the absence of interfering peaks at the SSS stretch (485 $cm^{-1}$), and the CS stretch (690 $cm^{-1}$) frequencies, suggested that background changes in headspace sampled SERS were not likely to compromise the assay for DMTS.

### *3.3.2. DMTS SERS unstirred, unheated*

These control experiments were followed up by attempts to experimentally detect DMTS from a SERS sensor that was placed in the headspace above ethanolic DMTS solutions. The SERS spectra gathered above a 50 and a 500 µM DMTS solution are shown respectively in Figure 34, and Figure 35.

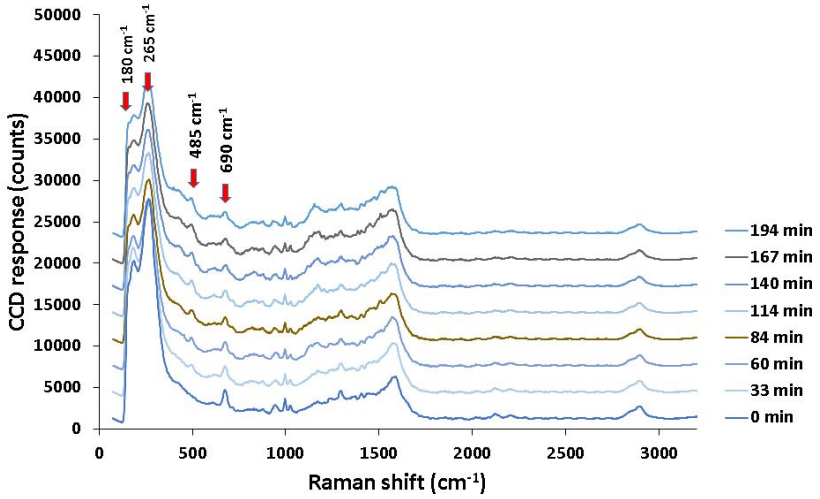


*Figure 34.* Room temperature 50 µM DMTS headspace SERS spectrum. Laser power: 10 mW, integration time: 5 s, raw spectra averaged per saved spectrum: 10.

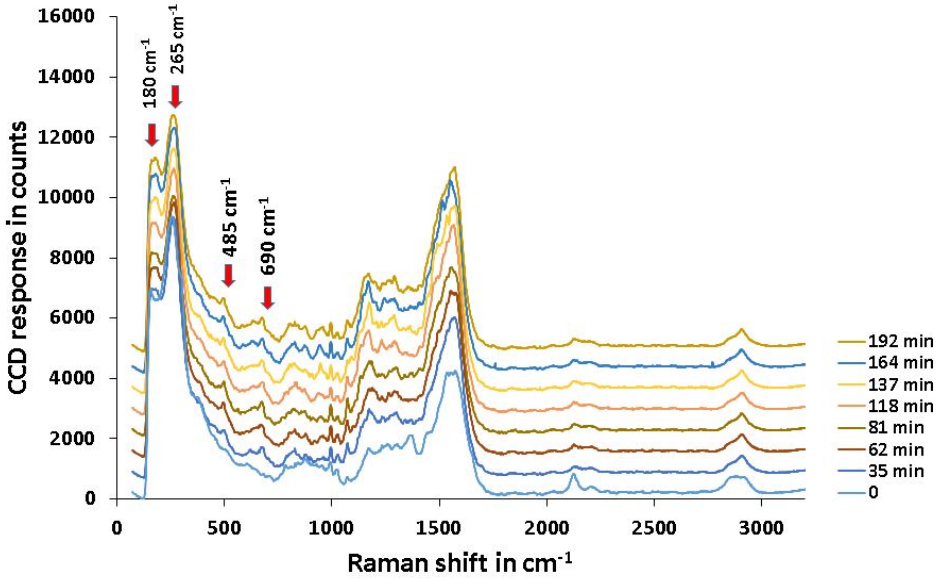


*Figure 35.* Room temperature 500 µM DMTS headspace SERS spectrum. Room temperature data Laser power: 4 mW, integration time: 5 s, raw spectra averaged per saved spectrum: 10.

In both cases, the CS and SSS stretches were observed to grow in respectively at 485 $cm^{-1}$ and 690 $cm^{-1}$. As in the prior experiments, the CS peak grows in first at the lower 50 µM concentration, and the v shape in the bend region between 180 and 265 $cm^{-1}$ diminishes with time as DMTS adsorbs to the sensor. It should also be noted that for the spectra shown in Figure 34 "zero hours" represents the first spectrum taken, but is not a true zero time. In reality, the time between addition of solution and gathering of the first spectrum took approximately 22 minutes.

In the headspace sampling from above the 500 µM solution the time between addition of solution and gathering of the first spectrum was reduced to 2 minutes by completing the optical alignment prior to adding the solution. The remaining delay was due to the time required to remove the positioning coupler to expose the fill port, add the solution through the fill port, reconnect the positioning coupler, and initiate the gathering of data. Additionally, in this experiment vacuum grease was used to seal the gap between

the top of the cuvette and the sensor holder for the first time. Since vacuum grease seals had not been employed in the 50 μM solution, we expected that this improved sealing would result in higher DMTS headspace concentrations, faster build-up of signal on the sensor, and final peaks that were at least as large as those obtained from the 50 μM headspace. However, in this experiment the laser power was also lowered to 4 mW. This should result in signals that are four tenths as large as would be expected for 10 mW excitation.

SERS signal did build up faster above the 500 μM solution than in the headspace above the 50 μM solution. This is seen in the rapid onset of the SSS stretch peak at 485 $cm^{-1}$ in Figure 35. It is not clear whether this increase in rate of deposition is due only to the higher concentration of the 500 μM solution, or to both the higher concentration and the improved sealing. Along with the expected increase in the deposition rate of DMTS on the sensor in the 500 μM headspace, the signal magnitudes were weaker than had been observed in the 50 μM headspace spectra. This was attributed to the decrease in the excitation power.

### *3.3.3. SERS DMTS stirred*

Speed is an important figure of merit for an analytical method. Both stirring and heating have the potential to increase the rate at which DMTS partitions into the headspace. Table 3 summarizes relevant characteristics of the three new, and one prior experiment that were carried out to investigate the role of stirring on the rate of detection. Three of the experiments summarized in Table 3 (100 μM unstirred, 100 μM stirred, and 500 μM stirred) were new experiments. The third row of the table summarizes a prior

experiment. This experiment, whose data was shown previously in Figure 35, was used as the unstirred control for the 500 μM experiment.

Table 3

*Stirring methods*

| Figure | Power (mW) | Stirrer | Stir Rate (rpm) | Temperature | [DMTS] (μM) | Condensation |
|---|---|---|---|---|---|---|
| Figure 36 a | 10 | Newport | 0 | Room | 100 | No |
| Figure 36 b | 10 | Qpod | 1400 | Room | 100 | not checked |
| Figure 37 a and Figure 35 | 4 | Newport | 0 | Room | 500 | No |
| Figure 37 b | 4 | Hotplate | 600 | Room | 500 | Yes |

SERS spectra collected above the 100 and 500 μM ethanolic DMTS solutions are shown respectively, in Figure 36 and Figure 37. The results of this stirring experiment are confusing. The unstirred control spectrum for DMTS was gathered under conditions recorded as identical to those used in the 50 μM solution. Surprisingly, no growth of peaks is observed in the unstirred 100 μM experiment (Figure 36a). Good growth of the SERS peaks is observed in the 100 μM experiment (Figure 36b). The appearance of the CS peak occurs approximately 24 minutes after exposure in the 100 μM stirred sample, and approximately 22 minutes after exposure in the unstirred 50 μM experiment (Figure 34). Thus, the results of the 100 μM stirring experiments do not support the conclusion that

stirring speeds up detection. Conversely, because of the lack of consistency between the 50 and 100 µM unstirred spectra, we also cannot conclude that stirring does not help.

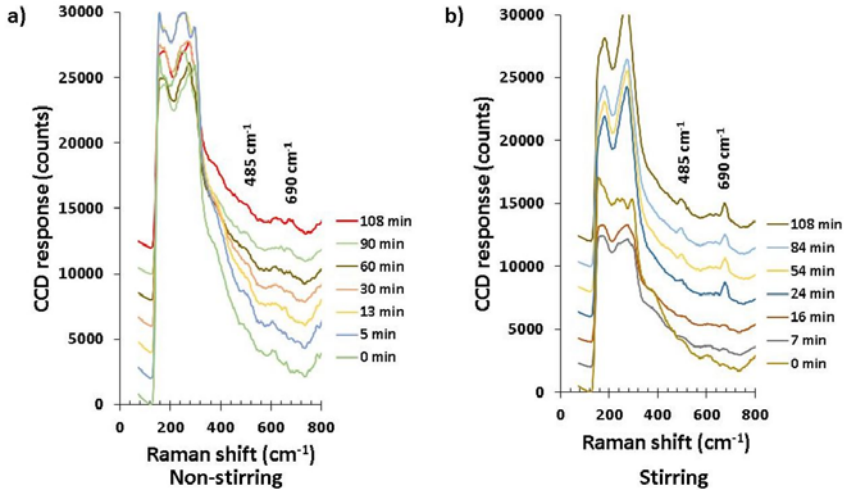


*Figure 36.* 100 µM DMTS non-stirring vs stirring comparison. a) Unstirred headspace SERS spectra b) Stirred (Qpod 1400 rpm) headspace SERS spectra. The interval of spectrum collection was 60 second. The laser power: 10 mW, integration time: 5 s, raw spectra averaged per saved spectrum: 10 were same for both experiment. Offset and scaling parameters are also similar for both a and b.

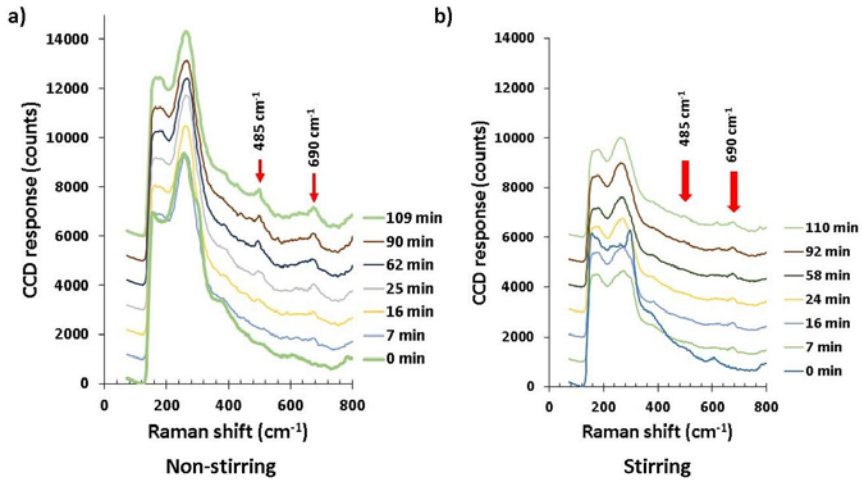


*Figure 37.* 500 µM DMTS non-stirring vs stirring comparison. Laser power: 4 mW, integration time: 5 s, raw spectra averaged per saved spectrum: 10. a) Unstirred headspace SERS spectra. b) Stirred (hotplate 600 rpm) headspace SERS spectra. Offset and scaling parameters are similar for a and b.

The results of the 500 μM experiments are shown in Figure 37. This experiment suggests that stirring actually shrinks the DMTS SERS signal. Close examination of the cuvette at end of the 500 μM DMTS stirring experiment revealed that a fog had condensed on the cuvette wall through which the SERS spectra were being gathered, and that the sensor also had condensation. Photographs showing these effects are presented in the next section, in which steps to overcome the problem are discussed. We hypothesize that condensation is favored by the improved grease seal, that the condensate is ethanol, and that it reduces SERS signals as it builds up. We also hypothesized that if the grease served as a sink into which DMTS could partition, that this would also decrease SERS signals.

Why did the stirred 100 μM solution yield cleaner signals? The 100 μM stirred measurements differed from the others in that they were carried out within the Quantum Northwest Qpod temperature controller, even though the temperature control capabilities were not used. Because alignment was tedious in the Qpod, the other measurements were carried out externally to the temperature controller. In repeated tests after the experiments reported here, we found that under identical room and sealing conditions, condensate would build up much more slowly on the walls of the cuvette when it was in the temperature controller. We hypothesize, that this is due to the large black aluminum structure that conducts a small amount of heat from the room into the cuvette. Another factor that was not held constant in these experiments was the illuminating laser power. It is possible that the 10 mW excitation focused at the sensor surface in the 100 μM experiments warmed the sensor surface more than did the 4 mW excitation power used in the 500 μM experiments. If so, the higher laser illumination power in the 100 μM experiments may have partially mitigated condensation on the sensor in those experiments.

### *3.3.4. DMTS SERS heated*

Following the stirring experiments, the role that heating might play in speeding up the rate of DMTS detection from the headspace was investigated.

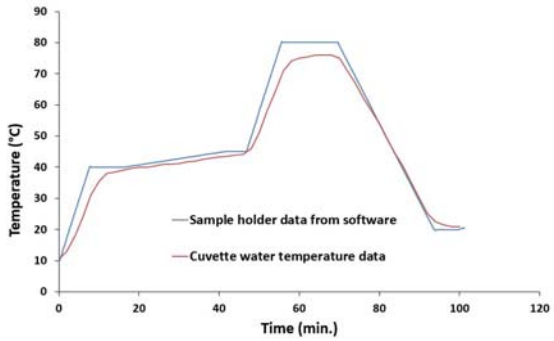


*Figure 38.* Temperature controller control experiment.

Figure 38 shows a control test of the temperature controller. The temperature change of 1 mL of DI water was measured with a classical glass thermometer and compared with the software value. The observed hysteresis has a magnitude of ~ 4° C. The conclusion drawn from this experiment was that the Qpod cuvette temperature controller was working as designed. The observed hysteresis is expected, because the thermal mass of the classical thermometer is large relative to the cuvette. A more careful calibration requires a temperature sensor whose heat capacity is small relative to that of the cuvette and its contents.

Following the Qpod cuvette temperature controller test, a SERS sensor was placed in the headspace of a sealed cuvette, and the cuvette was placed in the Qpod. An aliquot of 100 μM ethanolic DMTS was added to the cuvette below the sensor. A 2 $^{o}$C/min temperature ramp of the cuvette was initiated immediately upon addition of the solution. The collection of SERS spectra began ~2 minutes later. Figure 39 shows the spectra collected as the cuvette was warmed. The odor of ethanol indicated that the grease seal

failed at some point in the experiment. This is not surprising, given that an error in the experimental design had raised the solution temperature slightly above the boiling point of ethanol (78-79 °C).[50] Nonetheless, a strong CS peak had appeared in the spectrum by the 4 min (32 ºC) mark.

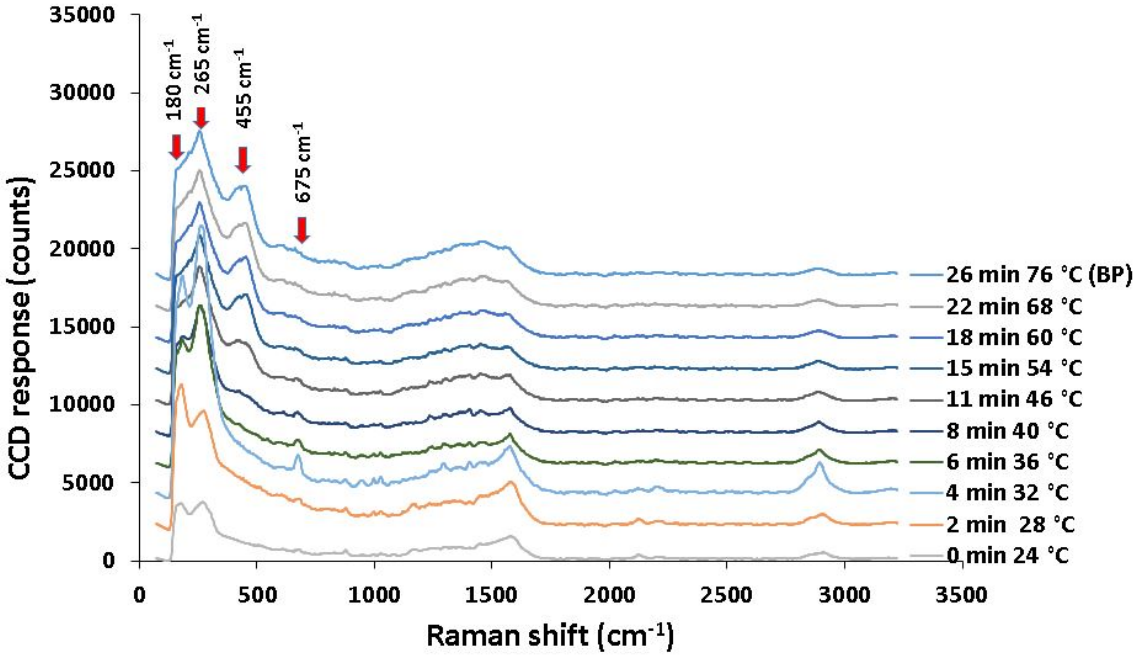


*Figure 39.* Headspace sampling SERS at elevated temperature. The sample was 100 μM DMTS. The temperature was ramped at 2°C/min from 20 to 80°C. (Laser power: 10 mW, integration time: 5 s, raw spectra averaged per saved spectrum: 10).

As the temperature increased above 32 ºC, the magnitude of the CS peak systematically dropped, and a much stronger peak grew into the SSS stretching region. This second peak is very broad, and its center is redshifted to 455 $cm^{-1}$. This is close to the ethanol peak at 430 $cm^{-1}$, and closer still to the predicted frequency for the SSS symmetric stretch which was predicted have a frequency of 460 $cm^{-1}$. If this were a bulk ethanol peak, then we would expect the rest of the ethanol spectrum to be present – it is not. It appears that higher temperature favors the SSS symmetric stretch peak at 455 $cm^{-1}$ over the asymmetric stretch

at 485 $cm^{-1}$ that has been prominent in the drop coating and immersion experiments. This experiment is encouraging because the time to detection is decreased from ~20 to ~4 minutes. The appearance of the new and large peak at 455 $cm^{-1}$ presents an interesting avenue for future study. Finally, the seal failure in this experiment highlights the need for seals that can withstand the elevation in vapor pressure that accompanies the elevation in temperature. For future experiments the vapor pressure of ethanol can be estimated by using the Antoine equation:[51]

*Eq. 22*

$$P = 10^{A-\frac{B}{c+T}}$$

Here, P = Pressure; A, B, C= Antoine equation parameters;[51] T = Temperature in °C. At 60 °C temperature the calculated vapor pressure of ethanol is 46.8 kPa.

## 4. SERS challenges

Two of the challenges encountered in the SERS experiments after implementing the grease sealing were increased window and sensor fogging. Because some SERS signals were reduced the possibility that grease might serve as a sink for DMTS represented another potential challenge. In this section, first experimental approaches to mitigating fogging were proposed and tested. The hypothesis that grease serves as a sink for DMTS was also experimentally tested in GC-MS experiments.

### 4.1. Condensation

Figure 40 shows the Silmeco sensor used in the 500 μM stirring experiment before and immediately after use in the experiment. The darker spot, seen in the sensor in Figure 40a, is the region that was preleaned by evaporation of a water droplet. As seen in Figure 40b, by the end of the experiment the dark area was greatly expanded, suggesting that

condensation had formed a liquid overlayer on that portion of the sensor. Another possibility that was considered, was that the grease being used to hold the sensor to the glass was seeping around and onto the sensor. To mitigate this second potential problem we switched to UV curing glue based attachment of the sensors to the glass support in subsequent experiments.

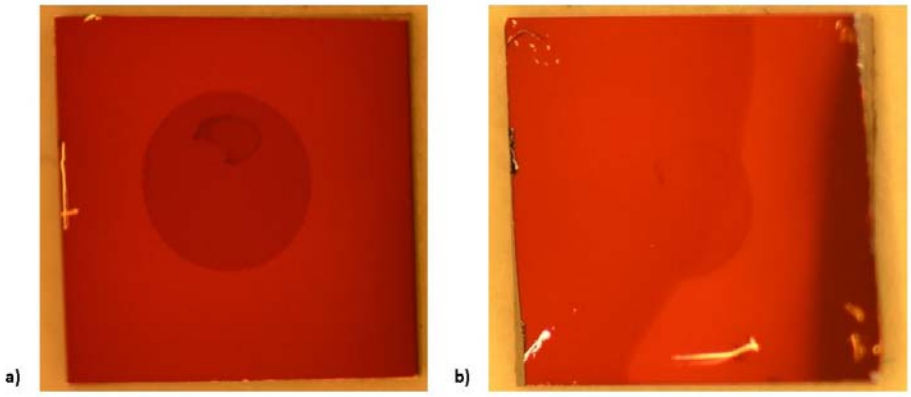


*Figure 40.* SERS sensor condensation. a) Before starting the experiment b) After the 500 μM DMTS stirring experiment.

Because solvent condensation is the most likely cause of the wetting effects seen in Figure 40, an important future direction will be to find a way to control the sensor surface temperature during experiments. Warming the sensor slightly should prevent condensation.

Photographs from experiments investigating the problem of condensation on the cuvette windows are shown in Figure 41. Figure 41a shows that after sitting for 30 minutes, a sealed cuvette sitting in the open air has developed condensation on the side windows. Figure 41c shows that when the same experiment is repeated in the Quantum Northwest Qpod minimal condensation has formed after 30 minutes. We hypothesized that this was due to the black aluminum surrounding the cuvette was conducting a small amount of heat, generated from light absorption, to the cuvette walls. To test this hypothesis, blackened

aluminum foil was attached to the side of a cuvette. As seen in Figure 41b, after a 30 minute incubation period, condensation was still present. Thinking that the heat capacity of the aluminum might be important, the experiment was repeated with the holder shown in Figure 41d. This holder has three thicker aluminum sides. Following a 30 minute exposure, these sides were clean. The fourth side of the cuvette holder has a thin aluminum cover. As shown in Figure 41d, this side developed condensation. At room temperature, placing the cuvette in a cage of blackened aluminum that is at least ¼ inch thick appears to be effective in mitigating the formation of condensation on the cuvette windows. In holders with aluminum walls, alignment is more time consuming because the view of the laser spot on the sensor surface is blocked by the aluminum. Although we have good alignment procedures that work in this setting, they are tedious, and thus an important goal for the future should be to develop more rapid alignment protocols for the cuvette holders.

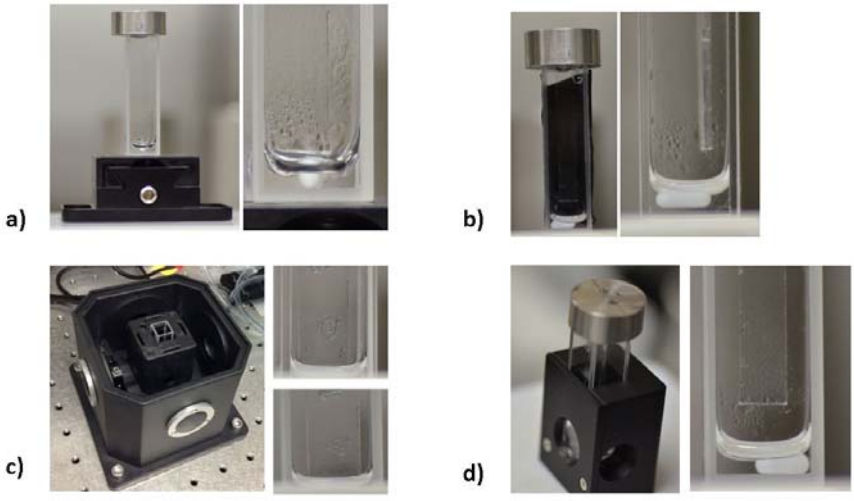


*Figure 41.* Condensation on cuvette wall. a) Cuvette on goniometer b) Cuvette wrapped with aluminum foil c) Cuvette inside temperature controller subsequent cuvette wall was shown top before and bottom after stirring, inside the sensor holder grease is visible d) Cuvette inside a steel cuvette holder.

An alternate solution to the condensation problem is to directly heat the window being used in the experiments. Toward this end, a glass microscope slide coated on one side with a thin film of indium tin oxide (ITO) was attached to the top of the cuvette window with double sided tape (Figure 42a). Two double A batteries were aligned in series, and connected with alligator clips to aluminum foil which contacted the ITO surface. The batteries generate a potential drop of ~3 volts across the ITO. The current running through the ITO window was measured to be 51.3 mA. This generated enough heat (Figure 42b) to completely remove the condensate within 30 seconds (Figure 42c), and is a first step toward independent control of the cuvette wall temperature.

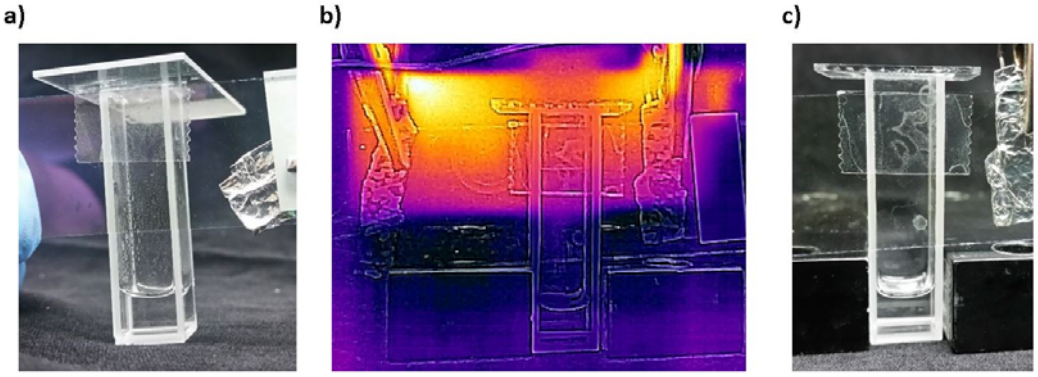


*Figure 42.* Condensation problem solution. a) After 2 hour the cuvette window forms condensation. b) IR picture of the ITO window when running electricity. c) The window turns clean within 30 second.

### 4.2. Grease challenge

During headspace SERS investigations of the effects of stirring, Dow Corning vacuum grease was used to seal the cuvette.[52] We hypothesized that grease might serve as a sink for DMTS, resulting in signal losses over and above those caused by condensation. The GC-MS experiments used to test this hypothesis are described here.

Figure 43 shows chromatograms collected from headspace above 500 μM DMTS using solid phase micro extraction (SPME) following different incubation times. In these chromatograms, the retention time of DMTS was 7.2-minutes. Control chromatograms of

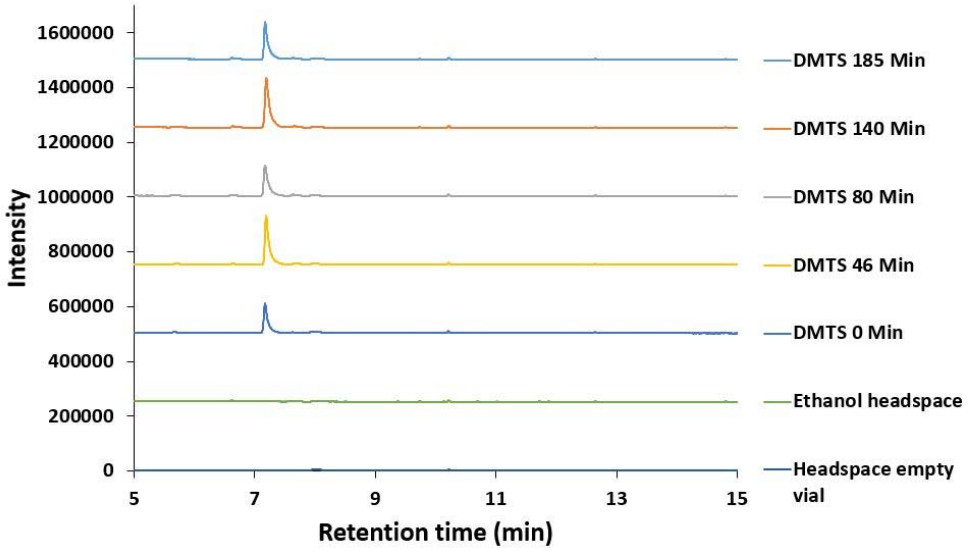


*Figure 43.* DMTS chromatogram extracted by SPME.

ethanol and the empty headspace were also collected. The DMTS peak was confirmed by the Agilent MS library from GC-MS computer in Dr. Petrikovics' lab. Peaks at 7.6, 10.2 and 12.6 are also observed with much lower intensities. The areas for these peaks were determined using the Gaussian fitting and integration approach described earlier. The peak areas calculated for the control chromatograms are listed in Table 4. In these control experiments, the headspace sampling vials were sealed by PTFE coated septa in screw top lids. No vacuum grease was used in the control experiments. The experiment was repeated but this time, grease was added to the inner walls of the glass vials, and was also placed between the lip of the vials and the PTFE coated septa. Screw tops were again used to tighten the septa onto the sampling vials. Representative chromatograms obtained from SPME sampling of a 500 μM ethanolic solution in a grease-sealed vial along with

appropriate controls are shown in Figure 44. The peak areas from this initial chromatogram and other chromatograms from similar vials sampled after longer and longer incubation periods with the grease are tabulated in Table 5.

Table 4

*DMTS peak areas in the absence of grease sealing*

| Sampling time (min) | Mass of grease used (mg) | DMTS Peak area | Peak at 7.6 min Peak area | Peak at 10.2 min Peak area | Peak at 12.6 min Peak area |
|---|---|---|---|---|---|
| 0 | 0 | 8368 | 100 | 219 | 105 |
| 46 | 0 | 14640 | 458 | 241 | 52 |
| 80 | 0 | 10090 | 444 | 229 | 52 |
| 140 | 0 | 16286 | 406 | 205 | 51 |
| 185 | 0 | 10747 | 218 | 169 | 71 |

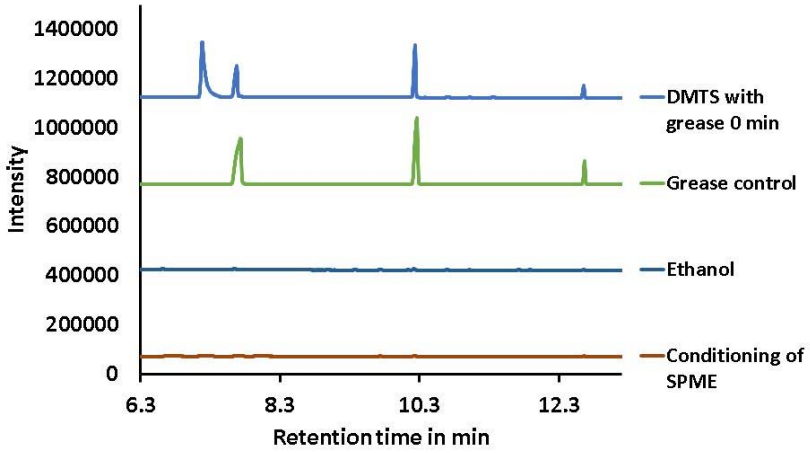


*Figure 44.* DMTS chromatogram extracted by SPME with grease interference.

Table 5

*DMTS peak areas in the presence of grease sealing*

| Sampling time (min) | Amount of grease used (mg) | DMTS Peak area | Peak at 7.6 min Peak area | Peak at 10.2 min Peak area | Peak at 12.6 min Peak area |
|---|---|---|---|---|---|
| Control | 6.1 | 0 | 16628 | 13283 | 2353 |
| 0 | 3.6 | 15628 | 6232 | 7229 | 1199 |
| 50 | 5.5 | 18683 | 2420 | 5387 | 1268 |
| 95 | 10.7 | 19180 | 5560 | 8429 | 1552 |
| 145 | 8 | 23661 | 3600 | 8138 | 1960 |
| 180 | 4.4 | 20506 | 1378 | 6615 | 1755 |

*Note. These areas are from chromatograms obtained via SPME sampling above a 500 μM DMTS solution held in grease sealed glass vials.*

Figure 45 compares the areas of the DMTS peaks obtained after incubation times ranging from 0 to180 minutes, with and without the presence of vacuum grease. Increased incubation times do not lead to a systematic loss of DMTS. This data supports rejection of the hypothesis that grease is serving as a sink for DMTS.

Because, the presence of grease in the seals leads to larger DMTS peaks in the chromatograms, we hypothesized that the increase in DMTS peak areas might be because low molecular weight silicone compounds in the polysiloxanes[53] of the grease interact with the carboxen/polydimethylsiloxane coating of the SPME fiber and promotes the binding of DMTS. (Carboxen fiber is suitable for adsorbing $C_2$-$C_5$ n-alkane molecule.[54]) The grease

may be providing a better seal so DMTS is not able escape from the headspace of the cuvette.

Or the increase in signals, that is seen when grease is present, may be due to an improved seal that prevents external oxidants from entering the cuvette and oxidizing the DMTS. This new hypothesis needs to be tested in future experiments.

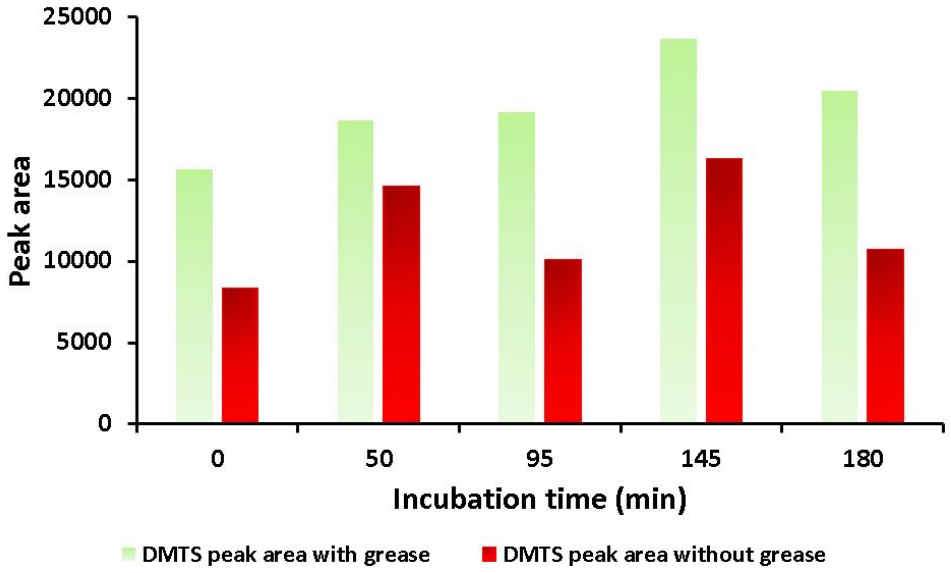


*Figure 45.* DMTS peak area comparison when using grease vs no grease.

## 5. DMTS reduction experiment

A faster detection method was hypothesized by reducing DMTS and producing methyl mercaptan, based on the idea that thiol molecules bind to noble metals faster than DMTS. For the reduction experiment three different reducing agents were used: iron(II) chloride ($FeCl_2$), sodium borohydride ($NaBH_4$), and dithiothreitol (DTT).

### 5.1. Iron(II) chloride

The first reducing agent optimized was iron(II) chloride. $FeCl_2$ was chosen since one of our lab member's research is about reaction of DMTS with hemoglobin. Her work provides a result of the reduction of DMTS by heme iron. So, we propose reduction by

iron(II) chloride as a primary reducing agent. Gas chromatography, ordinary Raman and SERS were used to test the reduction of DMTS by $FeCl_2$. The reaction we propose is:

$$4\ Fe^{2+} + CH_3\text{-}S\text{-}S\text{-}S\text{-}CH_3 + 4\ H^+ \rightarrow 4\ Fe^{3+} + 2\ CH_3\text{-}S\text{-}H + H_2S$$

### *5.1.1. Gas chromatography*

The first instrument used to test the reduction by $FeCl_2$ was gas chromatography.

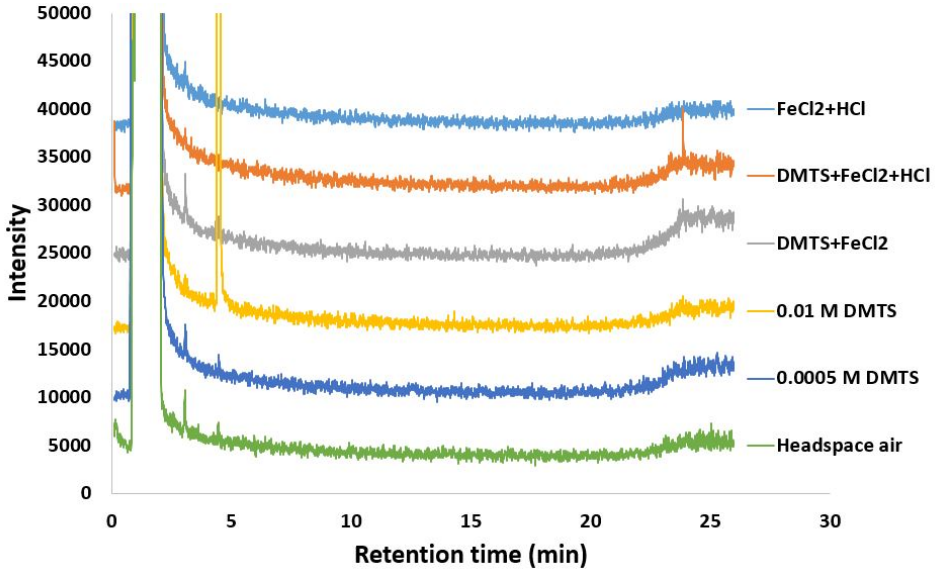


*Figure 46.* GC headspace analysis of reduction reaction. Headspace gas was extracted using gas syringe.

Figure 46 shows the chromatograms of the attempted reduction reaction with several controls. The 4.4-minute peak is observable from 0.01 M DMTS a clear evidence of DMTS. This is proved by having the confirmation from the GC library. None of the chromatograms shown have a peak at 23 minutes except the reaction mixture of DMTS and $FeCl_2$ in acidic medium. From the GC library, no identification has been found about the compound. Due to the very low boiling point of methyl mercaptan (5.95 °C), GC is not able to detect it under these conditions. The initial injection temperature of the GC was 110°C and the initial oven temperature was 35 °C. Later a more concentrated solution was used with same parameters to test the reduction.

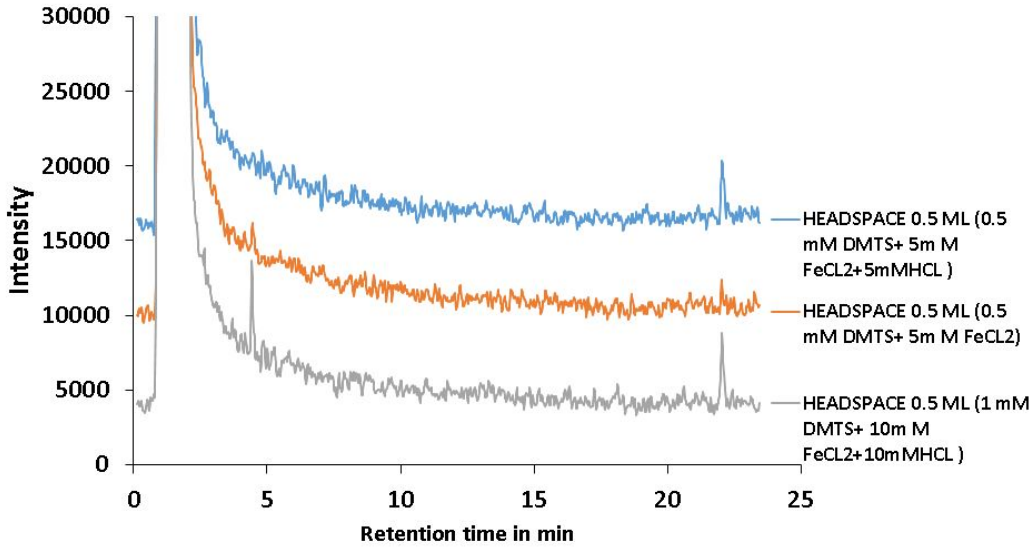


*Figure 47.* DMTS reduction product test by GC-MS. 0.5 and 1 mM is described in the materials and method section as 500 and 1000 µM.

In Figure 47 the reduction with acidic (blue and grey chromatogram) and non-acidic (orange chromatogram) medium is shown with high (1 mM, grey chromatogram) and low (0.5 mM, blue chromatogram) DMTS concentrations. The non-acidic chromatogram shows a small signal at 23 minutes compared to the reduction with acidic medium. Also, at high concentration (1 mM) a DMTS peak at 4.4 minutes is observed; this may suggest that the reduction of a high concentration of DMTS is slow.

Now let's compare the blue and orange chromatogram; both have the same concentration of DMTS. The only difference is that one is in acid medium and other is non-acidic. From this comparison, a sharp peak is observed at 23 minutes in terms of acidic medium compared to non-acidic medium. Also, the DMTS signal at 4.4 minutes is observable in the case of non-acidic medium. This suggests two hypotheses. First, the reduction is faster when using a low concentration. Second, even faster reduction can occur in acid medium. An extended study is needed to prove these hypotheses.

One of our lab member's work is to understand the reaction and study kinetics of DMTS with hemoglobin. From Xinmei's work it has been found that dimethyl disulfide or methyl disulfide may also be produced by the reduction of DMTS by heme iron. In section 5.1.3 production of dimethyl disulfide is supported by SERS study; which is discussed later in the SERS reduction experiment by $FeCl_2$.

### *5.1.2. Ordinary Raman*

The next step towards understanding the reduction by $FeCl_2$ was to study the reduction using ordinary Raman equipment. Because methyl mercaptan and hydrogen sulfide are toxic to human health, the experiment is carried out inside the fume hood. As discussed previously, the peaks from ordinary Raman spectrum of DMTS, 485 and 690 $cm^{-1}$ are from SSS and CS stretch respectively. We hypothesize that upon reduction the peak at 485 will lower in intensity and 690 may reduce because during reduction DMTS will decrease in amount and methyl mercaptan and hydrogen sulfide will be produced. Both are gases at room temperature and will partition in the headspace quickly and leave the solution.

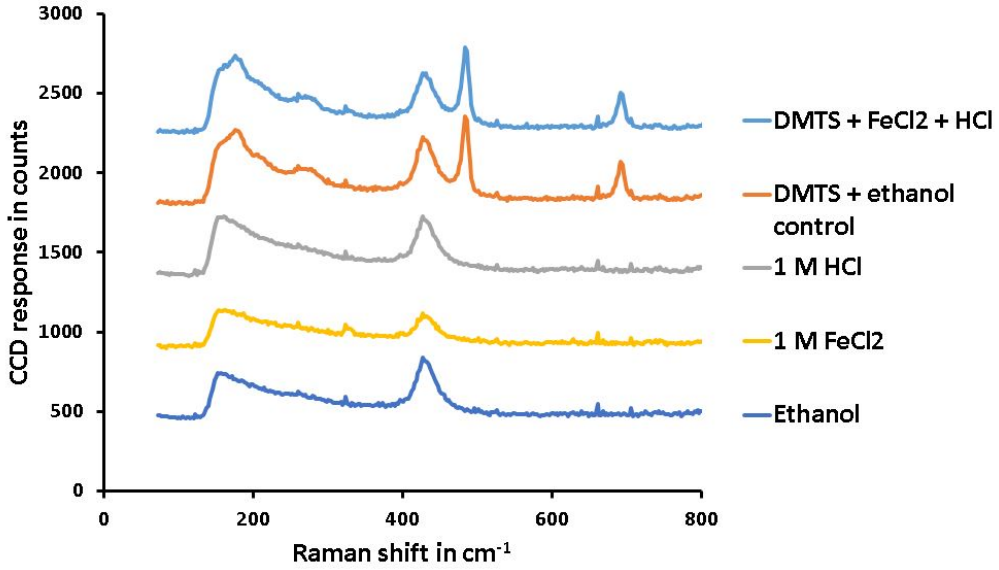


*Figure 48.* Ordinary Raman analysis of DMTS reduction by $FeCl_2$. Laser power: 10 mW, integration time: 5 s, raw spectra averaged per saved spectrum: 10. Data is shown up to 800 wavenumbers within the region of the interest signal.

Figure 48 shows the ordinary Raman spectrum of the reduction reaction (light blue spectrum) and the control (orange spectrum). The reduction spectrum (DMTS + $FeCl_2$ + HCl, light blue spectrum) is obtained by adding 200 µL 0.50 M DMTS with 200 µL 1 M $FeCl_2$ and 1 M HCl. The spectrum was collected immediately after mixing the solution. The control (orange) spectrum contains 200 µL DMTS + 383 µL ethanol. In terms of dilution both solutions contain similar concentration of DMTS.

Apparently, there is no change during the reaction. We hypothesized that the SSS stretch will decrease in intensity and CS may remain or lessen. To have a better understanding, we plotted the peaks with Gaussian peak fitting by using excel.

From the Gaussian peak fitting followings are the peak area calculated.

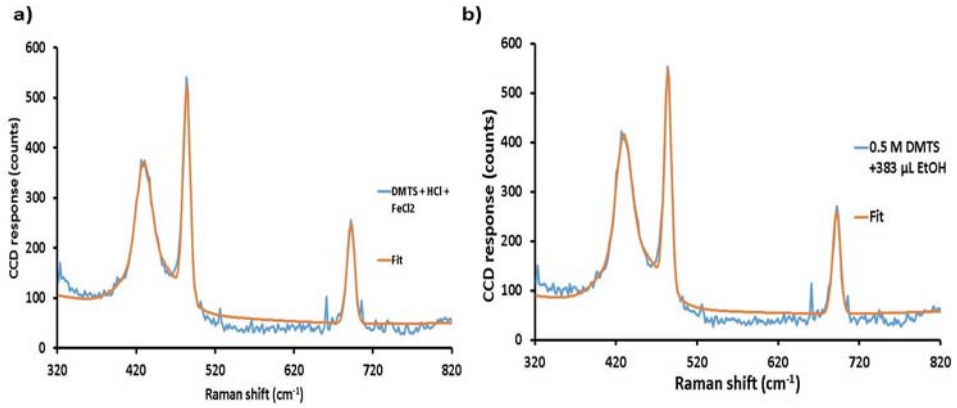


*Figure 49.* $FeCl_2$ reduction spectrum fit. a) For reduction reaction peak area at 485 $cm^{-1}$ is calculated 4790 and at 690 $cm^{-1}$ is calculated 2473, b) Control 0.5 M DMTS + 383 µL EtOH peak area at 485 $cm^{-1}$ is calculated 4862 and at 690 $cm^{-1}$ is calculated 2488.

Figure 49 shows the quality of the Gaussian peak fitting of the reduction and control peak at the SSS and CS stretch. In Figure 49, three peaks are shown at 430, 485 and 690 $cm^{-1}$, the peak at 430 $cm^{-1}$ is from ethanol and 485 and 690 $cm^{-1}$ arises from the SSS and CS stretch of DMTS, respectively. Here only the 485 and 690 $cm^{-1}$ peaks are considered for discussion.

From the peak area calculations, we found that the reduction spectrum contains a slightly smaller peak area (4790) at the SSS region compared to control (4862). And the peak area at 690 is also decreased in the reduction spectrum from 2488 to 2473. The change in the SSS stretch is 4862 – 4790 = 72 is larger compared to the CS stretch 2488 – 2473 = 15. This bigger change in the SSS stretch may suggest the reaction is happening, but not fast enough to have a significant difference. This result of a slow change is consistent with the GC analysis of $FeCl_2$ reduction. Because the spectrum in this experiment was collected immediately after mixing the solution, there may not have been enough time for complete reaction. A subsequent study will be to collect spectra from the reduction reaction for a longer period. But due to observation that the $FeCl_2$ solution was pale yellow, $Fe^{2+}$ is

already oxidized by air and converted to $Fe^{3+}$, because no extra care was taken to prepare the solution in an oxygen free environment.

### *5.1.3. SERS*

Since our major goal was to develop a detection method using SERS technique, here a SERS sensor is used to study the reduction by $FeCl_2$. This experiment is also carried out in the fume hood for the sake of safety.

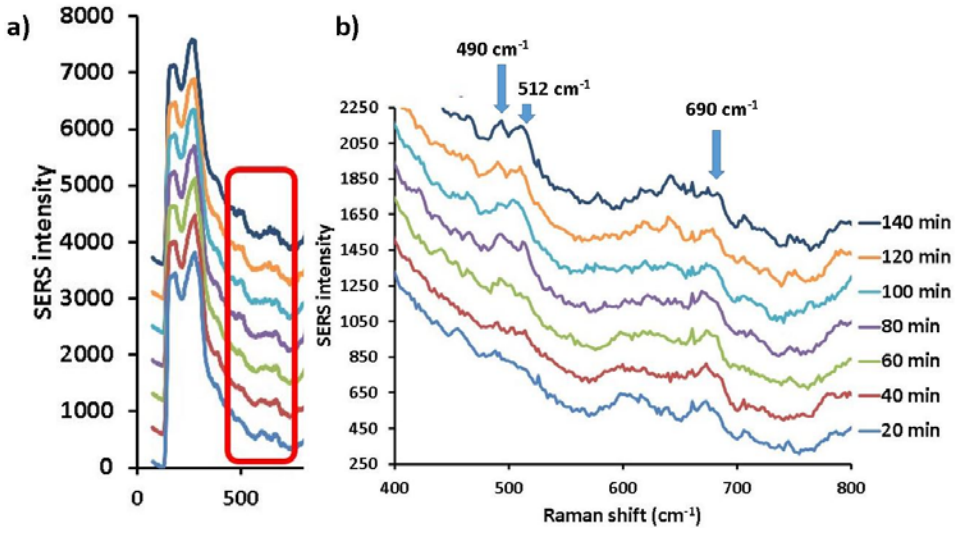


*Figure 50.* $FeCl_2$ SERS reduction. a) SSS and CS stretch of DMTS is shown with Red squared area. b) Red squared area is zoomed. Laser power: 3 mW, integration time: 5 s, 5 raw spectra averaged per saved spectrum: 5 and 1400 rpm stirring was used for this experiment.

Figure 50 shows the SERS spectra collected from the headspace of the reduction of DMTS by $FeCl_2$ in acid medium. Peaks at 490, 512 and 690 $cm^{-1}$ are the major concern for this analysis section. 490 and 690 is assigned to DMTS in accord with previous discussion. But the 512 peak is new here which we have never witnessed before. From the literature we learned that a double sulfur stretch occurs at 500-550 $cm^{-1}$.[29] Because of the probability of producing dimethyl disulfide or methyl disulfide we can assign this peak to either of

these disulfide compounds. Figure 50 b shows that at 20-minutes there are no 490 and 512 peaks. But the 690 peak is present in the 20-minute spectrum. With increasing time the area at 490 and 512 is increasing and the area at 690 peak is decreasing or remains the same. This decrease of the 690 peak is not clearly understood. This may suggest that methyl mercaptan is oxidizing and producing di-sulfur compound.

Two hypotheses can be posited from this experiment. One, DMTS reduction is slow. Two, a disulfide compound is produced. More careful work is needed to support these hypotheses.

### 5.3. Sodium borohydride ($NaBH_4$)

The result obtained from the reduction by $FeCl_2$ is promising in terms of cleaving DMTS into a sulfide or a disulfide product. Since the reduction apparently happens slowly with $FeCl_2$, a strong reducing agent is sought. The following experiment has been carried out by using a strong reducing agent sodium borohydride ($NaBH_4$). To study the reaction by $NaBH_4$ ordinary Raman and SERS instrument are used.

#### *5.2.1. Ordinary Raman reduction analysis*

$NaBH_4$ is a very strong reducing agent. The reaction of $NaBH_4$ with DMTS is very fast and strong. The solution changes color upon mixing the reactants. Table 6 describes the color changes observed during the reaction of DMTS with $NaBH_4$ in acidic and basic medium.

Table 6

*$NaBH_4$ reduction*

| Sample No. (All solutions contained 0.5 M DMTS and $NaBH_4$ in ethanol) | Ingredient | Result | Additional Ingredient | Result |
|---|---|---|---|---|
| Test tube 1 | None | Yellow solution (precipitate) | HCl | Clear (Transparent) |
| Test tube 2 | HCl | Clear (Transparent) | None | Clear (Transparent) |
| Test tube 3 | HCl | Clear (Transparent) | NaOH | Yellow solution (precipitate) |

*Note. The concentration of the DMTS, HCl, $NaBH_4$, NaOH solutions were 0.5 M, 1M, 1 M, and 50 wt%.*

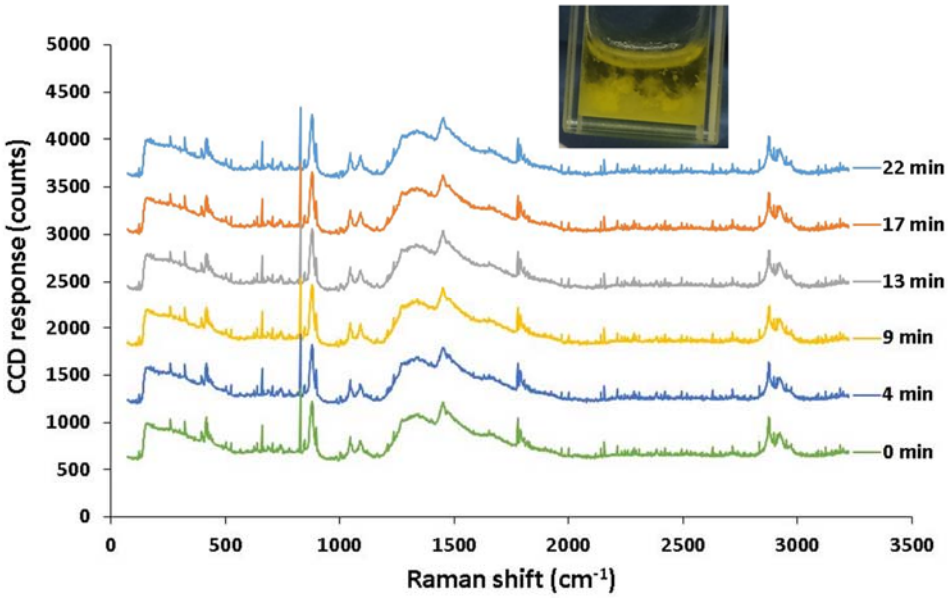


*Figure 51.* DMTS reduction by $NaBH_4$. The spectrum was collected with laser power: 10 mW, integration time: 20 s, raw spectra averaged per saved spectrum: 10. Inset precipitate formation is shown.

Ordinary Raman spectra of reaction mixture of 0.5 M DMTS and 1 M $NaBH_4$ are shown in Figure 51. The spectrum is showing unprecedented changes. The only sharp peak

is observed at 900 $cm^{-1}$ from ethanol. No signal was identifiable as DMTS, disulfide or methyl mercaptan. The reason for having low signal may be from the elemental sulfur formation. Because the solution turns yellow, this supports the hypothesis of elemental sulfur formation.

A follow up reduction experiment was carried out in acidic medium.

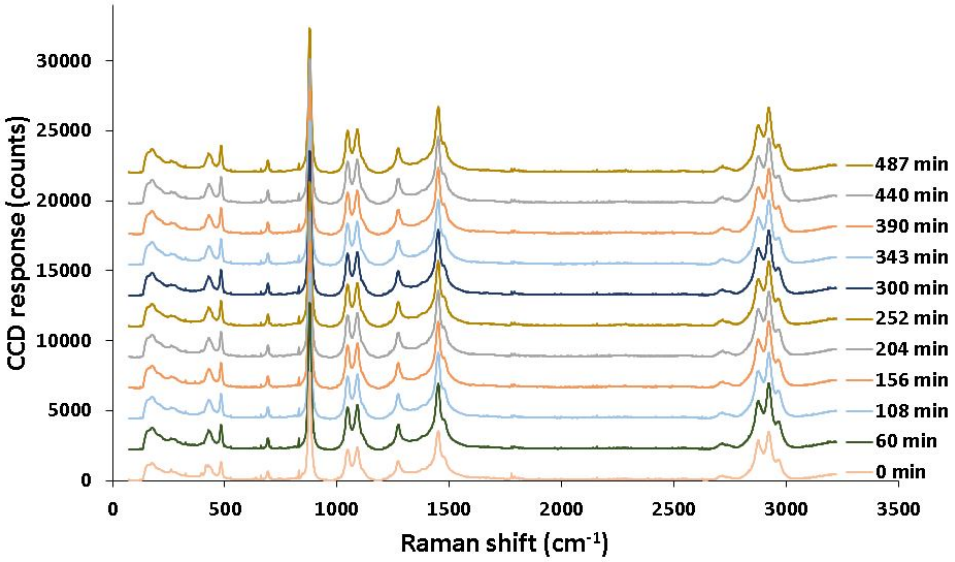


*Figure 52.* DMTS reduction by $NaBH_4$ in presence of HCl. Laser power: 10 mW, integration time: 20 s, raw spectra averaged per saved spectrum: 10.

While testing the reduction by $NaBH_4$ in an acidic medium no changes in the spectrum were observed over a longer period (Figure 52). The DMTS signal maintained its intensity during the period of the spectrum collection. The reason there was no reduction can be explained by the following hypothesis. $NaBH_4$ may reacting with HCl and producing diborane ($B_2H_6$) and hydrogen gas ($H_2$) with sodium chloride (NaCl) salt.

$2\ NaBH_4 + 2\ HCl \rightarrow 2\ NaCl\ (s) + B_2H_6\ (g) + 2\ H_2\ (g)$

### *5.2.2. SERS reduction analysis of $NaBH_4$*

From the result obtained by ordinary Raman analysis of $NaBH_4$ reduction it was found that reduction is occurring without any acid. For the SERS experiment the reaction of DMTS and $NaBH_4$ is studied without any acid.

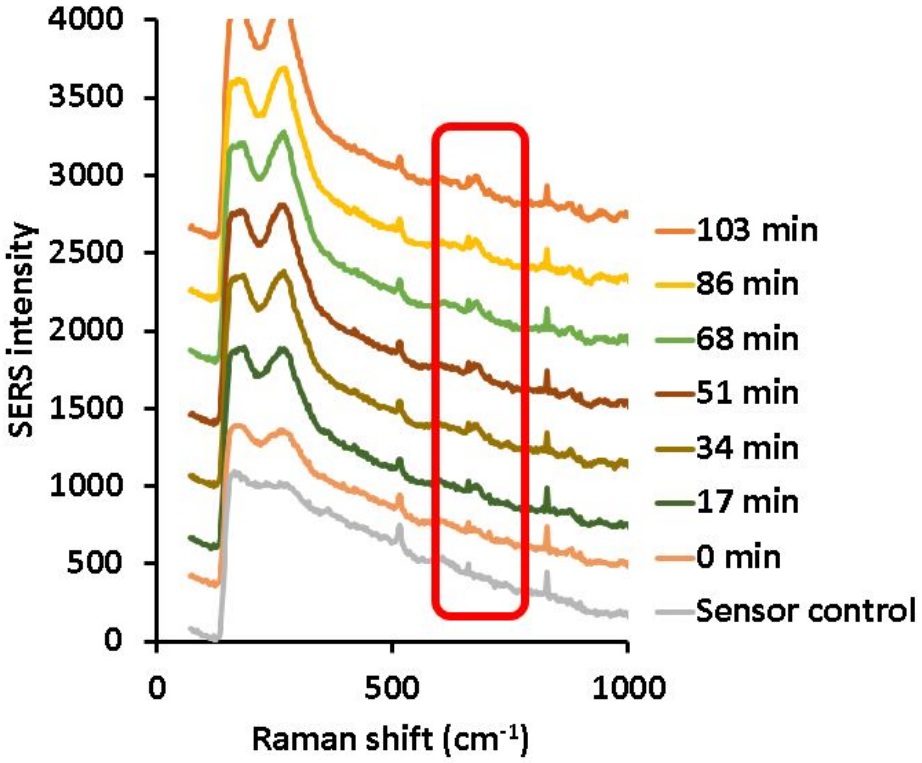


*Figure 53.* Reduction by $NaBH_4$ SERS spectrum. Laser power: 4 mW, integration time: 5 s, raw spectra averaged per saved spectrum: 10.

The SERS reduction reaction spectra from 0 minutes to 103 minutes are shown in Figure 53. An artifact peak is present at 507 $cm^{-1}$, in the disulfide stretching region. This peak is observed in the control spectrum; at that point no DMTS or its reductant product is expected. Because of the sensitivity of the SERS sensors, it may detect sulfur compound from human breath. The signal at 690 wavenumbers is increasing slowly with time, which supports methyl mercaptan production. The absence of any signal at 485 wavenumbers also supports the absence of DMTS in the headspace.

Qualitative analysis of the data demonstrates detection of methyl mercaptan within 520 seconds. Because the final concentration of the solution of this experiment is 250 μM, a more concentrated solution may provide a more intense signal and can test the hypothesis. Laser power can also be increased to produce a more intense signal.

The resulting less intense signal may also arise from the fact that the nanopillar leaning was done by evaporation of water from the sensor in an oven at 110 °C. Previous experiments were carried out by water evaporation at room temperature.

Research has been found that human breath contains hydrogen sulfide, methanethiol, dimethyl sulfide, and dimethyl disulfide.[55] Because no extra caution was taken during the exposure of the sensor in the air and nanopillar leaning upon evaporation of water, it is likely that the peak at 507 $cm^{-1}$ may result from the experimentalists' breath.

**5.3. Dithiothreitol (DTT)**

So far we have witnessed that $FeCl_2$ apparently gives a slow reduction reaction and $NaBH_4$ gives a fast reaction. An intermediate reducing reagent is sought. Dithiothreitol (DTT), or Cleland's reagent, has been extensively used in biochemical labs for selective reduction of disulfides of protein and peptides. The reduction potential of DTT has been found to be -0.33 V at pH 7 and its effectiveness is in the pH range of 6.5-9.[56]

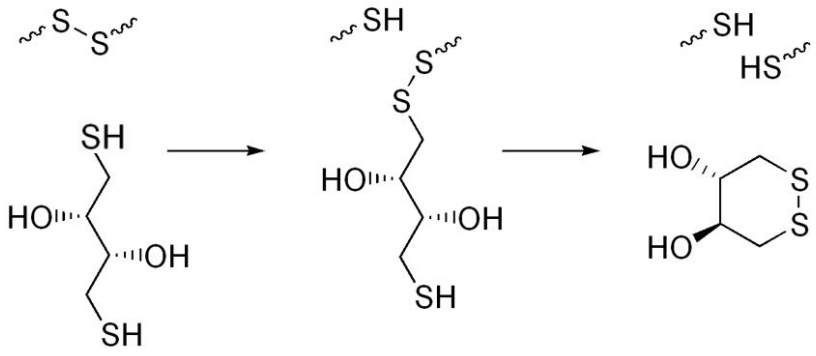

The reduction reaction mechanism of DTT[56] has been found to producing a cyclic disulfide compound. In this section ordinary Raman and SERS has been utilized to test the reduction reaction by DTT.

### *5.3.1. Ordinary Raman analysis*

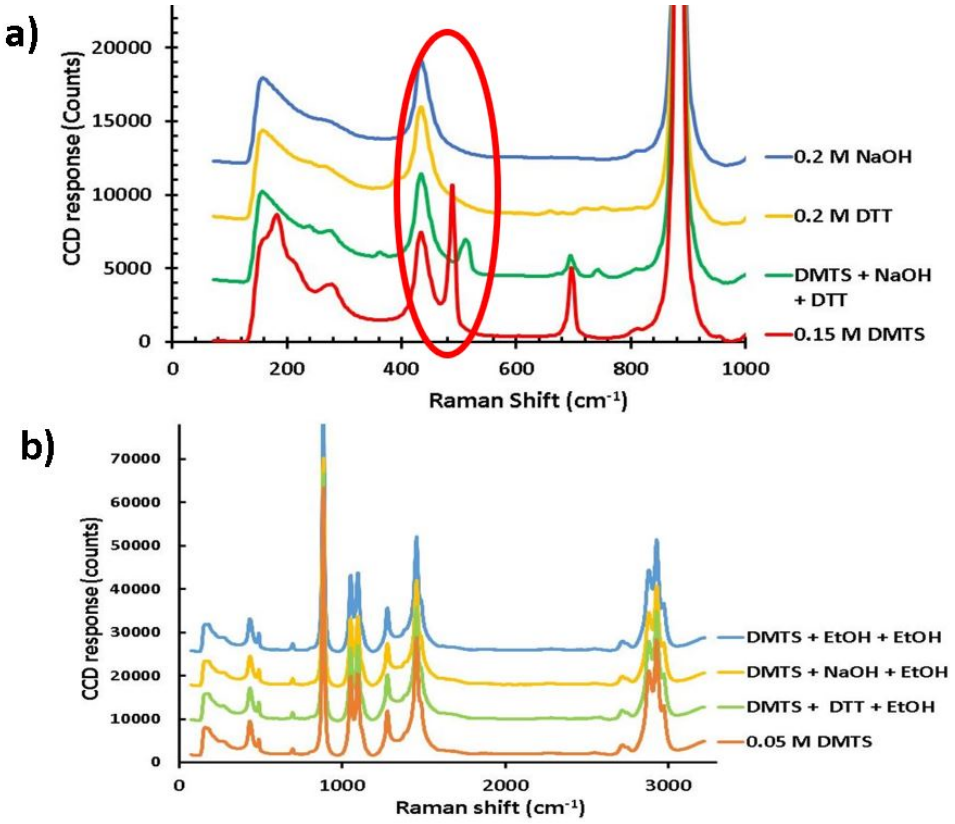


*Figure 54.* DTT reduction analysis by ordinary Raman. a) Peak at 485 $cm^{-1}$ from the reduction reaction is disappeared and a new peak at 512 $cm^{-1}$ is appeared. b) Control spectrum of different solution addition. Laser power: 480 mW, integration time: 1.5 s, raw spectra averaged per saved spectrum: 10

Figure 54 a shows 4 spectra: the red spectrum is of 0.15 M DMTS, the green spectrum is a reduction reaction spectrum, and the yellow and blue spectra represent 0.2 M DTT and 0.2 M NaOH, respectively. The 0.15 M DMTS spectrum clearly shows its signature two sharp peaks. But upon reduction the peak at 485 disappears and a new peak at 512 shows up, whereas the 690 remains at same place. That provides the evidence of

producing a disulfide compound and reduction of the trisulfide. The disulfide compound is the oxidized form of DTT described earlier. The measured pH of the reduction reaction mixture found to be 8.5. A test of the oxidation of DTT was not carried out.

No changes were found in the control spectra reaction of DTT and DMTS. (Figure 54 b).

### *5.3.2. SERS*

The ordinary Raman analysis of reduction by DTT showed a very promising result. In this section SERS result is presented from the reduction of DMTS by DTT.

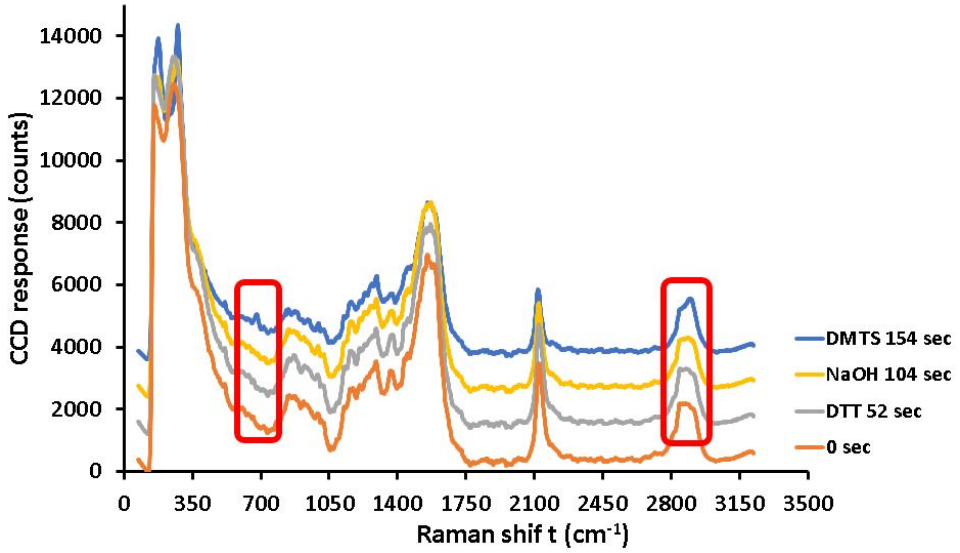


*Figure 55.* SERS analysis of DMTS reduction by DTT. DTT was added between 0 and 52 seconds, NaOH was added between 52 and 104 seconds, and DMTS was added in between of 104 and 154 seconds. Laser power: 10 mW, integration time: 5 s, raw spectra averaged per saved spectrum: 10.

Figure 55 shows the promising rapid detection of methyl mercaptan. Upon addition of DMTS, the reduction occurs quickly and provides methyl mercaptan signature peaks (blue spectrum). The methyl mercaptan signal grows within 50 seconds after addition of DMTS with DTT in presence of NaOH. According to the literature, the peaks at 680 and 2909 $cm^{-1}$ arise from methyl mercaptan, two feature clearly seen in the blue spectrum.[23]

The same peaks are also present in the headspace of DMTS but the time it took to bind to the sensor is longer than for methyl mercaptan. Figure 56 shows the reduction by DTT over 87 minutes.

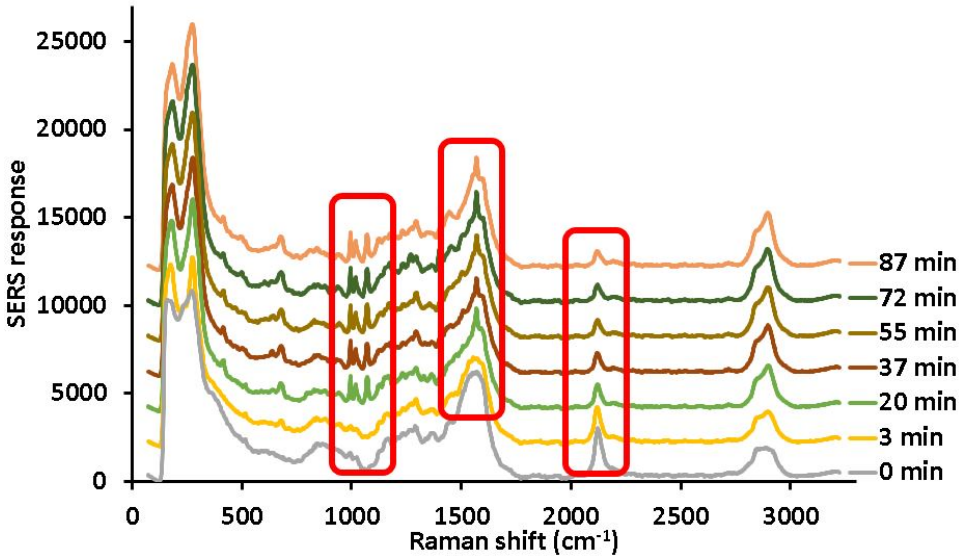


*Figure 56.* DTT reduction spectra with longer observation period.

Three red box regions are shown in Figure 56. Three additional changes near 1000, 1500 and 2100 $cm^{-1}$ have also occurred during the data collected from the headspace of the reduction by DTT. 1000 and 1500 $cm^{-1}$ are might come from benzenethiol. Because benzenethiol is used as the reference sensor for positioning, and the cuvette window is warmed by using ITO, so it is possible that benzenethiol desorption is occurring with a slight temperature increase of the headspace inside the cuvette (Figure 19). More study is required to support the hypothesis. But the 2100 peak decrease is consistent with the drop coating result.

Control of the reduction reaction of DTT with NaOH is also carried out as a blank and no substantial proof was recorded to have methyl mercaptan.

# CHAPTER IV

## Conclusion and Future Directions

Surface enhanced Raman spectroscopy (SERS) is a powerful vibrational spectroscopic technique that has been studied and used extensively in research. Due to its powerful sensitivity, SERS has been used for trace analysis. SERS has been applied in fields as diverse as forensic science, chemistry, physics, material science and life science.[57]

This work investigated different SERS methods for detecting DMTS from ethanolic solution. A thousand-fold improvement of detection was obtained by the SERS drop coating method relative to ordinary Raman analysis. The SERS drop coating method was able to detect DMTS at 5 μM concentrations. Signals were found in the fingerprint region that appear to vary monotonically over the concentration range of 5-5000 μM, that show promise for the quantitative determination of DMTS by SERS.

SERS headspace sampling experiments were explored because of their potential to improve selectivity while sampling from complex matrices. In the headspace sampling SERS experiments DMTS was detected at a concentration of 50 μM. Complex results were obtained from stirring experiments targeted at speeding up the detection of DMTS. The fogging of the cuvette window, and the sensor presented major challenges. A proof of principle experiment showed that the window fogging could be reversed by warming the window with current flowing through an indium tin oxide (ITO) coated glass slide, or by housing the cuvette in a holder with thicker aluminum walls that were painted black.

To prevent the solvent from condensing on the cuvette windows, the top of the cuvette needs to be kept at a slightly warmer temperature than the bottom. The most effective solution to this problem will likely be a dual zone temperature controller for the

cuvette. It may be possible to build a prototype of such a temperature control system with an ITO coated slide. The minimum current required to prevent condensation would need to be determined. Knowing the right amount of current, a follow up study might employ a specialized cuvette in which one window was adjoined with ITO window on top and glass at the bottom. So, that current can pass through the ITO and maintain required amount of heat to not have condensation on the glass window, and at the same time not changing the solution temperature.

Heating provided a clear improvement in the rate of DMTS sensing. The smell of ethanol during the heating experiment indicated that the cuvette seal had failed. The experiment with the qpod 2e temperature controller has confirmed that the grease seal fails above 49 °C. It would be advantageous to maintain the solution temperature below 49 ± 4 °C and study kinetics below that temperature.

Sub minute detection of DMTS from the headspace above a 100 μM ethanolic DMTS proved to be possible by using dithiothreitol (DTT) as a reducing agent. SERS spectra are supportive of the hypothesis that methyl mercaptan is produced during the reduction. In the future it would be useful to conduct a positive control experiment for detecting methyl mercaptan. Sodium methane thiolate can be used as a standard for this purpose.

No convincing evidence for the reaction of DMTS with iron (II) chloride was observed. Additionally, a disulfide compound may also have been produced with the reaction of $FeCl_2$. We concluded that the reaction with $FeCl_2$ is apparently slow. It may also be that the iron is oxidized so rapidly by dissolved oxygen that very little is able to react with DMTS. Oxygen free environments are needed to study this reaction more

carefully. A longer ordinary Raman experiment following the reduction of DMTS by $FeCl_2$ is also a potential future experiment to test the hypothesis of the slowness.

From the qualitative analysis of data, it was found that the methyl mercaptan detection time is 520 seconds, using sodium borohydride as the reducing agent. A yellow precipitate was observed while reducing DMTS with $NaBH_4$ in both cases (in acidic and in non-acidic media). It appears that the reaction of $NaBH_4$ with DMTS produces elemental sulfur. Raman spectra from the reaction mixture are needed to understand the reaction better.

## REFERENCES


(1) Agency for Toxic Substances & Disease Registry http://www.atsdr.cdc.gov/toxfaqs/tf.asp?id=71&tid=19 (accessed Oct 11, 2016).

(2) Centers for Disease Control and Prevention https://emergency.cdc.gov/agent/cyanide/basics/facts.asp (accessed Oct 12, 2016).

(3) Brennan, R. J.; Waeckerle, J. F.; Sharp, T. W.; Lillibridge, S. R. *Ann. Emerg. Med.* **1999**, *34* (2), 191–204.

(4) Greenfield, R. A.; Slater, L. N.; Bronze, M. S.; Brown, B. R.; Jackson, R.; Iandolo, J. J.; Hutchins, J. B. *Am. J. Med. Sci.* **2002**, *323* (6), 326–340.

(5) Shier, D.; Butler, J.; Lewis, R. *McGraw-Hill High. Educ.* **2009**, *10*.

(6) Kovacs, K.; Duke, A. C.; Shifflet, M.; Winner, B.; Lee, S. A.; Rockwood, G. A.; Petrikovics, I. *Pharm. Dev. Technol.* **2016**, 1–6.

(7) Kocić-Tanackov, S.; Dimić, G.; Lević, J.; Tanackov, I.; Tepić, A.; Vujičić, B.; Gvozdanović-Varga, J. *J. Food Sci.* **2012**, *77* (5), M278–M285.

(8) Chin, H. W.; Lindsay, R. C. *Sulfur Compd. Foods* **1994**, *564*, 90–104.

(9) CSID:18219 http://www.chemspider.com/Chemical-Structure.18219.html (accessed Oct 12, 2016).

(10) Wu, M.; Cui, Y.; Bhargav, A.; Losovyj, Y.; Siegel, A.; Agarwal, M.; Ma, Y.; Fu, Y. *Angew. Chemie - Int. Ed.* **2016**, *55* (34), 10027–10031.

(11) Chen, S.; Xu, Y.; Qian, M. C. *J. Agric. Food Chem.* **2013**, *61* (47), 11295–11302.

(12) Raman, C. V. The Molecular Scattering of Light, Nobel Lecture, Nobel Media AB, 1930. http://www.nobelprize.org/nobel_prizes/physics/laureates/1930/raman-lecture.html (accessed Jul 29, 2016).

(13) Albrecht, M. G.; Creighton, J. A. *J. Am. Chem. Soc.* **1977**, *99* (15), 5215–5217.

(14) Jeanmaire, D. L.; Van Duyne, R. P. *J. Electroanal. Chem. Interfacial Electrochem.* **1977**, *84* (1), 1–20.

(15) Sharma, B.; Frontiera, R. R.; Henry, A.; Ringe, E.; Van Duyne, R. P. *Mater. Today* **2012**, *15* (1–2), 16–25.

(16) Hossain, M. S. Dimethyl trisulfide (DMTS) detection by raman and surface-enhanced raman spectroscopy., Sam Houston State University, 2015.

(17) Biggs, K. B.; Camden, J. P.; Anker, J. N.; Van Duyne, R. P. *J. Phys. Chem. A* **2009**, *113* (16), 4581–4586.

(18) Deng, Z.; Chen, X.; Wang, Y.; Fang, E.; Zhang, Z.; Chen, X. *Anal. Chem.* **2015**, *87* (1), 633–640.

(19) Chen, P. C.; Joyner, C. C.; Patrick, S. T.; Benton, K. F. *Anal. Chem.* **2002**, *74* (7), 1618–1623.

(20) Schiller, G.; Auer, C.; Bessler, W. G.; Christenn, C.; Ilhan, Z.; Szabo, P.; Ax, H.; Kapadia, B.; Meier, W. *Appl. Phys. B* **2013**, *111* (1), 29–38.

(21) CSID http://www.chemspider.com/Chemical-Structure.18219.html (accessed Aug 11, 2016).

(22) Paik, W. K.; Eu, S.; Lee, K.; Chon, S.; Kim, M. *Langmuir* **2000**, *16* (26), 10198–10205.

(23) Hill, W.; Wehling, B.; Klockow, D. *Appl. Spectrosc.* **1999**, *53* (5), 547–550.

(24) Tripathi, A.; Emmons, E. D.; Christesen, S. D.; Fountain, A. W.; Guicheteau, J. A. *J. Phys. Chem. C* **2013**, *117* (44), 22834–22842.

(25) Rouhana, L. L.; Moussallem, M. D.; Schlenoff, J. B. *J. Am. Chem. Soc.* **2011**, *133* (40), 16080–16091.
(26) Pensa, E.; Cortés, E.; Corthey, G.; Carro, P.; Vericat, C.; Fonticelli, M. H.; Benítez, G.; Rubert, A. A.; Salvarezza, R. C. *Acc. Chem. Res.* **2012**, *45* (8), 1183–1192.
(27) Steudel, R. *Chem. Rev.* **2002**, *102* (11), 3905–3945.
(28) Lustemberg, P. G.; Vericat, C.; Benitez, G. A.; Vela, M. E.; Tognalli, N.; Fainstein, A.; Martiarena, M. L.; Salvarezza, R. C. *J. Phys. Chem. C* **2008**, *112* (30), 11394–11402.
(29) Rosario-Alomar, M. F.; Quiñones-Ruiz, T.; Kurouski, D.; Sereda, V.; Ferreira, E. B.; De Jesús-Kim, L.; Hernández-Rivera, S.; Zagorevski, D. V.; López-Garriga, J.; Lednev, I. K. *J. Phys. Chem. B* **2015**, *119* (4), 1265–1274.
(30) Bastian, EJ. Jr.; Martin, R. B. *J. Phys. Chem.* **1973**, *77* (9), 1129–1133.
(31) Kiss, L.; Holmes, S.; Chou, C.; Dong, X.; Ross, J.; Brown, D.; Mendenhall, B.; Coronado, V.; Silva, D. D.; Petrikovics, I.; Thompson, D. E. *J. Chromatogr. B* **2017**, 149–157.
(32) Atkins, P.; De Paula, J. In *Physical Chemistry*; Oxford University Press: Oxford, 2002; p 170.
(33) Sander, R. *Atmos. Chem. Phys.* **2015**, *15* (8), 4399–4981.
(34) Beilin, L. J.; Knight, G. J.; Munro-Faure, A. D.; Anderson, J. *J. Clin. Invest.* **1966**, *45* (11), 1817–1825.
(35) Saptalena, L. G.; Kerpen, K.; Kuklya, A.; Telgheder, U. *Int. J. Ion Mobil. Spectrom.* **2012**, *15* (2), 47–53.
(36) ChemSpider http://www.chemspider.com/Chemical-Structure.18219.html?rid=5d9d8b33-3a0e-4004-bb66-4c4305a65c6c (accessed Dec 5, 2016).
(37) Schmidt, M. S.; Hübner, J.; Boisen, A. *Adv. Mater.* **2012**, *24* (10), OP11-OP18.
(38) Yang, S.; Dai, X.; Stogin, B. B.; Wong, T. **2016**, *113* (2).
(39) Foresman, James B. ; Frisch, Æ. In *Exploring Chemistry with Electronic Structure Methods*; Gaussian, Inc. 2nd ed: Pittsburgh, PA, 1996; pp 61–64.
(40) MIT web.mit.edu/cortiz/www/PiranhaSafety.doc%0A (accessed Apr 4, 2017).
(41) Kaur, M. Strategies for attaching a cyanide metabolite (2-aminothiazoline-4-carboxylic acid) to gold-coated surface-enhanced Raman., Sam Houston State University, 2016.
(42) Johnson, E. V; Kroely, L.; Roca i Cabarrocas, P. *Sol. Energy Mater. Sol. Cells* **2009**, *93* (10), 1904–1906.
(43) NIOSH, CDC http://www.cdc.gov/niosh/idlh/74931.html (accessed Sep 24, 2016).
(44) NIOSH, CDC http://www.cdc.gov/niosh/idlh/7783064.html (accessed Sep 24, 2016).
(45) SIGMA-ALDRICH https://www.sigmaaldrich.com/content/dam/sigma-aldrich/docs/Sigma/Datasheet/6/646563dat.pdf (accessed Mar 2, 2017).
(46) Quijada, C.; Huerta, F. J.; Morallón, E.; Vázquez, J. L.; Berlouis, L. E. A. *Electrochim. Acta* **2000**, *45* (11), 1847–1862.
(47) Ancha, M. S. Characterization and formulation of selected sulfur molecules as potent antidotes in cyanide poisoning., Sam Houston State University, 2012.
(48) Bürgi, T. *Nanoscale* **2015**, *7* (38), 15553–15567.

(49) Gu, X.; Wang, H.; Schultz, Z. D.; Camden, J. P. *Anal. Chem.* **2016**, *88* (14), 7191–7197.
(50) PubChem https://pubchem.ncbi.nlm.nih.gov/compound/ethanol#section=Top (accessed Oct 17, 2016).
(51) GmbH, DDBST http://ddbonline.ddbst.com/AntoineCalculation/AntoineCalculationCGI.exe (accessed Sep 23, 2016).
(52) Dow Corning http://www.dowcorning.com/applications/search/default.aspx?R=112EN (accessed Oct 13, 2016).
(53) Dow Corning http://www.dowcorning.com/DataFiles/0902770182f90653.pdf (accessed Oct 17, 2016).
(54) Sigma Aldrich http://www.sigmaaldrich.com/analytical-chromatography/analytical-products.html?TablePage=14540720 (accessed Oct 17, 2016).
(55) Pysanenko, A.; Španěl, P.; Smith, D. *J. Breath Res.* **2008**, *2* (4), 046004/1-046004/13.
(56) Interchim http://www.interchim.fr/ft/0/054721.pdf (accessed Mar 14, 2017).
(57) Muehlethaler, C.; Leona, M.; Lombardi, J. R. *Anal. Chem.* **2016**, *88* (1), 152–169.

# APPENDIX

Calculation of MeSH produced from 200 µL 0.5 M DMTS reduction:

$$\frac{0.5\ mol\ DMTS}{L_{soln}} * 200\ \mu L * \frac{2\ mol\ MeSH}{1\ mol\ DMTS} * \frac{48.108\ g\ MeSH}{1\ mol\ MeSH} * \frac{m}{10^{-3}} * \frac{10^{-6}}{\mu} = 9.6\ \text{mg MeSH}$$

The lab volume is 20 (Length) ft ·15 ft (Width) · 10 ft (Height) => (20·30.48) cm·(15·30.48) cm·(10·30.48) cm (1 ft=30.48 cm); 609.6 cm·457.2cm·304.8cm=> $8.495 \cdot 10^7$ $cm^3$ or $8.5 \cdot 10^7$ $cm^3$ or mL. 9.6 mg/$8.5 \cdot 10^7$ mL is lower than recommended exposure limit published in NIOSH.[43]

Calculation of $H_2S$ produced from 200 µL 0.5 M DMTS:

$$\frac{0.5\ mol\ DMTS}{L_{soln}} * 200\ \mu L * \frac{1\ mol\ H2S}{1\ mol\ DMTS} * \frac{34.081\ g\ H2S}{1\ mol\ H2S} * \frac{m}{10^{-3}} * \frac{10^{-6}}{\mu} = 3.4\ \text{mg } H_2S.$$

3.4 mg/$8.5 \cdot 10^7$ mL is lower than recommended exposure limit published in NIOSH.[44]

# VITA

Md Nure Alam was born on January 01, 1987 in Bangladesh. He grew up in Comilla, a culturally rich town in Bangladesh. After completing his undergraduate studies in 2010 from the University of Dhaka, he finished his masters in 2012 from the same institution. After the graduation in 2012, he joined SGS-Bangladesh. He worked there for three months. Later he enrolled in the Master of Chemistry at SHSU, in 2014. During his graduate studies, he received the opportunity to do research under the supervision of Dr. David E. Thompson. During his graduate studies, he has presented his research at the 2016 Southwest Regional Meeting of the American Chemical Society, November 10-13, 2016, Galveston, TX and in Memphis, TN on November 4-7, 2015. He is planning to start his Ph.D. at Oregon State University in August 2017.